NASA/TM-2009-215730
NESC-RP-05-98/04-073-E

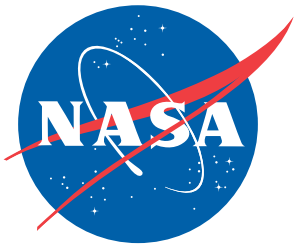

Stratospheric Observatory for Infrared Astronomy (SOFIA) Acoustical Resonance Technical Assessment Report

Michael W. Kehoe/NESC
Dryden Flight Research Center, Edwards, California

Michael G. Gilbert/NESC
Langley Research Center, Hampton, Virginia

Kajal K. Gupta
Dryden Flight Research Center, Edwards, California

Jerry H. Ginsberg
Georgia Institute of Technology, Atlanda, Georgia

Michael A. Kegerise
Langley Research Center, Hampton, Virginia

Ramesh Kolar
Naval Postgraduate School, Monterey, California

May 2009

NASA STI Program . . . in Profile

Since its founding, NASA has been dedicated to the advancement of aeronautics and space science. The NASA scientific and technical information (STI) program plays a key part in helping NASA maintain this important role.

The NASA STI program operates under the auspices of the Agency Chief Information Officer. It collects, organizes, provides for archiving, and disseminates NASA's STI. The NASA STI program provides access to the NASA Aeronautics and Space Database and its public interface, the NASA Technical Report Server, thus providing one of the largest collections of aeronautical and space science STI in the world. Results are published in both non-NASA channels and by NASA in the NASA STI Report Series, which includes the following report types:

- TECHNICAL PUBLICATION. Reports of completed research or a major significant phase of research that present the results of NASA programs and include extensive data or theoretical analysis. Includes compilations of significant scientific and technical data and information deemed to be of continuing reference value. NASA counterpart of peer-reviewed formal professional papers, but having less stringent limitations on manuscript length and extent of graphic presentations.

- TECHNICAL MEMORANDUM. Scientific and technical findings that are preliminary or of specialized interest, e.g., quick release reports, working papers, and bibliographies that contain minimal annotation. Does not contain extensive analysis.

- CONTRACTOR REPORT. Scientific and technical findings by NASA-sponsored contractors and grantees.

- CONFERENCE PUBLICATION. Collected papers from scientific and technical conferences, symposia, seminars, or other meetings sponsored or co-sponsored by NASA.

- SPECIAL PUBLICATION. Scientific, technical, or historical information from NASA programs, projects, and missions, often concerned with subjects having substantial public interest.

- TECHNICAL TRANSLATION. English-language translations of foreign scientific and technical material pertinent to NASA's mission.

Specialized services also include creating custom thesauri, building customized databases, and organizing and publishing research results.

For more information about the NASA STI program, see the following:

- Access the NASA STI program home page at *http://www.sti.nasa.gov*

- E-mail your question via the Internet to help@sti.nasa.gov

- Fax your question to the NASA STI Help Desk at 443-757-5803

- Phone the NASA STI Help Desk at 443-757-5802

- Write to:
  NASA STI Help Desk
  NASA Center for AeroSpace Information
  7115 Standard Drive
  Hanover, MD 21076-1320

NASA/TM-2009-215730
NESC-RP-05-98/04-073-E

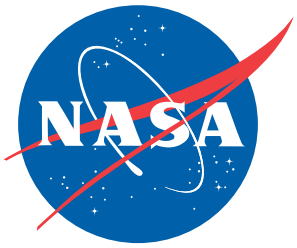

Stratospheric Observatory for Infrared Astronomy (SOFIA) Acoustical Resonance Technical Assessment Report

Michael W. Kehoe/NESC
Dryden Flight Research Center, Edwards, California

Michael G. Gilbert/NESC
Langley Research Center, Hampton, Virginia

Kajal K. Gupta
Dryden Flight Research Center, Edwards, California

Jerry H. Ginsberg
Georgia Institute of Technology, Atlanda, Georgia

Michael A. Kegerise
Langley Research Center, Hampton, Virginia

Ramesh Kolar
Naval Postgraduate School, Monterey, California

National Aeronautics and
Space Administration

Langley Research Center
Hampton, Virginia 23681-2199

May 2009

The use of trademarks or names of manufacturers in the report is for accurate reporting and does not constitute an official endorsement, either expressed or implied, of such products or manufacturers by the National Aeronautics and Space Administration.

Available from:

NASA Center for AeroSpace Information
7115 Standard Drive
Hanover, MD 21076-1320
443-757-5802

STRATOSPHERIC OBSERVATORY FOR INFRARED ASTRONOMY (SOFIA) ACOUSTICAL RESONANCE TECHNICAL ASSESSMENT REPORT

SEPTEMBER 1, 2005

NESC Request No. 04-073-E

TABLE OF CONTENTS

VOLUME I: REPORT

1.0 AUTHORIZATION AND NOTIFICATION 4

2.0 SIGNATURE PAGE 5

3.0 TEAM MEMBERS, EX OFFICIO MEMBERS, AND CONSULTANTS 6

4.0 EXECUTIVE SUMMARY 7

5.0 TECHNICAL ASSESSMENT PLAN 10

6.0 DESCRIPTION OF THE PROBLEM, PROPOSED SOLUTIONS, AND RISK ASSESSMENT 11
6.1 Description of Aircraft Modification 11
6.1.1 Telescope Assembly 14
6.2 SOFIA Cavity Design Process (Project solution and Technical Assessment) 16
6.2.1 Aero-Acoustic Analysis/Wind Tunnel Tests 16
6.2.2 Structural Integrity 23
6.2.3 Approach to Flight Test 43
6.2.4 NESC Risk Assessment 50

7.0 RESULTS OF STRUCTURALL ANALYSIS 55
7.1 A Simple Model of Structural Response Due to an Interior Cavity Resonance 55
7.2 Two-Dimensional Model of Coupled Acoustic Cavity – Structural Resonance 56
7.3 A General Analysis of the Response of an Acoustic Cavity Bounded by and Elastic Structure to Acoustic Excitation 56

8.0 FINDINGS AND RECOMMENDATIONS 58
8.1 General Findings 58
8.1.1 Specific Findings 59
8.2 Recommendations 62

9.0 LESSONS LEARNED 64

10. DEFINITION OF TERMS 65

11.0 LIST OF ACRONYMS 66

12.0 REFERENCES 67

13.0 MINORITY REPORT 69

List of Figures

6.1.1 Boeing 747SP Dimensions 12
6.1.2 Aircraft Modifications 13
6.1.3 Telescope Cavity Door System 14
6.1.1-1 Sketch of the Telescope Assembly Mounted in the SOFIA Aft Fuselage 15
6.2.1-1 Seven Percent Wind Tunnel Model Telescope Assembly Cavity 18
6.2.2-1 Section 46 Structure of the SOFIA Airplane 23
6.2.2-2 Structural Life Assurance Process Diagram 24
6.2.2-3 Cavity Fluctuation Pressure Environment for the Cruise Flight Condition 26
6.2.2-4 Cavity Fluctuation Pressure Environment for the Door Failed-Open Descent Condition 27
6.2.2-5 PSD Envelope for Engine and Boundary Layer Noise 28
6.2.2-6 Forward Bulkhead Assembly 30
6.2.2-7 Aft Bulkhead Assembly, Looking Forward 31
6.2.2-8 Right Side Fuselage Panels 32
6.2.3-1 DC-10 Wasp Airplane 45
6.2.4-1 Risk Matrix 52

VOLUME II: APPENDICES

Appendix A. NESC ITA/I Request Form (NESC-003-FM-01) 70
Appendix B. Tutorials 74
Appendix C. A Simple Method of Structural Response Due to an Interior Cavity Resonance 83
Appendix D. Two-Dimensional Model of Coupled Acoustic Cavities – Structure Resonance 121
Appendix E. A General Analysis of the Response of an Acoustic Cavity Bounded by an Elastic Structure 157
Appendix F. Tables – Door Position and Test Objectives 181

1.0 Authorization and Notification

A request was submitted on September 2, 2004 concerning the uncertainties regarding the acoustic environment within the Stratospheric Observatory for Infrared Astronomy (SOFIA) cavity, and the potential for structural damage from acoustical resonance or tones, especially if they occur at or near a structural mode. The requestor asked for an independent expert opinion on the approach taken by the SOFIA project to determine if the project's analysis, structural design and proposed approach to flight test were sound and conservative.

Michael Freeman, the NASA Engineering and Safety Center (NESC) chief engineer at the Ames Research Center (ARC), presented a risk assessment of the Telescope Assembly (TA) cavity acoustical resonance interacting with the airplane structural modes on September 16, 2004 to the NESC Review Board (NRB) which resulted in the authorization to develop a Technical Assessment plan. The Technical Assessment plan was developed and approved by the NRB on October 14, 2004. The NRB authorized the review of existing SOFIA technical reports and Technical Interchange Meetings (TIM) with project personnel. The scope of this assessment was to determine if the SOFIA project plans and preparations were adequate for performance of their proposed door open flight test activity. The focus of the technical assessment was on the TA cavity acoustic environment, which included the cavity door failed partially open configuration. The scientific mission phase of the program was not part of this assessment.

2.0 Signature Page

Assessment Team Members

_____	_____
Michael W. Kehoe, Lead	Michael G. Gilbert, Deputy Lead
_____	_____
Kajal K. Gupta	Jerry H. Ginsberg
_____	_____
Michael A. Kegerise	Ramesh Kolar

3.0 Team Members, Ex Officio Members, and Consultants

Team Members

Michael W. Kehoe	Chief Engineer, Lead	NASA/DFRC
Michael G. Gilbert	Chief Engineer, Deputy Lead	NASA/LaRC
Ramesh Kolar	Acoustics, Vibration, and Fatigue	Naval Post Graduate School
Jerry H. Ginsberg	Structural Acoustics	Georgia Institute of Technology
Kajal K. Gupta	Multidisciplinary Analysis (Structural Dynamics)	NASA/DFRC
Michael A. Kegerise	Aero-acoustics	NASA/LaRC
Pamela B. Fullen	Program Analyst	NASA/LaRC
Stacey E. Walker	Admin. Assistant	NASA/LaRC

Ex-Officio Members

Anthony Briceno	Safety and Mission Assurance	NASA/ARC
Douglas R. Fraser		
Nans Kunz	Project Representative, Chief Engineer	NASA/ARC

Consultants

Ivatury Raju	Structures (Fracture Mechanics)	NASA/LaRC

4.0 Executive Summary

General Description

The SOFIA Program provided the National Aeronautics and Space Administration (NASA) and the world's research and education communities with a state-of-the-art airborne observatory for infrared and submillimeter astronomy. The requirements of the program are to modify and test a Boeing 747SP aircraft with a 2.7 meter telescope, integrate the telescope, test the observatory and implement the Science and Mission Operations Center (SSMOC) and associated infrastructure.

The SOFIA system consists of two major components, the Airborne Observatory (the airplane and TA) and the SSMOC. The SSMOC is the ground support unit for Airborne Observatory.

The 747SP is a Boeing-built aircraft, modified to incorporate all mission systems and the TA for the SOFIA system. The aircraft modification consists of changes to the aircraft structure and skin components within fuselage Section 46, in order to accommodate an aperture, a cavity door assembly, and environmental conditioning for the TA. As part of the modifications, not only is there a large opening in the aircraft aft fuselage when it is flying, but there are also two new bulkheads. The forward bulkhead of the cavity is the new pressure boundary for the cabin, and it is also the mechanical interface to which the telescope is mounted. The aft bulkhead is required, in part, to minimize the overall cavity size, for aero-acoustic purposes, during the cavity door-open flight operations. The cavity and the section of the fuselage aft of it remain unpressurized during flight.

The size of the opening required in the fuselage of the SOFIA airplane exceeded any previous known experience for open port cavities in flying aircraft. Therefore wind tunnel tests (3 percent and 7 percent scale models) were conducted early in the SOFIA development to verify the feasibility of a cavity opening of this size. A 90 degree fuselage circumference opening, from the top centerline to about midline at the side was necessary to allow for the required TA elevation range.

It is critical for this airborne observatory to provide the shear layer control required to have a quiet cavity and a stable aircraft while cruising in the stratosphere at Mach 0.84. To accomplish this, a cavity door system consisting of three major components, an Upper Rigid Door (URD), a Lower Flex Door (LFD), and a Shear Layer Control Device was designed and fabricated.

Despite numerous wind tunnel tests and extensive analysis there remained uncertainties regarding the acoustic environment within the cavity, especially in the off nominal failed cavity door open descent flight regime, where some degree of an uncontrolled acoustic resonance is

expected to occur. The potential for structural damage from uncontrolled acoustic resonances in the SOFIA telescope cavity, especially if they occur at or near a structural mode was also stated as a concern. At the request of the Associate Director for Astrobiology and Space Programs at ARC, the NESC conducted a Technical Assessment with a team of subject matter experts (SME) to determine if the analysis, structural design, and proposed approach to flight tests, taken by the project, were sound and conservative.

The primary focus of the assessment was on the cavity acoustic environment and its effect on the surrounding structure. This was accomplished by the review of existing technical reports, TIMs with engineers assigned to the project, and through independent parametric studies conducted by the assessment team. Determination of whether the operational functions of the telescope met design requirements was not an objective of this assessment. However, the fuselage structural modification and the TA cavity opening have simultaneous influences on other areas such as structural dynamics (flutter), and stability and control. The potential effect on these areas was part of the evaluation.

The general findings of the Technical Assessment are:

The SOFIA project appropriately accounted for and designed an aperture treatment for flow control to mitigate or suppress telescope cavity resonances. The final design, a semi-circular aft-ramp, was found to be robust with respect to changes in airplane sideslip angle, TA elevation angle, and airplane angle of attack in the 7 percent scale model wind tunnel tests. These test results also indicated that there were no strong resonant conditions over a Mach number range of 0.4 to 0.88. However, there were no analyses and only limited wind tunnel test results for the cavity door failed open configuration. Therefore, there are uncertainties whether an uncontrolled cavity resonance will occur with the cavity door failed open during descent to landing from cruise altitude. These uncertainties are mitigated through a thorough, incremental building-block approach to opening the door during the flight test phase of the program.

The cavity fatigue analysis and damage tolerance analysis (DTA) was started, but not completed, during the time period of this assessment. The validity of some aspects of the proposed approach could not be substantiated and require verification prior to flight. This technical area requires further evaluation before flight with the cavity open door.

Flight test planning for either the door-closed or opened-door flights has not been completed. Some initial planning for technical areas related to this assessment, such as opening the cavity door, has been completed, and indicates a cautious approach to hazardous testing and to areas where uncertainties exist. Instrumentation in some areas requires supplementation for appropriate, real-time monitoring during flight, and for adequate post-flight data reduction.

The assessment team provided 22 specific findings, 3 observations, and 7 recommendations to the SOFIA project which can be found in the detailed findings and recommendations section (Section 8.0) of this report. The recommendations, once implemented, will reduce the uncertainties and lead to a better understanding of the acoustical environment within the cavity.

Overall, the analysis, structural design and proposed approach to the cavity door open flight test taken by the project was found to be sound and conservative, with the exception of the acoustic fatigue and damage tolerance assessment, which the project had not completed at the time of this review.

5.0 Technical Assessment Plan

The scope of this Technical Assessment was to determine if the SOFIA project plans and preparations were adequate for performance of their proposed cavity door open flight test. The focus of the technical assessment was on the TA cavity acoustic environment, which included the failed open door configuration. The scientific mission phase of the program was not part of this assessment.

The NRB authorized the SOFIA Acoustical Resonance Technical Assessment plan on October 14, 2004. The objective of this activity was to review the available technical reports that have been produced by the project in preparation for the flight test phase of the program. This assessment was to culminate with a technical opinion to the program on whether the approach in the analysis, structural design, and proposed flight test taken by the project, was sound and conservative.

The approach developed by the team was to first formulate a strategy to delineate a method on how each technical area should be properly evaluated. A multidisciplinary approach was taken by the team. Although the focus of this assessment was on the TA cavity and its surrounding structure with the cavity door open, the simultaneous influence of the cavity on other areas was also considered during the course of the assessment. The assessment problem resolution strategy indicated that several other technical disciplines, in addition to those associated with aero-acoustics, structural-acoustics, and acoustic fatigue, such as structural dynamics, and stability and control, required evaluation.

The specific sequence of events for the Technical Assessment was:

1. Gain a comprehensive understanding of the SOFIA project with an emphasis on the TA cavity design and test methodology.

2. Define the standard engineering tests and analyses requirements for a SOFIA type airplane modification (problem resolution strategy).

3. Compile the list of reports for review and evaluation.

4. Develop models and conduct parameter studies to better understand the interaction of cavity acoustics with the cavity structure.

5. Compile the findings and recommendations for the SOFIA Project Office.

6.0 Description of the Problem, Proposed Solutions, and Risk Assessment

This section describes the modifications made to the SOFIA Boeing 747SP aircraft. Specifically, the description focuses on the large structural modification and its effect on the areas that the assessment team was assigned to review. A description of the analyses and tests performed by the project is provided followed by a technical assessment of that work.

6.1 Description of Aircraft Modification

The SOFIA airplane is the replacement for the Kuiper Airborne Observatory (KAO) C-141A airplane. The final observing flight of the KAO airplane was in 1995, and SOFIA development commenced in 1996. SOFIA is a joint project between NASA and Deutsches Zentrum für Luftund Raumfahrt (DLR), which is Germany's national aerospace research center as well as the national space agency.

The Boeing 747SP airplane, shown in Figure 6.1-1, was selected as the aircraft best suited to meet the project's requirements. The B-747SP airplane has proven to be reliable, and maintainable, in worldwide fleet usage, and the SOFIA airplane had the remaining service life to continue flying for another 20 years.

The goal for SOFIA was to design a telescope and telescope accommodation that yielded the largest possible telescope primary mirror diameter. Early studies indicated that the modifications required to locate the telescope in the forward fuselage section were economically prohibitive. Therefore, it was decided to locate the telescope cavity in the aft fuselage area, which was a significantly less expensive aircraft modification.

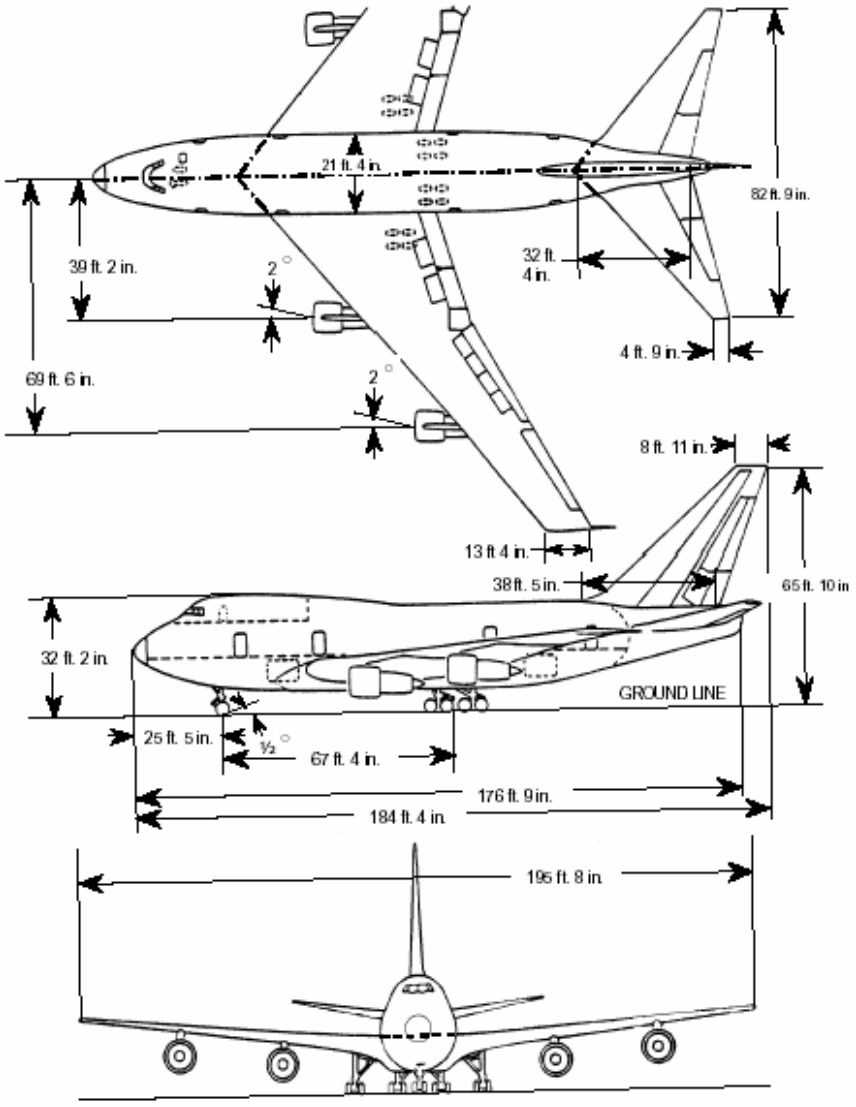

Figure 6.1-1. Boeing 747SP Dimensions.

The aircraft has been modified to incorporate all mission systems and the TA for the SOFIA system. The aircraft modification consisted of changes to the aircraft structure and skin components, within fuselage Section 46, in order to accommodate an aperture, door assembly, and environmental conditioning for the TA. As part of the modifications, not only is there a large hole in the aircraft when it is flying, there are also two new bulkheads. The forward bulkhead of the cavity is the new pressure boundary for the cabin, and it is also the mechanical interface to which the telescope is mounted. The aft bulkhead was required, in part, to minimize the overall cavity size for aero-acoustic purposes during the door-open flight operations. The aft portion of the fuselage remains unpressurized during flight. Figure 6.1-2 shows the modification to the SOFIA airplane.

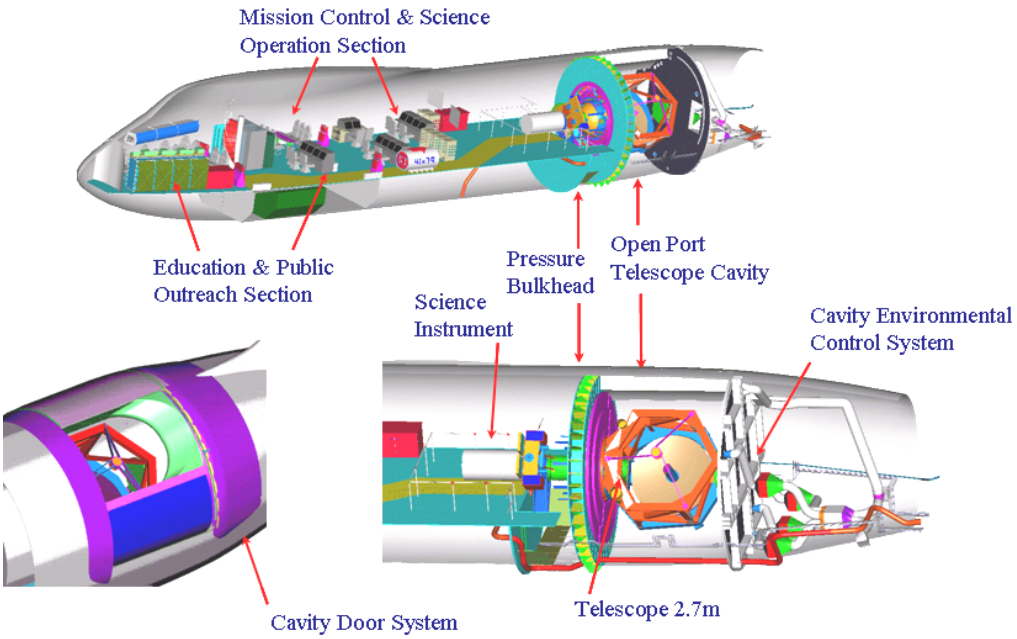

Figure 6.1-2. Aircraft Modifications

The size of the opening required in the fuselage of the SOFIA airplane exceeded any previous known for open port cavities in flying aircraft. Therefore, wind tunnel tests (3 percent and 7 percent scale models) were conducted early in the SOFIA development to verify the feasibility of a cavity opening of this size. A 90 degree fuselage circumference opening, from the top centerline to about midline at the side is necessary to allow for the required TA elevation range.

It is critical for this airborne observatory to provide the shear layer control required to have a quiet cavity and a stable aircraft while cruising in the stratosphere at Mach 0.84, with a very large opening in the fuselage. To accomplish this, a cavity door system consisting of three major

components, an URD, a LFD, and a Shear Layer Control Device was designed and fabricated. Figure 6.1-3 shows the components of the cavity door system.

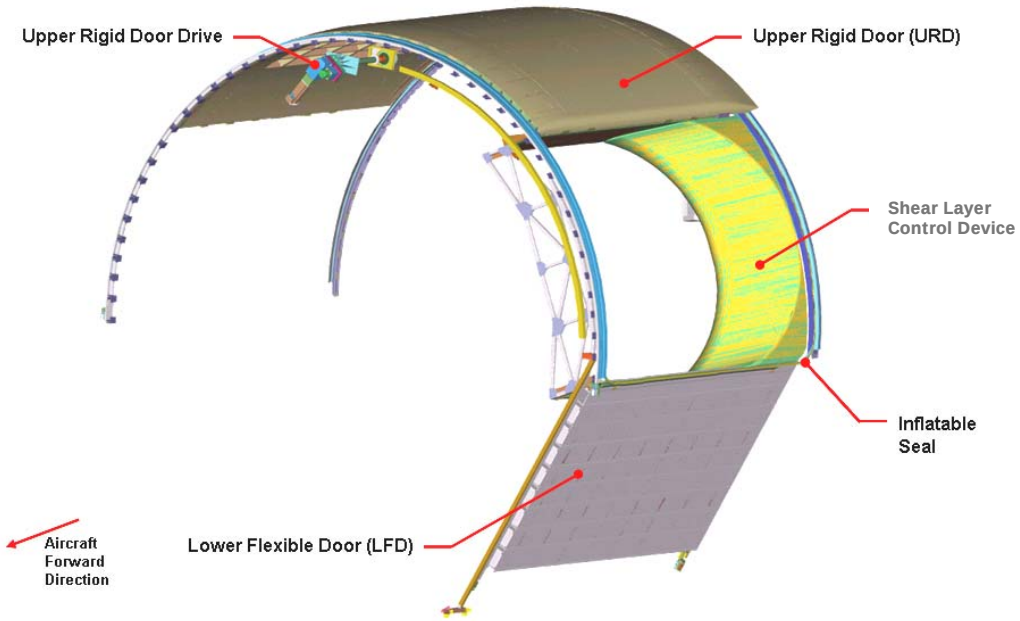

Figure 6.1-3. Telescope Cavity Door System.

The cavity door is closed during take-off and landing, as well as climb to and descent from the telescope observation altitude. The cavity door will only be opened at altitudes between 39,000 and 45,000 ft. This is the stratospheric altitude band for normal telescope operation. Once the aircraft achieves the desired observing flight conditions, the URD opens, exposing the telescope and the shear layer control features on the door system aperture. The shear layer concept was developed to minimize the aerodynamic disturbance to the telescope, and is a critical part of the system. Once the URD is open, the URD, Shear Layer Control, and LFD move together to track the telescope as it moves to the desired elevation angles, closing off the portions of the structural opening not required by the telescope for unobstructed viewing. The LFD closes off the lower portion of the structural opening when the telescope is observing at the higher elevation angles. In order to move freely, the cavity door system components were designed to be isolated from carrying fuselage loads.

6.1.1 Telescope Assembly

The TA, which weighs approximately 22,000 pounds, consists of the telescope metering tube assembly located in the cavity, the science instrument located in the cabin, and the Nasmyth tube. The Nasmyth tube, which is a combination framework and circular tube structure, provides

a connection between the telescope metering assembly, and the science instrument and a mounting for the hydrostatic bearing support, which provides a connection to the aircraft structure. This approach requires that the center of mass be located at the center of the bearing sphere, which is accomplished by the use of movable and removable counterweights on the science instrument end of the telescope. The hydrostatic bearing supports the entire weight TA structure and floats on a film of hydraulic fluid.

The TA structure is a stiffness driven design, based on optical requirements for image quality and pointing stability. It provides sufficient strength and stability to safely hold its own mass within the aircraft environment. The load path leads from the Nasmyth tube to the bearing sphere, through the vibration suspension system to the mounting bulkhead. A sketch of the telescope mounted in the aft fuselage is shown in Figure 6.1.1-1.

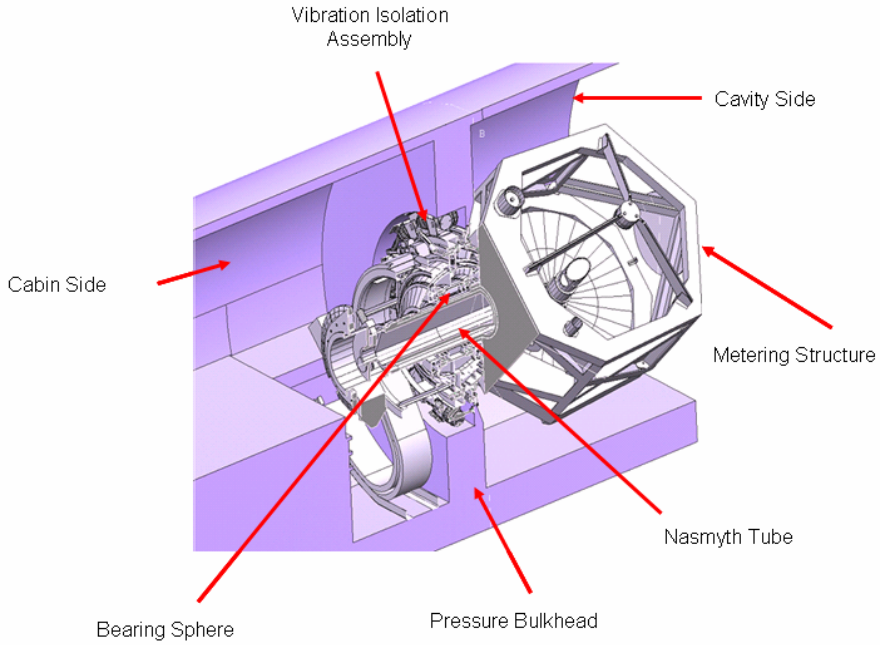

Figure 6.1.1-1. Sketch of the Telescope Assembly Mounted in the SOFIA Aft Fuselage.

The bearing sphere separates the TA from the aircraft structure but it does not separate it from the aero-acoustic environment. A suspension system, consisting of the vibration isolation system and the rotation isolation system with the rotation drive assembly as a subsystem, provides the required isolation.[1]

[1] Eberhard, S. and Ulrich, W., "The Suspension Assembly of SOFIA, the Key Subsystem Connecting the Telescope with the Aircraft." Proceedings of the Society of Photo-Optical Instrumentation Engineers (SPIE) Conference, Munich, Germany, Vol. 4014, March 2000.

The Vibration Isolation System is a passive spring-damper system (airbags and hydraulic dampers) with active altitude adjustment capability. This system is functional when the engines are operating (taxi and flight) and is designed to isolate the telescope from the aircraft vibrations.

The Rotation Isolation Assembly is a hydrostatic oil-bearing, separating the telescope from rotational excitations of the aircraft. This system is functional when the engines are operating (taxi and flight). It is designed to have minimal friction, so that the aircraft rotational excursions are isolated from the pointing portion of the telescope assembly, and the telescope remains fixed in inertial space while the aircraft moves around the telescope.

The Rotation Drive Assembly is a spherical linear torque motor for positioning of the telescope. It consists of Coarse and Fine Drive Systems with brakes. The assembly is caged during flight below 35,000 ft. because of expected high aircraft loads from turbulence.

Compensation is required for the structural bending of the Nasmyth tube. This is accomplished through flexible body compensation, which is used to counter the quasi-static Nasmyth tube bending during turbulent flight conditions, and to counter the effects of aero-acoustic excitation. Low frequency compensation is accomplished with the fine drive torque motors, while high frequency tube bending motions caused by aero-acoustic excitation are controlled by steering the secondary mirror mechanism, which has a fast tilt and chop capability.

6.2 SOFIA Cavity Design Process (Project Solution and Technical Assessment)

This section provides a summary of results obtained from the project in three general areas; aero-acoustic analysis/wind tunnel tests, structural integrity and the approach to flight test. The aero-acoustic analysis/wind tunnel tests (Section 6.2.1) focuses on the approach taken to design and validate the aft fuselage cavity acoustic environment. The structural integrity section (Section 6.2.2) examines the effect of acoustic resonances on the cavity structure in terms of fatigue and DTA. Other technical areas that were affected, such as flutter, the ground vibration test and stability and control, were also considered. The approach to flight test (Section 6.2.3) looks at the steps taken by the project to expand the flight envelope with the cavity door open. Each summary is followed by an evaluation made by the assessment team.

6.2.1 Aero-Acoustic Analysis/Wind Tunnel Tests

The primary objective of early SOFIA aero-related studies was to ensure that the SOFIA cavity was aerodynamically feasible, and to develop a shear layer control concept that provided the quietest cavity environment with minimal impact to the aircraft performance. Wind tunnel testing was used, as the primary tool, to investigate and validate aerodynamic design concepts.

Computational fluid dynamics (CFD) analyses were also performed during the early stages of the wind tunnel testing. However, because of the complexity of the problem, a single configuration required hundreds of Cray supercomputer processing hours to converge on a solution. As a result, wind tunnel testing was relied upon as the primary design tool.

A 7 percent scale model was developed and tested within the ARC 14 ft wind tunnel. A series of tests were completed between 1990 and 1997, prior to the start of final system development. A brief description of each test is given below:

SOFIA I – This was a wind tunnel test of the B-747 fore body section with a partial wing span and a telescope cavity opening located just ahead of the wing root. Concepts of aerodynamic contours required to eliminate cavity resonance were studied.

SOFIA II – The model wing span was extended, an aft section added, and the telescope cavity was moved to the aft fuselage area for this wind tunnel test. This model could be converted from an SP configuration to a 100/200 series B-747 section. The effects on airplane stability and control and candidate cavity aerodynamic treatments were studied. A model of the telescope was placed in the cavity to measure telescope unsteady torque.

SOFIA III – This was a 747SP configuration only. This test series included a cavity with a telescope tube type structure holding the secondary optics and a truss type telescope. Some aspects of a potential cavity door design were also tested.

SOFIA IV – This test series evaluated the cavity door system, using a shear layer design, and its ability to produce a benign cavity environment. Pressures were measured at 20, 40, and 60 degree telescope elevation angles. After proving feasibility, with respect to the cavity environment/acoustic issues, these tests were further used to derive and optimize cavity door and aperture shear layer control design concepts.

SOFIA V – A fifth wind tunnel test series was conducted with the 7 percent model after final flight hardware development was underway to measure the cavity environment and the telescope disturbances, using scaled model implementations of the actual designs, of both the cavity door system and the telescope configuration.[2] Kulite pressure transducers were put on the cavity forward and aft bulkheads and on the telescope structure. The design was tested over a Mach

[2] McIntyre, M. J. *SOFIA V Wind Tunnel Test Report, Telescope Loads and Cavity Aero-acoustics*. NASA Ames Research Center, Moffett Field, CA, Document number 05-N-19980423-001, April 23, 1998.
Rose, W.C. "SOFIA V Design Validation Test Final Report", NASA Ames Research Center, Moffett Field, CA, Document number 05-N-19980415 - 001, April 15, 1998.

number range of 0.78 to 0.86. The TA was modeled geometrically but not dynamically. This was a geometrically accurate wind tunnel model and only addressed the cavity acoustics. Figure 6.2.1-1 shows the wind tunnel model TA cavity.

Figure 6.2.1-1. Seven Percent Wind Tunnel Model Telescope Assembly Cavity

In addition to the 7 percent scale tests, wind tunnel tests were performed on a 3 percent scale model of the SOFIA configuration.[3] The aperture treatment for that model was based on the final design from the 7 percent scale tests. The primary objective of the 3 percent tests was to examine the effects of the cavity on the stability and control of the SOFIA aircraft. The cavity on this model was also instrumented with unsteady pressure transducers (on the forward and aft bulkheads). Acoustic data collected from these sensors was compared to the 7 percent model test data.

Extensive wind tunnel tests were performed on the 7 percent scale model to determine the robustness of the aperture treatment to a range of flow conditions. This assessment was made with unsteady pressure transducers located inside the cavity on the fore and aft bulkheads. The nominal cruise condition for observation with the SOFIA telescope is Mach 0.85, angle of attack equal to 2.5 degrees, 0 degrees sideslip, and a T/A elevation angle of 40 degrees. At cruise Mach number, no change in the overall sound pressure levels (SPL) was observed for a +/- 3 degree change in the sideslip angle. For T/A elevation angles ranging from 20 to 60 degrees and sideslip angles of +/- 3 degrees, no significant change in the overall SPL was observed. As angle of attack was varied from 2 to 3 degrees, no significant change in the overall SPL occurred. Finally, a Mach number sweep revealed a decreasing overall SPL with decreasing Mach number for a range of sideslip angles (+/- 3 degrees) and T/A elevations (20 to 60 degrees). Power spectral density (PSD) plots of unsteady pressures within the cavity for a range of Mach numbers (0.4 to 0.88) do not exhibit any strong resonant conditions.[4]

6.2.1.1 Assessment of Aero-Acoustic Analysis/Wind Tunnel Tests

Flight of the SOFIA aircraft, with no aperture treatment, such as a cavity leading edge fence or aft ramp, would not be possible due to the resulting large-amplitude acoustic resonance. Therefore, some form of flow control or flow management is necessary to mitigate or suppress the cavity resonance. The SOFIA program selected a trailing-edge ramp geometry for control of cavity resonance.

Industry practice of designing cavity treatment, through the use of wind tunnel testing of rigid

[3] Rose, J. A. "Wind Tunnel Test Report for the Stratospheric Observatory for Infrared Astronomy (SOFIA) Program." Raytheon Systems Company Technical Report, Sept., 21, 2000.
Rose, W. C. *Synopsis of Low-speed Wind Tunnel Test Report*. NASA Ames Research Center, Moffett Field, CA, Document number 05-N-19980930-001, September 30, 1998.
_____. *Synopsis of High-speed Wind Tunnel Test Report*. NASA Ames Research Center, Moffett Field, CA, Document number 05-N-19981118-001, November 18, 1998.

[4] McIntyre, M. J. *SOFIA V Wind Tunnel Test Report, Telescope Loads and Cavity Aero-acoustics*. NASA Ames Research Center, Moffett Field, CA, Document number 05-N-19980423-001, April 23, 1998.

models, was followed by the project to design an aperture treatment for flow control to suppress telescope cavity resonances. The ramp design was carried out through a series of five wind tunnel tests (SOFIA I to SOFIA V) on a 7 percent scale model of the B-747SP. The final design was a 30 degree ramp with a semi-circular geometry in the spanwise direction and a rounded leading edge. The three dimensional aft ramp was selected, because the flow approaching the front edge of the cavity was not orthogonal. This design was developed, first for the forward fuselage cavity configuration, and the same design concept was used when the cavity was moved to the aft fuselage. The aft corner fillets appear to provide robustness for a flow condition that is angular over the opening. This results in a weaker acoustic feedback and an overall reduction in the amplitude of the acoustic resonance.

An examination of the 3 percent scale model wind tunnel PSD data for a range of Mach numbers and T/A elevations reveals an uncontrolled resonance in the cavity. Comparing PSD data at cruise conditions for the 3 percent and 7 percent models indicates similar frequency content and therefore it can be said that the essential physics is the same. In the 3 percent model PSD data, however, a resonant tone at 47 Hz is approximately 20 dB above the PSD level for the 7 percent model. Essentially, the 3 percent model aperture treatment (ramp) is failing to provide suppression of cavity resonance. In addition, the PSD data for the 3 percent model were found to be strongly dependent on the T/A elevation. Finally, the PSD data for the 3 percent model displayed a strong dependence on the Mach number. Uncontrolled levels of cavity resonance occur over a wide Mach number range with tone frequencies that vary with Mach number. This behavior is characteristic of an uncontrolled cavity flow. In contrast, the cavity pressure PSD data for the 7 percent model display very little dependence on Mach number.[5]

The 7 percent model is a better representation of the full-scale airplane. During flight testing of the baseline SOFIA aircraft (prior to modifications), measurements of the fuselage boundary layer at the aperture location were made. Using that data, appropriate boundary-layer trips were selected for the 7 percent model to match the scaled boundary layer to that in flight. This is critical because cavity resonance is highly dependent on the state of the incoming boundary layer. In the 3 percent model tests, Boeing "trip dots" were used to trip the boundary layer. These trips were designed to match the overall characteristics of the model to flight data, but do not address particular boundary-layer characteristics. The resulting boundary layer on the 3 percent model is too thin relative to that expected in flight. Thinner boundary layers (relative to the cavity depth) are known to result in higher amplitude cavity tones. Progressively thicker boundary layers reduce the amplitude of the cavity resonance. Since the boundary layer on the 3 percent model was not properly scaled, the acoustic data from that test should be viewed with caution.

[5] McIntyre, M. J. *Comparison of NASA and RSC Wind Tunnel Test Results*. NASA Ames Research Center, Moffett Field, CA, Document number 02-N-20000616-001, June 16, 2000.

Wind tunnel tests of the 7 percent scale model were conducted with and without the TA present in the cavity and the results showed that the cavity SPLs were slightly lower when the TA was present.[6] The amplitudes of the pressure fluctuations in the cavity of the SOFIA airplane should be lower than observed during wind tunnel tests due to the damping effect of the flexible cavity wall structure (Appendix C) that were not represented in the wind tunnel models and the lack of pressure spatial coherence over the large cavity area.

Limited wind tunnel testing was accomplished for the cavity door failed opened configuration and as a result there are still uncertainties whether an uncontrolled cavity resonance will occur under these conditions.[7] Wind tunnel results from the 7 percent scale wind tunnel model indicate that the cavity door in the 25 percent and 75 percent open positions produced SPLs within 2dB of the door fully open level. The 3 percent scale wind tunnel model acquired data over the entire Mach number range from cruise altitude, through descent, to landing with the door in the full open configuration, and exhibited cavity acoustic resonances. However, due to the boundary layer scale issue, it is not certain that these results reflect the conditions that will be present during flight. Ultimately, the uncertainties of the effect of a partial door opening will become known and resolved during the flight test phase. Preliminary flight test plans (Appendix F) provide for a conservative build-up approach to opening the cavity door. Extensive instrumentation for monitoring SPLs, accelerations, and strains in addition to tufting, with monitoring, of the internal cavity and the surrounding external structure including the empennage is needed to measure and understand the acoustic environment during flight.

Scaling of model frequencies to flight conditions is based on a Strouhal number (St = fU/L). The 3 percent and 7 percent model data at cruise conditions suggest that this is an appropriate scaling. Experience with weapons bay cavities also indicates that the Strouhal number is the appropriate scaling parameter for comparing model and flight data. Unsteady pressure amplitudes are scaled with the freestream dynamic pressure.

If the SOFIA aircraft exhibits uncontrolled cavity resonance during initial flight testing, several contingency plans have been set forth to mitigate the problem. SOFIA III wind-tunnel tests considered the use of foam linings on the cavity walls. This approach resulted in a lower overall SPL by only 2 dB so it is not likely to be a fix. In SOFIA IV, leading edge fence devices/spoilers were considered. These devices shifted the frequency content in the cavity and

[6] Rose, W. C. *SOFIA-Telescope Torque Wind Tunnel Test, SOFIA III Final Report.* Incline Village, NV: Rose Engineering & Research, Inc., 31 March 1995.
[7] Rose, W. C. *SOFIA-Conceptual Door Design and Aero-Optics Wind Tunnel Test, SOFIA IV Final Report.* Incline Village, NV: Rose Engineering & Research, Inc., 31 March 1996.

lowered the overall SPL. Leading-edge devices tend to thicken the incoming boundary layer and modify the stability characteristics of the cavity shear layer. The thicker boundary layer typically results in a reduction in the unsteady cavity pressures. A drawback of these devices is that they increase aircraft drag, and therefore, reduce the observation time per flight. They also result in a degradation in aero-optical performance. If a leading-edge device is required to mitigate an uncontrolled resonance, it is likely that additional wind tunnel testing will be needed to optimize the geometry.

6.2.2 Structural Integrity

The assessment team focused its efforts on the structural modification in Section 46 of the airplane (Figure 6.2.2-1), in particular on the effects of the acoustics on the cavity structure. This area contained the new forward bulkhead head (a pressure bulkhead), the supporting structure for the telescope, the telescope assembly, the new aft bulkhead, the cavity shear layer control device, and the cavity door system.

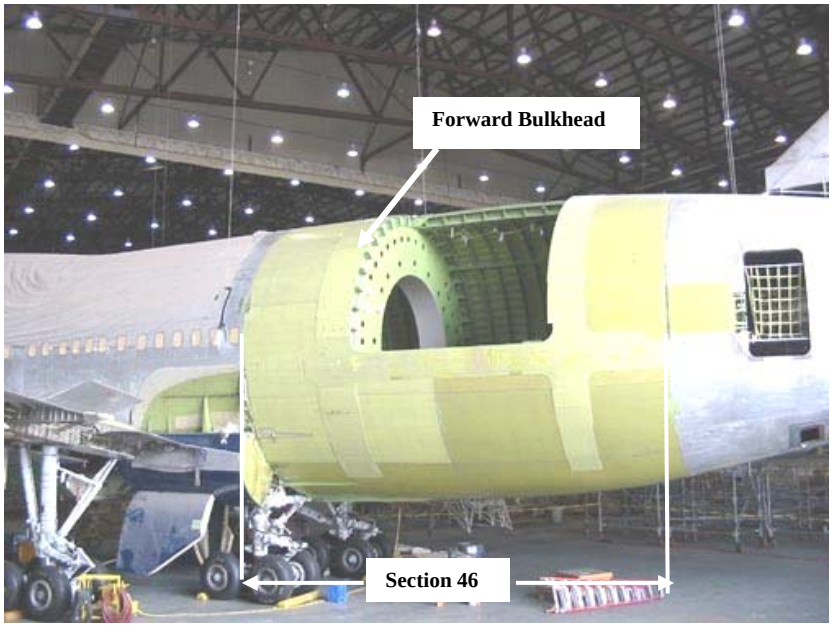

Figure 6.2.2.-1 Section 46 Structure of the SOFIA Airplane.

The process that the project followed to verify structural life assurance is depicted in the flow diagram shown in Figure 6.2.2.-2. The blocks shaded yellow on the diagram show where the assessment team focused its evaluation of the project's assessment of the cavity acoustic effects on the surrounding structure. Areas specifically not evaluated were the acoustic effects on the structure due to the jet engine noise, and airframe boundary layer noise. It should be noted that much of the cavity door open fatigue and damage tolerance assessment work was in a preliminary stage and not complete.

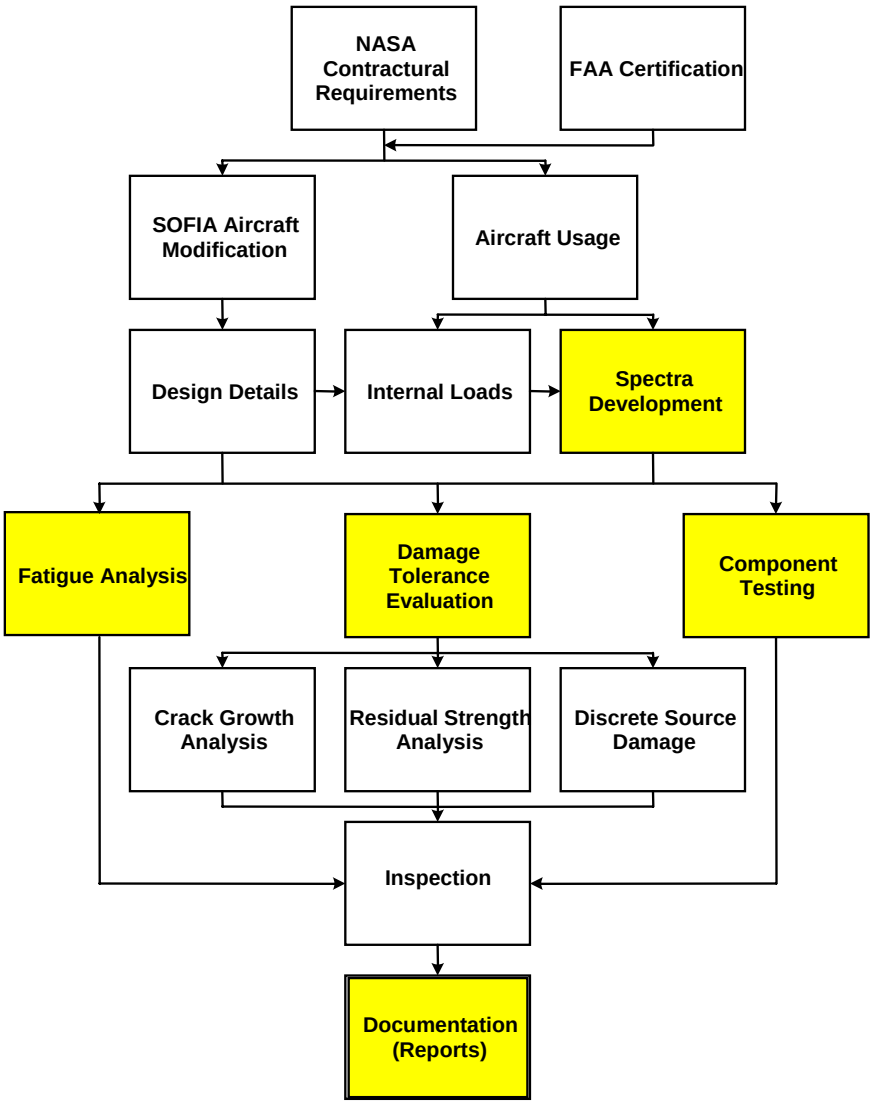

Figure 6.2.2-2. Structural Life Assurance Process Diagram.

6.2.2.1 Spectra Development

Wind tunnel fluctuating cavity pressure data from the 3 percent scale model wind tunnel tests were used as the input forcing spectra for the cavity structure. These data were taken from low and transonic speed wind tunnel tests, and envelope the overall broadband noise as well as discrete tones generated by cavity resonance or vortex shedding from the leading edge of the

cavity. These envelopes were used to assess the effect of the cavity aeroacoustics on the surrounding cavity structure, during telescope operation at cruise flight conditions, and for emergency descent with the door partially open.

Three cavity fluctuation pressure environment envelopes are shown in Figure 6.2.2-3 for the cavity door open cruise flight condition. One envelope is defined in the SOFIA Systems Interface Requirements Specification SOF-1030, one is a response curve of the maximum cavity pressures levels measured in the 3% scale wind tunnel test at a Mach number of 0.85, and one envelope is a curve defining the SOFIA door fully open cruise operating envelope.[8] The SOFIA operating envelope shown in the figure encloses the wind tunnel data. In the lower frequency range (0.5 Hz to approximately 9.0 Hz), the SOFIA operating envelope overlays the envelope specified in SOF-1030. The operating envelope spectrum was the fluctuating pressure environment data used in the acoustic fatigue analysis and represents a worse case environment for long term fatigue over the life of the airplane at normal cruise flight conditions. This data is used with the Miles equation.[9]

[8] *Stratospheric Observatory for Infrared Astronomy (SOFIA) Systems Interface Requirements Specification SOF-1030*. Moffett Field, CA: National Aeronautics and Space Administration Ames Research Center, Original Issue August 1988, Revision 4 June. 2001.

[9] Miles, John. "On Structural Fatigue Under Random Loading." *Journal of the Aeronautical Sciences* (November 1954).

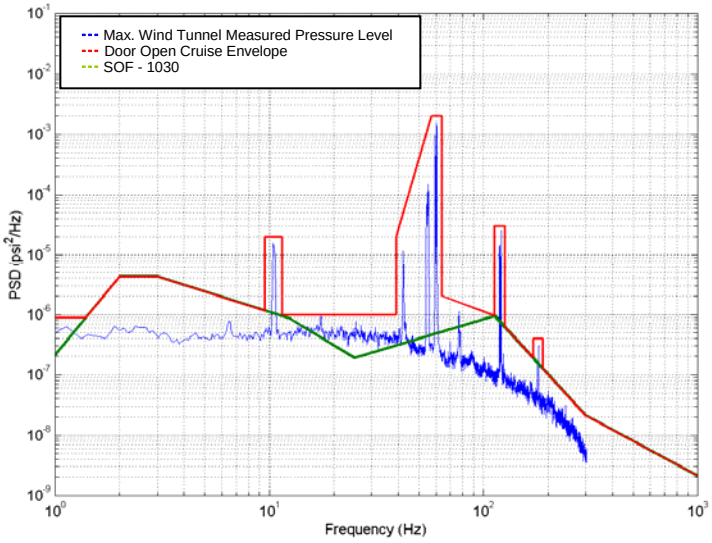

Figure 6.2.2-3. Cavity Fluctuating Pressure Environment for the Cruise Flight Condition.

Three cavity fluctuating pressure environment envelopes are shown in Figure 6.2.2-4 for the failed cavity door open descent condition. One envelope is defined in the SOFIA Systems Interface Requirements Specification SOF-1030, one is a pressure response curve for Mach numbers of 0.2, 0.4 and 0.6 (which were measured in the 3% scale wind tunnel test), and a SOFIA operating envelope, which encloses the wind tunnel data.[10] The wind tunnel data represents off-nominal observation flight conditions that the airplane would be exposed to in a descent if the cavity door failed to close. The door failed operation envelope shown in the figure encloses the wind tunnel data and has a higher amplitude than either wind tunnel or SOF-1030 requirement levels. The door failed open operating envelope spectrum has higher levels of fluctuating pressure in the cavity due to the expected higher dynamic pressures that would be experience during descent and represents a worse case environment.

[10] *Stratospheric Observatory for Infrared Astronomy (SOFIA) Systems Interface Requirements Specification SOF-1030*. Moffett Field, CA: National Aeronautics and Space Administration Ames Research Center, Original Issue August 1988, Revision 4 June. 2001.

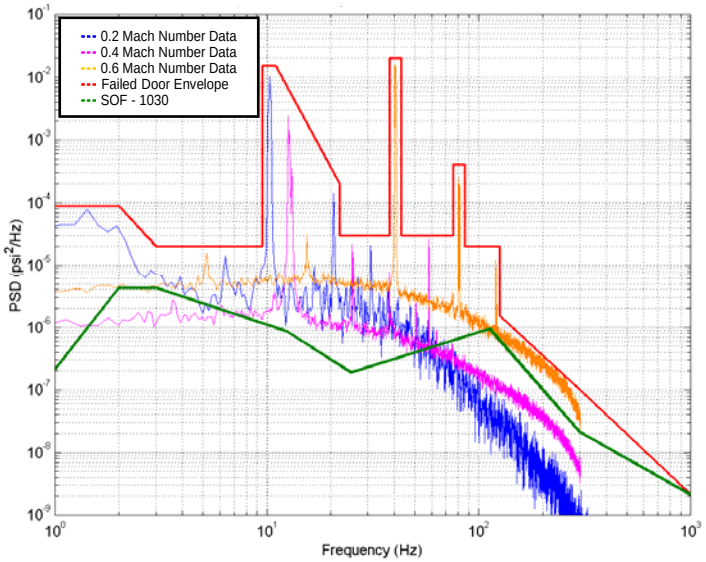

Figure 6.2.2-4. Cavity Fluctuating Pressure Environment for the Door Failed-Open Descent Condition.

The 3 percent scale wind tunnel data exhibited large amplitude peaks and uncontrolled acoustic resonances that were not present in the 7 percent scale wind tunnel data. As an example, PSD data for the cruise flight condition indicated that the acoustic response at 47 Hz for the 3 percent model was 20dB greater than the 7 percent model at the same frequency. In addition, it is important to note that the reduction in fluctuating pressure load within the cavity that results from the lack of spatial coherence and damping that is provided by the flexibility of the cavity structure was not taken into account. Therefore, the input spectra used for fatigue calculation was considered conservative.

The PSD envelope for the exterior environment, which included engine and boundary layer acoustics is shown in Figure 6.2.2-5. This PSD envelope was summed with the PSD envelope of the fluctuating pressures in the open cavity (Figures 6.2.2-3 and 6.2.2-4) to create a PSD fluctuating pressure envelope for the fuselage skin panels.

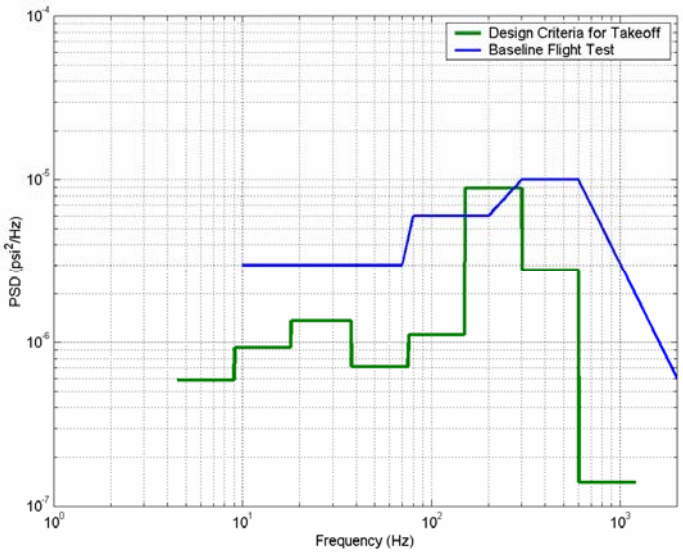

Figure 6.2.2-5. PSD Envelope for Engine and Boundary Layer Noise.

6.2.2.2 Fatigue

The following methodology was followed to determine the fatigue life of the forward bulkhead, the side fuselage panels, and the aft bulkhead:

1. Calculate the resonant frequencies of the structure.

2. Integrate the fluctuating pressure PSD curves defined by the envelope encompassing the measured wind tunnel data and then apply to the fundamental resonant frequency of the structure being analyzed.

3. Calculate the root mean square stress of the structure.

4. Calculate cycles to failure at a given stress level from S/N curves to determine fatigue life.[11]

5. Assess acoustic fatigue life by calculating the total number of hours to failure based on mission profiles.

[11] *Metallic Material and Elements for Aerospace Vehicle Structures*. MIL-HDBK-J1, 31 January, 2003.

The project established a short term fatigue life requirement for the condition when the airplane must descend from its observation cruising altitude with the cavity URD failed in a position from partially to full open. The requirement was established for a design life of 80 minutes, with a safety factor of four on life (yielding 20 minutes flight life), which was representative of the flight time required to perform a descent for a cruising altitude of 40,000 ft. The philosophy was to provide a finite structural life, which ensured a safe operation during flight testing should a cavity resonance occur during a descent with the cavity URD partially open.

6.2.2.2.1 Cavity Forward Bulkhead Structure

For the forward bulkhead (Figure 6.2.2-6), fatigue of the unit as well as individual panels (shaded) between stiffeners was considered. Acoustic fatigue was considered for the cruise flight and the failed door descent cavity fluctuating spectra.

Data presented at the Critical Design Review (CDR) indicated that the largest bulkhead panel has a resonant frequency of 401 Hz. This frequency is well above the cavity fluctuating pressures defined in either spectra envelope. Consequently, acoustic fatigue was considered negligible.

The fundamental resonant frequency of the built-up bulkhead structure, with the telescope assembly isolated and off of the hard-stops, is 66 Hz which is the cruise configuration with the cavity door open. The project has stated that the bulkhead assembly has sufficient acoustical fatigue life.

The bulkhead resonant frequency decreases to 14 Hz, with the telescope against the hard-stops which is the configuration planned for the cavity door failed open descent. The project has stated that the bulkhead assembly has sufficient acoustical fatigue life for the door failed open descent condition.

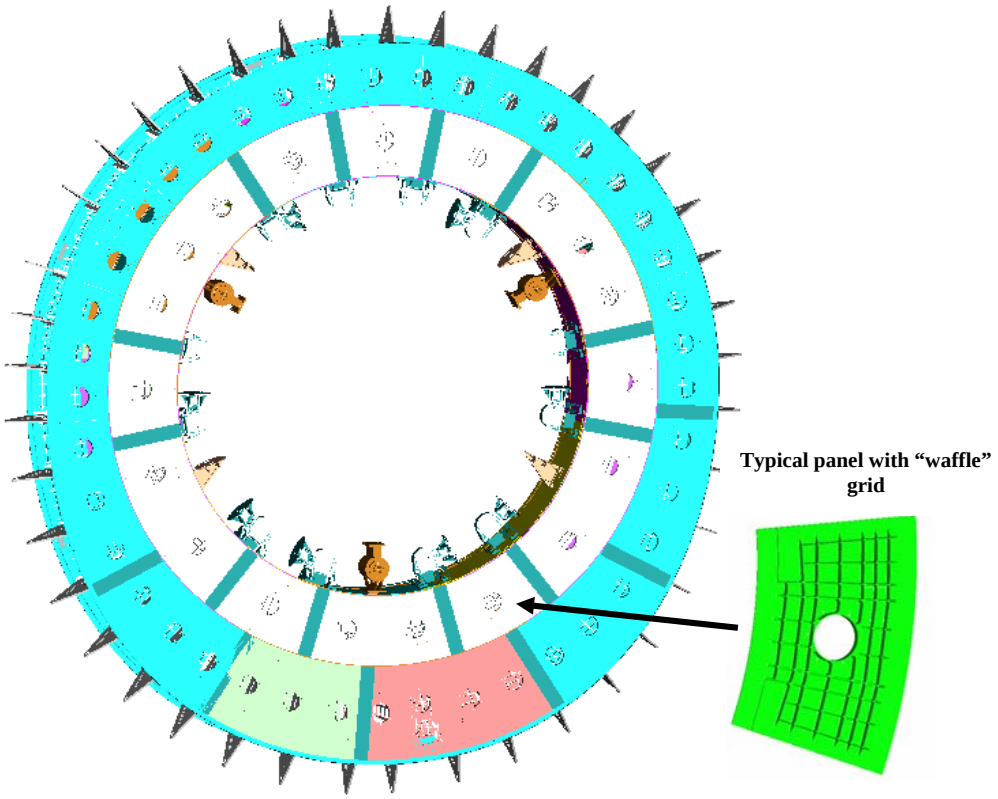

Figure 6.2.2-6. Forward Bulkhead Assembly

6.2.2.2.2 Cavity Aft Bulkhead

For the cavity aft bulkhead (Figure 6.2.2-7), fatigue of the unit as well as of individual panels between stiffeners was considered. The shaded panels in Figure 6.2.2-7 were representative panels chosen for analysis. Typical panels are 8 in. by 11 in., while the radial panels are smaller and have higher resonant frequencies. Data presented at the CDR showed that all resonant frequencies are greater than 150 Hz and acoustic fatigue was considered to be negligible, since the fluctuating pressure levels in the cavity for either the cruise or the door failed-open flight condition have a low amplitude at frequencies greater than 150 Hz.

A preliminary acoustic fatigue analysis of the aft bulkhead as a unit was performed by the project.[12] A simplified method of applying the loads from the power spectrum density (PSD) curves and generating stress output was adopted to relate the stress on an equivalent flat plate (which simulated the stiffness of the aft bulkhead) under a 1 psi load to the final magnified dynamic stress. A damping level of 1 percent was assumed in the analysis. The fundamental resonant frequency of 28 Hz was calculated. The project has stated that sufficient acoustic fatigue life has been predicted at this resonant frequency.

The bulkhead frequency and damping will be measured during the ground vibration test as well as in flight. These data will be used to update the analysis.

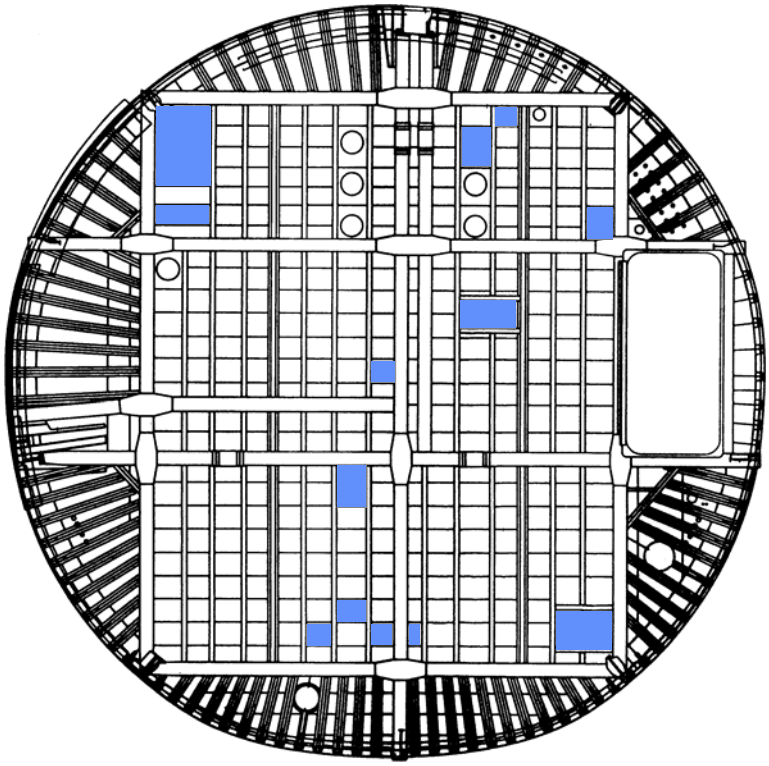

Figure 6.2.2-7. Aft Bulkhead Assembly, Looking Forward.

[12] Matthews, L.S. *Vibroacoustic Assessment of SOFIA's Aft Bulkhead*. Rep No. LDG-00-004-SDS, Raytheon Systems Company, March, 2000.

6.2.2.2.3 Fuselage Side Panels

Selected panels were chosen for analysis for the sides of the fuselage. Typical panel dimensions are 20 in. long and 7-9 in. wide. The right side fuselage panels which were selected (shaded) are shown in Figure 6.2.2-8. Panel thickness is indicated for each bay on the figure. Thickness increases required for static strength resulted in high fundamental resonant frequencies which provided for longer acoustic fatigue life for each panel. Panels on the left side of the fuselage were similarly selected.

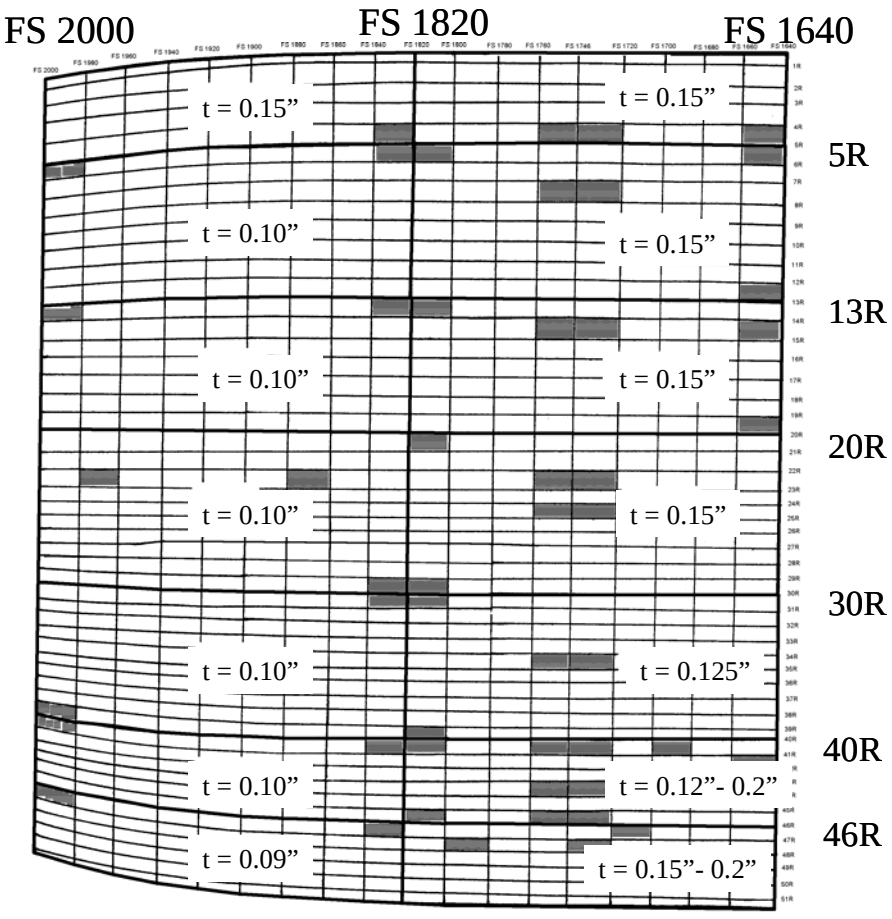

Figure 6.2.2-8. Right Side Fuselage Panels.

6.2.2.2.4 Telescope Assembly

Stress levels that result from the aero-acoustic loads has been a concern particularly during a descent of the aircraft with the cavity door failed in a partially open position. An analytical assessment was performed using the aero-acoustic pressures represented by the 3-sigma equivalent aero-acoustic forces applied as static forces and then additionally scaled with an assumed dynamic amplification factor of 25.[13] The results indicate that the highest telescope stresses are approximately 40 percent less that the stresses calculate for the worst-case proof of strength analysis. Worst-case margin of safety, was calculated to be 1.95. Since the stress levels were so low, there was not a concern from a fatigue perspective.

6.2.2.2.5 Cavity Door/Shear Layer Control Device

Two different methods were used to determine the dynamic response of the URD, LFD, and Shear Layer Control Device to the fluctuating pressure input spectra defined in section 6.2.2.1. The "Peak Shift" method was used in cases where the aircraft velocity was changing and the cavity door was failed open. The "Random Only" method was used in cases where the airplane velocity was constant and the cavity door was open for viewing.[14]

The "Peak Shift" method consisted of integrating the individual wind tunnel pressure PSD data to get the total energy in the spectrum and then calculating the RMS pressure. The pressure is then scaled to account for proper dynamic pressure, and then applied as a harmonic, spatially coherent pressure at each structure natural frequency below 100 Hz. Damping was assumed to be a constant 2 percent. Any mode with a computed strain above 25 percent of the maximum allowable was considered an active mode, and used for the final frequency response in each load case. The maximum total force (inertial and applied) was determined for the entire structure through an entire half cycle of applied load. This result was then used to determine the fatigue life, as outlined in an earlier section.

For the "Random Only" method, applicable wind tunnel pressure PSD data were applied as random load inputs, without being applied at a specific frequency. The appropriate fluctuating pressure PSD was converted according to the Miles' equation, to a magnified quasi-static pressure in both the positive and negative directions, which is combined with other static loads to

[13] Honaker, Michael, "Preliminary Assessment of Stress Levels in the TA Due to Aero-Acoustic Loads and 1 G Gravity Effects", SOFIA project Technical Note TN-MAH-013, August 10, 2000.

[14] Ospring, M. J. "SOFIA Dynamic Analysis Procedures, Revision B", SOFIA Project Memo for the Record, December 21, 2002.

_____. "SOFIA Cavity Door Analysis Procedures", SOFIA Project Memo for the Record, October 3, 2003.

produce peak and alternating loads and stresses. Damping was assumed to be a constant 2 percent. The distribution of this pressure is assumed to be normal, and therefore, assumed to have a one sigma probability of exceedance. The pressure is applied to all cavity exposed surfaces as a static load and then it is combined (positive and negative) with other loads to get peak and range values.

Should a failure in the door drive mechanism occur, requiring SOFIA to land with the door in an open position, a design criterion for the worst-case loading situation (cavity resonant type of behavior) was considered. To be conservative, it was assumed that the frequency of the resonant behavior was equal to the URD fundamental mode, and that the pressure loading profile was completely coherent with the mode shape. For this loading condition, the structure of the URD was designed for a total design life of 80 minutes with a safety factor of four on life (yielding 20 minutes flight life).

Flight data will be acquired during the flight test phase which will provide the actual loading profile and door response. As an additional measure of safety, a mass damper can be installed, if needed, on the URD for the initial flight tests to damp out the door response.

Structural proof tests of the URD, LFD, Shear Layer Control Device, and critical subassemblies have been completed. In addition, modal testing of the URD and LFD has taken place in which component structural frequencies, damping values, and mode shapes have been measured. These data were used to validate analytical models.

6.2.2.3 Damage Tolerance Assessment and Component Testing

The DTA is to be performed after the initial flight tests, but before FAA certification. DTA typically includes the assessment of the number of cycles required for a given inspectable crack to grow to critical proportions, calculating residual strength at critical stress riser locations, and performing discrete damage event analyses.

A draft Fatigue and Damage Tolerance Component Test Plan has been published by the project.[15] The project is to perform DTA and the analysis is to be validated by means of four structural component tests. Two components are new structural detail design parts, the forward bulkhead lug, the forward bulkhead fore and aft pressure panels. The other two components are representative details of the new structure, namely, fuselage skin splices. These components were selected for validation of the analytical methods only and not based on the criticality of the structure.

[15] Lee et al. *Fatigue and Damage Tolerance Component Test Plan for the SOFIA 747SP*. Raytheon Aircraft Integration Systems, Doc. No. 96188003-002, 2001.

There are three types of tests planned for each cavity structural component: fatigue tests, crack growth analysis tests, and residual strength tests. Fatigue test loads will be applied until fatigue cracking initiates or for a minimum of two lifetimes (one lifetime is defined as 40,000 flight hours or approximately 4500 flights). Fatigue loading will be applied as a flight-by-flight and cycle-by-cycle spectrum loading. Crack growth testing will be performed to validate crack growth analytical methodology by measuring crack growth rates. The loading will be similar to the fatigue spectrum loading. Residual strength testing will be performed to determine the residual strength of the structural component at the end of the crack growth testing. The test spectrum for each component will be a randomized, flight-by-flight spectrum, generated using an in-house spectrum generation program and the SOFIA airplane mission utilization. The loading spectra are developed from external loads and the effects of internal cabin pressure. Acoustic loads are incorporated into these tests through the acquisition of flight data. Test component instrumentation is placed in the same location as the actual flight hardware. Loading sequence will be in the form of cyclic, flight-by-flight, generated in maximum-minimum end-point format.

6.2.2.4 Technical Assessment of Structural Integrity

Preliminary fatigue analyses have been accomplished on the cavity structural components. The philosophy is to acquire flight test data which will be used to update the fatigue analyses during the flight test phase of the project. There were no numerical values of structural fatigue life presented in any of the documents reviewed by the assessment team. Much of the detailed fatigue and damage tolerance assessment for the cavity door open configuration is on hold, including documentation, due to a focus on flying the airplane with the cavity door closed. Consequently, the assessment team could not perform an in-depth review in this area.

Of most concern to the assessment team was the acoustic fatigue life, with the cavity door open for observation flight and the cavity door failed in an open position during descent from 40,000 ft. The 3 percent scale wind tunnel data was used as input spectra because these data are assumed to have conservatively large magnitudes in comparison with the 7 percent scale data. However, as noted earlier in this report, the 3 percent model is not the best representation for the cavity acoustics and acoustic response data may be overly conservative. There is additional conservatism as a result of assuming full cavity spatial coherence and not incorporating the flexibility effects of the cavity wall structure in the acoustic response. There is essentially no wind tunnel data, either 3 percent or 7 percent, with the cavity door in a partially open position.

6.2.2.4.1 Fatigue Life Calculation at The Structural Fundamental Frequency

The project assumed that the structural components will have the shortest fatigue life at their fundamental frequency. Typically, there are three ways that components fail due to fatigue at constant amplitude as presented in literature:

1. The first method is applying certain stress amplitude and allowing it to break after certain number of cycles.
2. The second method is applying certain strain-amplitude and allowing it to break after a certain number of cycles.
3. The third method of fatigue failure – a component is subjected to variable amplitude loads – here the stress/strain history is monitored and the number of cycles is counted and fatigue life expended (or remaining fatigue life) is calculated.[16]

The project adopted a procedure where the fatigue life is calculated for a single degree of freedom system under random loadings.[17] These references describe how the input PSD, when matched in frequency to a structure resonance, can result in very high response and short fatigue life. It has been shown that the response of the structure is the important parameter, and the response is maximized when the input energy is focused where structural response is relatively high (at fundamental or higher frequencies). The basic reason for this is that when the cyclic stresses are high, fatigue damage is prevalent. Although fatigue may certainly occur at any frequency due to forced vibration, such as the acoustic loadings PSD, it is common for resonance of the structure to magnify the response and result in problems. It was noted that such issues were encountered in practice in several wind tunnel facilities. Mitigative measures used in those cases include using control algorithms to avoid operation at the first five natural frequencies of the wind tunnel components.

The team concluded that although high displacements result at the first fundamental frequency, it is possible that higher stresses occur at higher resonant frequencies due to greater mode shape deformation slopes. Consideration should be given for the inclusion of higher frequency modes to ensure that this approach is conservative.

[16] Metallic Materials and Elements for Aerospace Vehicle Structures. MIL-HDBK-5J, 31 January, 2003.
[17] Ospring, M.J., and Harry Gobler. *Dynamic Analysis Using Power Spectral Density.* Project Memo for the Record, December, 1983.
Steinberg, David. *Designing Electronic Equipment for Random Vibration*. Seminar Handout, 1983.
Thompson, W.T. *Theory of Vibrations with Applications*. 5th Ed. Prentice-Hall, 1965.

6.2.2.4.2 Aft Cavity Bulkhead Fatigue Life Calculation

A preliminary acoustic fatigue analysis of the aft bulkhead was performed.[18] A simplified method of applying the loads from the input spectra PSD curves and generating the stress output on an equivalent flat plate (which simulated the stiffness of the aft bulkhead) was adopted. One of the reference equations in the analysis (labeled as "random") is the standard Miles equation which is commonly used to approximate the response of a single degree of freedom oscillator to relatively flat, broad band random vibration input. It is frequently used in the calculation of sonic fatigue. The other equation (labeled "sin") is not in a standard form, and could not be verified in any reference. The difference between these two algorithms was evaluated.[19] In summary, calculations of peak structural response using the Miles equation are sensitive to the input load. The verified form of this equation is the "random" algorithm and it is only intended for use when the input PSD has a very flat, broad nature. In the case under consideration, the envelope PSD is not flat and the standard form for the Miles equation has not been used. As a result, the calculation of dynamic response of the rear bulkhead is possibly unconservative. The project needs to provide further verification of the non standard form to ensure that it is appropriate to use for the aft bulkhead fatigue life calculation.

6.2.2.4.3 Crack Growth

The acoustic fatigue analysis, performed to date, used the classic "safe life" approach which does not take existing cracks in the structure into account. The approach cannot assure that a small crack near a rivet hole within the cavity structural components, will not reach critical unsafe proportions during the flight test phase of the program. To mitigate this possibility, an inspection of critical structure should be performed on each open door before flight. If cracks are found, DTA analyses should be performed to insure that the growth of the crack remains below critical length for the planned duration of the next flight.

There are always some cracks present near holes, joints, etc. That is the basic assumption that the Federal Aviation Administration (FAA), NASA, the United States Air Force, and to a limited extent Navy and Army, aircraft fatigue and fracture methodology assume (i.e. Damage Tolerance). The question needs to be addressed as to how these cracks behave as the airplane undergoes various phases of flight testing, with the uncertainties of the structural-acoustic coupled loads due to the SOFIA's cavity configuration. One way to address, assess, and mitigate such risks is a conservative build-up approach during the door open flight testing phase. Strain

[18] Matthews, L.S. *Vibroacoustic Assessment of SOFIA's Aft Bulkhead*. Rep No. LDG-00-004-SDS, Raytheon Systems Company, March, 2000.
[19] Ospring, M. J. "SOFIA Dynamic Analysis Procedures, Revision B", SOFIA Project Memo for the Record, December 21, 2002.

histories at the critical stress locations, and loads, due to acoustical coupling, should be monitored, in addition to the inspection for cracks at critical locations. This information would be used to perform incremental DTA to assure structural integrity during the flight test program.

6.2.2.4.4 Damage Tolerance Assessment

Damage tolerance assessments are best carried out by representative tests on full-scale structure. Since this would be economically unfeasible, a large amount of reliance must be based on analysis. This is the case with the SOFIA project, and the project is conducting sufficient component testing to validate all analysis methods.

6.2.2.4.5 Structural Integrity Of The Structure Surrounding the Cavity Opening

In the SOFIA V wind tunnel design validation test (a 7 percent scale model), steady-state pressures were measured around and downstream of the cavity aperture.[20] From this data, static-load specifications were formed for the aperture ramp, aperture fairing, partial external door assembly, and surround fuselage. Static pressures on the aft fairing and downstream fuselage indicated the possibility of sonic or supersonic flow. This could set the stage for unsteady shock buffeting in this region and additional drag on the aircraft. It was strongly suggested, in the report, that the tested aft fairing be modified, in the final design, to reduce the local Mach number by reducing the local curvature of the fairing surfaces. The project has stated that this design change was made but was never validated in any subsequent wind tunnel tests.

Unsteady pressures were also measured around and downstream of the cavity opening as well as on the door. It was found that the overall SPL on the fuselage downstream of the cavity was on the order of 3-5 dB greater than the closed-door levels. It was suggested in the SOFIA V design validation test report that the increased levels be taken into account in the structural design and fatigue-life calculations.[21] The report also provided conservative unsteady load levels on the ramp, fairings, and fuselage surrounding the cavity opening to be used in structural design. It could not be determined if these load levels were used in the design. Results of design and fatigue life calculations accounting for these increased load levels are required before the open door flight testing begins.

There still remains some uncertainty as to how these load levels will be altered in the instance of an uncontrolled resonance, which has a possibility of occurring in the case where the door fails in a partially opened configuration. There were no analyses available to address this critical

[20] Rose, W. C. "SOFIA V Design Validation Test Final Report", NASA Ames Research Center, Moffett Field, CA, Document number 05-N-19980415 - 001, April 15, 1998.
[21] Ibid.

question. Sufficient analyses are required to understand the magnitude of the load levels, along with a conservative approach to flight test to account for this uncertainty.

6.2.2.5 Airplane Flutter

In the case of the B-747SP, the fuselage is a monocoque type structure, where the primary structural load path elements include the skins, stringers, and frames. Therefore, to create an opening that is about 15 feet long and one fourth of the circumference of the fuselage requires a modification that includes substantial reinforcement of the remaining structure. This structural modification has potential adverse effects on flutter. These effects are predicted through analyses and verified through ground vibration and flight testing.

The project initially did not have a dynamics finite element model to perform either vibration analyses or flutter analyses. A ground vibration test of the baseline airplane was conducted to acquire modal data for verification and tuning of a dynamics finite element model that was eventually created. Flight testing of the baseline B-747SP was accomplished with an excitation system to excite structural modes and accelerometers to measure the structural response. Frequency and damping values were calculated from the flight data for correlation with the flutter analysis. Baseline flutter analyses were performed after the completion of the baseline flight flutter testing.[22] The results calculated were comparable to documented Boeing results.

The same process is being undertaken for the SOFIA airplane. The finite element model has been modified to represent the cut-out in the aft fuselage including changes in fuselage mass and stiffness distribution. A ground vibration test of the SOFIA configuration will be conducted and the dynamics model of the structure will be tuned to match the test data. Final flutter analyses will then be performed followed by flight flutter testing.

The structural mode frequencies that participate in the flutter mechanism of the basic B-747SP are between 2 and 3 Hz. The flutter mechanism involves the antisymmetic first wing bending mode coupling with an engine nacelle lateral mode. There is some aft fuselage torsion motion that is part of the flutter mechanism mode shape. However, the fuselage torsion mode is at a higher frequency, and is not coupled with the other two modes.

Preliminary predictive flutter analyses have been performed for the SOFIA airplane, and the predicted flutter speeds are 5 to 10 knots less that the baseline configuration. These results were for a door-closed configuration and with the telescope assembly in a braked condition (rigid

[22] Martin, E. L., *Baseline Flutter Analysis for the Stratospheric Observatory for Infrared Astronomy (SOFIA) Program*. L3 Communications Document 96186001-001, February 18, 2005.

mount). Springs have been inserted (based on telescope data from Germany) into the analysis to model the telescope in the floating mode to analyze the potential for coupling with the structure. No coupling was noted and the flutter speed did not change. Analyses are also planned for various cavity door openings and telescope elevation angles to determine changes in mass distribution.

The CDR indicated that the aft fuselage stiffness of the SOFIA airplane (vertical, lateral, and torsional) had increased by as much as 20 percent. Recent structural analyses indicate that there is a slight decrease in the vertical and lateral stiffness and the torsional stiffness is the same as the baseline configuration. Currently, consideration is being given to perform flutter analysis that included parametric variations of the aft fuselage stiffness in order to determine the effect of stiffness variation on flutter speed.

Modeling of the unsteady aerodynamics on the aft fuselage cut-out area (door open and closed positions) will not be changed from what was used for the baseline configuration. Rationale for this decision was developed through analyses, which reduced the effects of the aft fuselage unsteady aerodynamic paneling, and the results showed that there was no effect on the flutter mechanism or predicted speed of the airplane.

There are no plans to conduct flutter analysis of the upper rigid door, since is not a load bearing structure. In addition, the likelihood of panel flutter, defined as the self-excited oscillation of the external skin surface, is remote, based on the design and operational speed (subsonic) of the airplane.

6.2.2.5.1 Technical Assessment of Airplane Flutter

The project appropriately created baseline B-747SP analytical models, and validated the models through ground vibration tests and flight tests. Final baseline flutter analysis results have been shown to match Boeing predicted flutter analysis results. The baseline model was modified to represent the SOFIA configuration. The project will validate the SOFIA model with a ground vibration test and verify the absence of flutter through flight flutter testing.

The project is performing a thorough aeroelastic investigation of the SOFIA airplane. The baseline airplane has provided data to validate models and provide an in-depth understanding of the structural dynamics of the airplane.

There are 33 structural modes with a frequency less than 10 Hz. Predicted flutter frequencies are less than 5 Hz. Low amplitude acoustics are always present in the cavity during door-open cruise flight. The acoustic frequencies have been predicted to be above 10 Hz, and are

considerably higher than the basic structural modes of the B-747SP airplane, and cannot couple with the airplane elastic modes to cause flutter.

6.2.2.6 Airplane Ground Vibration Test

A Ground Vibration Test (GVT) of the SOFIA airplane is planned.[23] The primary purpose of the test is to measure the modal characteristics of the modified airplane and then tune the dynamics finite element model used for flutter analysis. Modal data will also be compared to the baseline GVT results to better understand the effects of the structural modifications to the airplane.

The baseline B-747SP dynamics model, used in the baseline flutter analysis, has been correlated/updated with the baseline GVT data. The same process will take place for the SOFIA model, and, if a similar correlation is achieved between SOFIA GVT data and the SOFIA dynamics model, there will be high confidence in the predicted flutter speeds and margins for the SOFIA configuration.

Modal data will be acquired for the cavity (bulkheads and fuselage panels), telescope assembly, and the cavity door system. Current plans call for testing with the telescope in multiple configurations (caged, uncaged, braked, unbraked, different elevation angles, etc), and with the cavity door at various openings. Data from these components will be used for the validation of models used in the acoustic fatigue analysis.

6.2.2.6.1 Technical Assessment of the Airplane Ground Vibration Test

The GVT planned for the SOFIA airplane is adequate to acquire modal data of sufficient resolution and bandwidth to validate the dynamics finite element model used for vibration and flutter analyses. This data will ensure proper representation of the mass and stiffness distribution. The comparison of modal data to the baseline airplane modal data will further the understanding of the effects of the structural modification to the structural dynamics of the airplane.

Acoustic fatigue life of many of the cavity structural components was computed using the resonant frequencies of these components. Measurement of these frequencies during the GVT should be performed to verify that the correct resonant frequency was used in these analyses. It is currently planned to apply direct structural excitation to the aft bulkhead, the URD, the LFD and the Shear Layer Control Device to acquire frequency response functions. There are no plans

[23] Puglise, J. *Observatory Ground Vibration Test Plan for the Stratospheric Observatory for Infrared Astronomy (SOFIA) Program*. L3 Communications Document TP96157011-000, December 15, 2004.

to directly excite the forward bulkhead in the configuration that fatigue analyses were performed (telescope assembly isolated from the bulkhead and off/on the hard stops). Excitation of nearby structure will not provide adequate levels of excitation to this structure. Measurement of the fundamental resonant frequency of the two representative forward bulkhead panels used for fatigue life calculations should also be accomplished.

Acoustic fatigue life of the aft bulkhead was determined by using selected panels from the structure. The resonant frequency of the panels that are dimensionally different should be measured during the GVT in addition to the fundamental resonant frequency of the aft bulkhead structure in the fore-aft direction. Similarly, the fundamental resonant frequency of the fuselage sidewall panels used in the fatigue analysis should also be measured.

The modal response of the door located in the aft bulkhead and the pressure relief panels located on the door should be measured during the GVT. This information will be important during the cavity door open flights.

Servoelastic tests of the telescope are not called out in the test plan. An understanding of the potential coupling of the structure with the telescope assembly is essential. Sine sweeps of the telescope assembly should be performed as part of the airplane GVT.

6.2.2.7 Airplane Stability and Control

A six degree of freedom flight simulation of the Boeing 747SP airplane was created. The initial aerodynamic model, and stability and control derivatives, used in the model development, were verified/updated with flight test data acquired during the baseline flight testing and wind tunnel testing.

Low speed and transonic wind tunnel model (3 percent scale) tests were conducted to investigate the stability and control characteristics of the airplane with an opening in the aft fuselage.[24] The wind tunnel tests provided data on how the stability and control characteristics were influenced by the aft fuselage cavity with the door closed, with the door open, and with the telescope at elevation angles of 20, 40 and 60 degrees. The cavity opening and the selected shear layer control design has minimal impact on the performance of the 747SP airplane, from both an aerodynamic drag perspective and from a stability and control and handling qualities perspective.

---

[24] Rose, W. C. *Synopsis of Low-speed Wind Tunnel Test Report.* NASA Ames Research Center, Moffett Field, CA, Document number 05-N-19980930-001, September 30, 1998.
_____. *Synopsis of High-speed Wind Tunnel Test Report.* NASA Ames Research Center, Moffett Field, CA, Document number 05-N-19981118-001, November 18, 1998.

The aerodynamic model of the simulation was up-dated with the measured changes in the aerodynamic coefficients from the wind tunnel tests. The simulation of the SOFIA airplane was used to analyze handling qualities for different cavity configurations (door open and closed and various telescope angles) at different points in the operating envelope.

6.2.2.7.1 Technical Assessment of Airplane Stability and Control

There have been no significant changes found in either stability and control or handling qualities for the modified SOFIA airplane compared to the baseline B-747SP airplane. The project has performed analyses, wind tunnel testing and flight testing to reach this conclusion. Even though no significant changes are evident, a comprehensive series of flight tests are being planned for the SOFIA airplane to evaluate its flight characteristics.

6.2.3 Approach To Flight Test

6.2.3.1 Baseline Flight Testing

The project has taken a two stage approach to flight testing. Initial flight test data was acquired for the baseline airplane in a 17 flight program.[25] The baseline flight data provided the project with essential data to construct and validate engineering analytical models. The airplane was extensively instrumented (nearly 1000 parameters) during the baseline phase for data acquisition in nearly every technical discipline.

The baseline flight test program acquired basic airplane flight data for:

1. basic flight characteristics
2. a six degree-of-freedom flight simulation
3. structural loads and strains (including the empennage)
4. flutter (structural frequencies and damping)
5. performance, stability and control, runway performance, stall characteristics, and high speed characteristics
6. airframe acoustics/vibration
7. boundary layer measurements

[25] Page, D. L. *Baseline Flight Test Report for the Stratospheric Observatory for Infrared Astronomy (SOFIA) Program*. L3 Communications Document 96156002-001, Revision A, September 10, 1998.

6.2.3.1.1 Technical Assessment of Baseline Flight Testing

The data acquired and experienced gained from the baseline flight test program has greatly benefited the SOFIA project. The baseline flight test data has been used to validate analytical models, aided in the design of wind tunnel models, and will be used during the SOFIA flight tests to track and trend differences between the two configurations.

It was also noted that the Boeing Airplane Company is not involved, either as a subcontractor or a consultant, with the SOFIA airplane modification. Boeing declined to bid on the proposal solicitation for the modification work. This, in part, required a baseline flight test program to acquire data for the airplane and for analytical model development and validation. It was noted that some project members have extensive B-747 experience which includes structures engineers, as well as the pilot for the flight test program. The assessment team concluded that participation by Boeing, as a consultant at this stage of the project, would be beneficial, but also noted that the project team has gained an in-depth knowledge of the basic airplane through the development of analytical models, and data acquired through wind tunnel testing and flight testing.

6.2.3.2 DC-10 Widebody Aircraft Sensor Platform (WASP) Flight Test

A DC-10 airplane, with a large cavity in the forward fuselage, serves as a sensor platform test-bed for another government agency and is shown in figure 6.2.3-1. The cavity design and flight test activity of this program was reviewed by the assessment team to determine similarities to the SOFIA program.[26]

[26]Ospring, M. J. "Trip Report – ATS Engineering Modified DC-10", SOFIA Project Memo for the Record, October 30, 2003.
Kunz, N., "Trip Report for Visit to DC-10 Open Cavity Project", SOFIA Project Memo for the Record, December 17, 2003.

Figure 6.2.3-1 DC-10 WASP Airplane.

The length of the primary cavity of the DC-10 is about the same as the SOFIA cavity, although the cavity is considerably shallower. Although the DC-10 primary cavity shear layer control concept was based on SOFIA developed technology (aft ramp geometry, etc.), substantial differences exist including:

1. Aft ramp geometric differences such as an incomplete aerodynamic lip.
2. No telescope in the cavity (acoustical impedance).
3. Cavity volume to aperture area is much smaller.

Another important difference is the ratio of free stream cavity length to boundary layer thickness. This is a well established parameter for open port cavities. A lower ratio provides a better probability for a well behaved cavity that does not resonate. The cavity length of the DC-10 cavity is about the same as the SOFIA cavity, however, with the SOFIA cavity in the aft fuselage, the boundary layer is several times thicker.

The flight conditions (Mach 0.71 & 0.58 at 29,000 ft), chosen for the first door open attempt of the DC-10, were neither the planned operational speed, nor the minimum speed to test landing stability and control issues. These speeds were chosen to accommodate the chase airplane. A flight test, at a Mach number of 0.71 and 29,000 ft altitude, revealed an uncontrolled cavity resonance of 143 dB with predominant frequency of 37 Hz. The resonance occurred with the cavity door partially open (1/3 of the way). A resonance of 143 dB was also present at a reduced Mach number of 0.58, at the same altitude, and a similar frequency. The cavity door on the

aircraft was never fully opened, so it is unknown whether the resonant amplitude had peaked or would continue to worsen as the door was opened beyond this point. When the door was opened at 1/3 of its maximum travel, fairly hard shaking was present on the door drive system (causing the design engineer to cease operations) as well as physical shaking in the cockpit (causing the pilot to relay his command to close the door). The aircraft was decelerated from 230 psf to 180 psf at a constant altitude but the resonance persisted.

The decision to cease operations was subjective, and nearly simultaneous, from both the design engineer who was located near the cavity and the pilot in the cockpit. The instrumentation, that was installed to monitor the cavity activity, was recording data below predetermined limit values. However, the video record of the tufting of the cavity interior and exterior structure was an important data record, as it provided clear evidence of flow attachment and separation, and of structural performance (to supplement strain gage data). It was this record that was used to locate the additional instrumentation for future flights.

The DC-10 program was a fast track program with the associated higher risks. The designs for the cavity and shear layer control hardware were not wind tunnel tested on a DC-10 wind tunnel model prior to developing full-scale hardware. The designs used on the DC-10 were based on the SOFIA wind tunnel developed and tested design concepts and then modified to suit other requirements not related to the aerodynamic or aero-acoustic performance.

6.2.3.2.1 Technical Assessment of DC-10 WASP Relevance to SOFIA

There are some important differences between SOFIA and the DC-10 aircraft. The placement of the cavity just behind the cockpit on the DC-10 results in a very thin boundary layer at the cavity leading edge. The SOFIA cavity, in contrast, is at a position on the fuselage where the boundary layer is much thicker and should by itself result in lower unsteady pressures. No wind tunnel tests were performed on the DC-10 to develop the cavity aperture treatment. There are no "standard" formulas for designing a ramp geometry, and, without wind tunnel testing, the design is just a guess. Extensive wind tunnel tests were performed on the SOFIA aperture treatment, and its robustness to varying flow conditions was thoroughly examined, thereby decreasing the risk of an in-flight resonance.

There are some interesting lessons learned from the DC-10 WASP program that are applicable to the SOFIA project. The important lesson learned is that the effects of the resonance may not subside rapidly as flight condition changes. This means that for some particular Mach numbers, the onset of an uncontrolled resonance may occur and last over a range of flight Mach numbers. If the door were to fail and remain open, the aircraft may be subjected to an uncontrolled resonance for a period of time. The pilot may not be able to "back-off" of a particular flight

condition and eliminate the resonance immediately. This will have to be considered in the build-up approach to opening the cavity door during flight testing.

Tufting of the cavity interior and surrounding exterior structure provides important information, not only for understanding the physics of the cavity flow and its effect on the surrounding structure, but also for providing data for the location of additional instrumentation should it be required to resolve a problem discovered during flight.

6.2.3.3 SOFIA Cavity Door Open Flight Test

Airworthiness testing will initially be conducted with the cavity door closed to evaluate stability and control, structural loads, flutter, and then with the cavity door open to determine cavity acoustics levels. SOFIA mission systems that are installed to support the operation of the telescope will be tested concurrently or through dedicated testing. Data from the SOFIA flight test will be compared to analytical predictions as well as the baseline flight data.

There were components of open door flight test plans (albeit in a draft status) available for review by the assessment team (Appendix F).[27] These test plans delineated the flight envelope expansion process for opening the cavity door in flight, as well as an initial cavity instrumentation list. Both plans delineated an incremental opening of the cavity door and a gradual build-up in dynamic pressure.

6.2.3.3.1 Technical Assessment of the SOFIA Cavity Door Open Flight Test

The assessment team reviewed the preliminary test plans for an understanding of the project's initial intentions for flight testing. It was understood by the assessment team that these plans would evolve and change as the project progresses toward the door open flight phase.

The uncertainties associated with the acoustic SPLs of the cavity, particularly in the failed door open configuration, dictate that a conservative build-up approach to opening the door in flight be undertaken. The flight test plan found in Appendix F provided the appropriate build-up approach to expanding the cavity door open flight envelope. This plan is recommended to be the starting point for planning cavity door expansion flights and changed accordingly as flight test data and other data become available.

Initial recommendations for a suite of flight instrumentation, to be used in the SOFIA aircraft, were put forth by the project in the draft flight test plan found in Frey's document.[28]

[27] Frey, M. L., "Observatory Flight Test Plan for the Stratospheric Observatory for Infrared Astronomy (SOFIA) Program", L3 Communications Document 96160001-001, September 29, 2003.
[28] Ibid.

Instrumentation for the forward and aft bulkhead is suitable for measuring critical data. Instrumentation for the cavity door system is extensive and will provide a wealth of data for correlation with analysis and for fatigue and DTA. The cavity instrumentation consists of a small number of microphones. Given the uncertainty of the acoustic environment, the cavity should have more extensive instrumentation. This includes placement of tufting on the interior and exterior surfaces around the cavity (including the empennage), video monitoring of the tufting, static pressure taps, and dynamic pressure transducers. This instrumentation should be functioning for any build-up flight testing for the open-door configuration.

6.2.3.4 Cavity Structural Integrity Verification

Flight test data will be acquired to evaluate the effect of cavity environment on the empennage and telescope cavity structure. The cavity and surrounding structure are instrumented with strain gages, unsteady pressure transducers, accelerometers and microphones.

Preliminary flight test plans have been formulated (Appendix F).[29] These are the same plans that have been formulated for the cavity door open flight test (Section 6.2.3.3). The plans will evolve as fatigue and DTA analyses mature and as initial flight data becomes available.

6.2.3.4.1 Technical Assessment of Cavity Structural Integrity Verification

The energy contained in an unstable cavity acoustical resonance can cause sonic fatigue damage to the structure on which this energy impinges. There is a large amount of instrumentation in the cavity to record structural data. The preliminary flight test plans indicate a number of door and telescope configurations are being considered for flight testing.

Currently, there is no cavity structural inspection plan in place. An inspection plan is needed, not only for routine cavity door-open flights, but also in the event that an unstable acoustic resonance occurs.

6.2.3.5 Flight Flutter Testing

A draft flight test plan has been written for the SOFIA cavity door closed flights.[30] Flight flutter testing will be accomplished during this phase to verify that there are no instabilities within the flight envelope of the airplane. Frequency and damping data will be acquired during the flight test to establish trend information so that the flutter envelope can be incrementally expanded for each fuel configuration.

[29] Ibid.

[30] Preliminary Phase One Flight Test Plan for the Stratospheric Observatory for Infrared Astronomy (SOFIA) Program. L3 Communications Document 9616XXXX-000, December 2004.

The current version of the test plan indicates that three different fuel loadings are to be flown, with the telescope assembly in the floated, caged and braked condition at 40 degrees elevation with the cavity door closed. A total of five test altitudes, ranging from 15,000 to 35,000 feet, are to be flown. The maximum dynamic pressure and Mach number occur simultaneously at 23,000 ft. which is one of the test altitudes.

A very early version of the cavity door open flight test plan revealed that flutter testing would be performed with the cavity door open to a critical position, at altitudes outside of the observation altitude band of 39,000 ft to 45,000 ft, and as low as 15,000 ft.[31] Acoustic levels of the cavity were be monitored, during this testing, along with structural frequency and damping values.

The control surface cables have been significantly rerouted in the aft fuselage area of the cavity. The project has performed control cable tension and strength tests, comparison of control surface rotation frequencies for the baseline and SOFIA configurations, and control surface freeplay tests. Indication of adverse effects from the rerouting of the control surface cables will be monitored closely during the flight flutter test phase.

6.2.3.5.1 Technical Assessment of Flight Flutter Testing

The project has defined a comprehensive matrix of flight conditions and airplane configurations to demonstrate that the SOFIA flight envelope is free of flutter with the cavity door closed. Appropriate analyses have been conducted and models have been validated with ground vibration test results.

Very preliminary flight flutter test planning with the cavity door open was reviewed by the assessment team. Testing was proposed at altitudes outside of the telescope observation altitude band of 39,000 ft to 45,000 ft. The reasoning for this is not clear. The door open flutter characteristics should be checked, within the telescope observation altitude band, over the operational Mach number range and in several different fuel configurations. Flying with the cavity door open, at off design altitudes, may cause a cavity acoustic resonance. While the resonance will not affect the flutter characteristics, it may have an effect on sonic fatigue life. Flutter testing with the cavity door open should only be performed at the cavity door open design altitude.

Flutter testing is considered to be hazardous testing and typically requires a safety chase airplane. The chase airplane pilot helps detect other aircraft in the test range and can provide a visual

[31] Frey, M. L., "Observatory Flight Test Plan for the Stratospheric Observatory for Infrared Astronomy (SOFIA) Program", L3 Communications Document 96160001-001, September 29, 2003.

inspection of the SOFIA aircraft, should an abnormal response occur to the structural excitation. As a minimum, a chase aircraft is required at the high dynamic pressure and high Mach number test points.

Although not defined in the flight test plan, discussions with project engineers have confirmed that flight flutter test points, with autopilot on and the yaw damper off, will be conducted at selected flight conditions to verify that the structural modifications have not had an adverse effect.

6.2.4 NESC Risk Assessment

The risk matrix is shown in Figure 6.2.4-1. *Likelihood* is the probability that an identified risk event will occur. *Consequence* is an assessment of the worst credible potential result(s) of a risk. The consequence is assigned for three areas: safety, mission success and the impact to national significance.

The initial risk assessment performed by the NESC Chief Engineer at the ARC indicated that there were no immediate safety risks but there appear to be significant (potentially catastrophic) risks to both crew and vehicle, which must be addressed prior to the first flight of the SOFIA aircraft with the cavity door open.

Initial Risk Assessment

The *Likelihood* of this problem occurring was rated as 4. Adequate data was not available to conclude that acoustical resonances will not interact with structural modes. No specific operational constraints or design modifications have been put in place to preclude it.

The *Consequence* of this problem happening with respect to **Safety** was rated at 5. It could result in the loss of vehicle and crew.

The *Consequence* of this problem happening with respect to **Mission Success** was rated at 5. It could result in failure to meet any of the Mission Objectives.

The *Consequence* of this problem happening with respect to impacting **National Significance** was rated at 5. It could result in the loss of a major NASA asset and mission.

The estimated *Consequence* and *Likelihood* of occurrence for each of the above hazards is annotated on the matrix shown in Figure 6.2.4-1.

Nomenclature
S – Safety
M – Mission Sucess
N – National Visibility

Subscripts
i – Initial Assessment based on a cursory review of technical data
f – Final Assessment pending completion of NESC recommendations

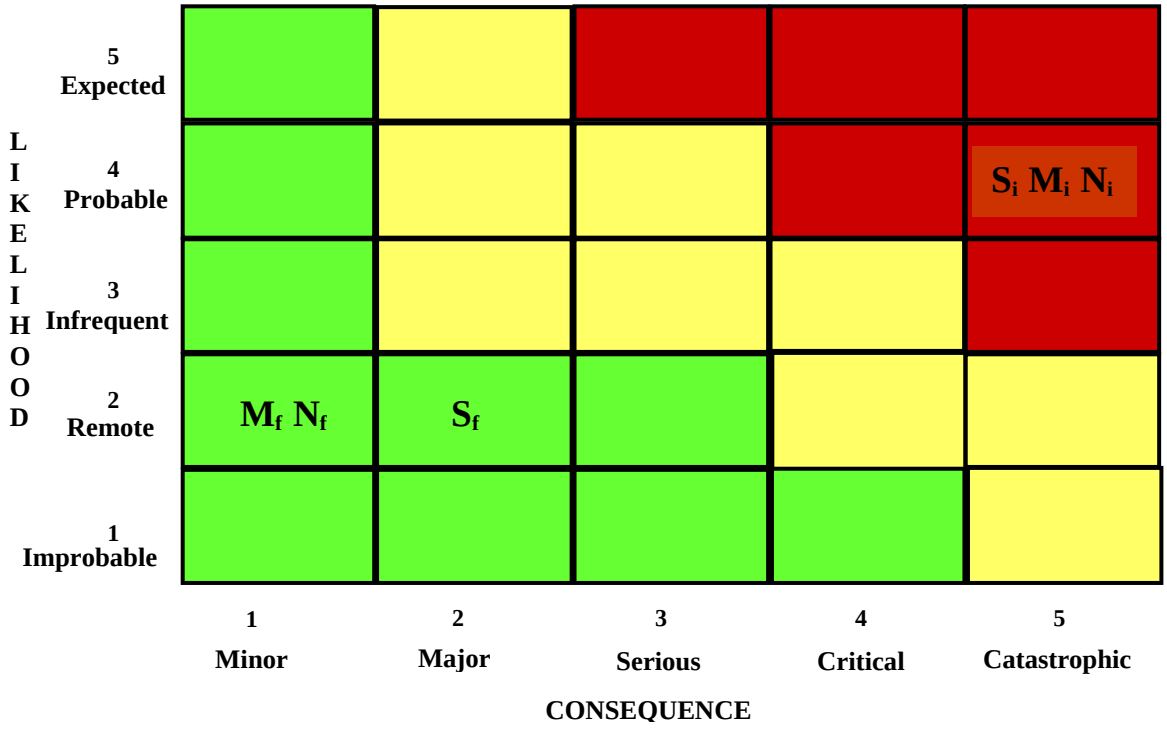

Figure 6.2.4-1 Risk Matrix

Final Risk Assessment

The Likelihood of this problem occurring is rated as 2. Adequate data is available to conclude that acoustical resonances will not interact with structural modes in a catastrophic manner. The cavity acoustic instability occurs when a Rossiter mode is at the same frequency as a cavity acoustic mode. The project has performed analyses which estimate the cross-over of Rossiter frequencies with cavity acoustic frequencies. Independent NESC Technical Assessment analysis has shown that a "triple" resonance (a Rossiter mode that interacts with an acoustic mode and a structural mode) does not occur and that the cavity acoustics and cavity structure becomes a system that resonates at its own unique frequencies. The 7 percent scale wind tunnel model

data, acquired for the cruise observation flight condition, as well as off-nominal flight conditions with the cavity door fully open, did not indicate an acoustic instability within the cavity.

Only limited cavity door failed-open data was acquired during wind tunnel testing which leaves some uncertainty whether an acoustical resonance will occur during a descent from cruise altitude with the cavity door failed partially open. Flight test planning includes a detailed plan to incrementally open the cavity door with a slow build-up in flight condition severity. This approach will ensure that any acoustical resonant condition will be identified in advance before it is fully encountered.

Data from the DC-10 Widebody Aircraft Sensor Platform (WASP) airplane indicated that an acoustical resonance of 143dB was not catastrophic and the airplane was recovered without damage. Many important lessons learned from the DC-10 WASP flight test are being incorporated into the SOFIA flight test program.

Several contingency cavity design modifications have been considered to mitigate an uncontrolled resonant condition should one be exhibited during the flight test program. Wind tunnel testing has shown foam linings on the cavity walls and cavity leading edge fence devices/spoilers to reduce overall sound pressure levels.

The *Consequence* of this problem happening with respect to **Safety** is rated at 2. The build-up approach being taken during the flight test program will minimize the magnitude of any cavity resonance encountered. The DC-10 WASP flight test experience indicates that an acoustical resonance can be encountered without loss of vehicle and without any major damage occurring to the airplane. The DC-10 WASP configuration was not tested in the wind tunnel and the flight test was not conducted in a build-up fashion. The design of the critical cavity structure provides a fatigue life that ensures structural integrity throughout a descent from the design observation altitude to landing with a cavity door failed partially open.

The *Consequence* of this problem happening with respect to **Mission Success** is rated at 1. If a resonance occurs while flying at observation altitudes, a porous fence or other cavity leading edge device may have to be installed in order to attenuate the resonance. The SOFIA project has tested several contingencies in the wind tunnel. Installation of a cavity leading edge device will degrade flight time per mission which will require more flights than originally planned to accomplish all of the science objectives. Failure to meet **any** of the mission objectives is not a credible consequence.

The *Consequence* of this problem happening with respect to impacting **National Significance** is rated at 1. The likelihood of a complete loss of the aircraft or science mission is remote based on the likelihood rationale stated above. Any acoustic and/or fatigue problems encountered can be

resolved through an engineering modification albeit cost and schedule will be affected. This will be of minor national significance.

The estimated consequence and likelihood of occurrence for each of the above hazards is annotated on the matrix. These risk levels are based on the assessment of the technical materials reviewed and analyses performed by the team.

6.2.4.1 In-flight Crew Escape System

The SOFIA aircraft does not have an in-flight crew escape system such as ejections seats or a slide chute similar to the one used for the B-747 Shuttle Carrier Airplane (SCA) during the Shuttle approach and landing tests.

A crew escape system was not deemed to be necessary for the SOFIA airplane. Although there are uncertainties to whether an unstable cavity acoustic resonance will occur and its effect on the surrounding structure as well as uncertainties in other areas, each can be approached in a controlled manner during the flight test.

There are always uncertainties at the beginning of a flight test program. However, a conservative build-up approach, in the areas of each uncertainty, ensures that unexpected or catastrophic events do not occur. Each area of the uncertainty for SOFIA can be approached using the build-up flight test technique and as such, the assessment team considers an escape system as unnecessary.

This is unlike the situation of the B-747 SCA during the release of the Orbiter. A build-up to the release of the Orbiter from the SCA was not possible; the Orbiter was either going to strike the vertical stabilizer or it wasn't.

7.0 Results of Structural-Acoustics Analysis

The primary charter of the Technical Assessment was to review the project's analytical and test results and then formulate an opinion on whether the project's approach was sound and conservative. The Technical Assessment requestor stated a concern over the potential for structural damage caused by an acoustical resonance occurring at or near a structural mode. A worst-case scenario is that cavity Rossiter mode frequencies could align with the frequencies of the cavity acoustic resonances frequencies and cavity structure vibration mode frequencies. If such a possibility were to occur, one is confronted with a "triple resonance," which would imply the potential for a catastrophic condition.

The compliance of the SOFIA cavity structure can substantially change the cavity pressure distribution, and no account was taken of the coupling of interior cavity pressure with the structural displacement in a resonance in either wind tunnel measurements, or supporting computational fluid dynamics evaluations. In order to better understand the coupling of the acoustic resonance with an elastic cavity structure, and the possibility of a "triple resonance" occurrence, a set of progressively more refined models, that were amenable to fundamental analytical techniques, were formulated. The basic intent of these analyses was to explore how the transfer function given the structural response to a known acoustic source was affected by the dynamic nature of the acoustic cavity.

7.1 A Simple Model of Structural Response Due to an Interior Cavity Resonance

The first model selected for study was the simplest one in which acoustic cavity and structural resonances can occur (Appendix C). In it an air-filled tube of constant cross section is driven at one end by a source at specified amplitude and frequency. The other end of the tube is terminated by a one-degree-of-freedom damped oscillator in which the mass is a piston that is driven by the acoustic pressure. The walls of the tube are taken to be rigid, so the acoustic field constitutes a pair of plane waves propagating in the forward and backward directions. The pressure applied to the piston is the sum of the pressures in these waves, and the velocity of the piston must match the particle velocity in the fluid.

The analysis disclosed that there is only a single set of frequencies at which resonances occur. Contrary to the initial expectation, these frequencies are neither the structure's natural frequencies, nor the purely acoustic resonant frequencies of the cavity. The worst-case scenario places a Rossiter mode frequency at a coupled cavity-structural resonance, which is not a "triple resonance" effect. Another important conclusion derived from this model, was that damping in the structure, is extremely beneficial in reducing the acoustic pressure field as well as the structural displacement.

7.2 Two-Dimensional Model of Coupled Acoustic Cavity - Structure Resonance

The rectangular cavity model represented features like those of SOFIA (Appendix D) compared to the air-filled tube model. The model was sufficiently uncomplicated to permit direct analysis of the governing equations. The cavity could sustain acoustic waves propagating in multiple directions, and the structure was distributed over a spatial region, so it had multiple natural frequencies. The specific model was a rectangular cavity open at x=L, while the opposite end at x=0 is an elastic plate whose edges are clamped. The side walls at y=0 and y=b were taken to be rigid. An acoustic source was placed at one edge of the open end, comparable to a Rossiter mode, in which the source is at the trailing edge. Only situations in which there was no variation of the response in the z direction was considered, in order to make the analysis tractable. Thus, the acoustic excitation is a line source in a three-dimensional perspective.

Despite the differences of the air-filled tube and rectangular cavity models, the qualitative aspects of the results were the same. The cavity acoustic resonant frequencies are neither the structure's natural frequencies, nor the purely acoustic resonant frequencies but a set of frequencies of the coupled system. The flexible cavity acoustic resonance frequencies approach the rigid cavity resonance frequencies with increasing cavity structural stiffness.

7.3 A General Analysis of the Response of an Acoustic Cavity Bounded by an Elastic Structure to Acoustic Excitation

The assessment team also performed a completely general analysis by combining the governing equations for a structural response to a known surface pressure and an acoustic response to known motion of structure and acoustic source (Appendix E). General conclusions from this analysis are:

1. Structural natural frequencies will not match resonance frequencies of the coupled acoustic-structure system.

2. The displacement will not be large at the structure’s natural frequencies.

3. The flexible acoustic resonance frequencies approach rigid acoustic natural frequencies as the cavity structural stiffness increases.

4. Acoustic resonance frequencies identified in the wind tunnel, after scaling, will not match frequencies for SOFIA.

5. The measured wind tunnel pressure field after proper scaling to full scale will be higher than in the SOFIA cavity.

The implication from these analyses is:

The procedures used for dynamic analysis will over predict the structural response, because the pressure PSD that acts on the full-scale SOFIA structure will be less than the properly scaled PSD measured in the wind tunnel. Thus, the dynamic design procedures yield conservative designs even though the cavity structural flexibility and coupling with the acoustic resonance was neglected in the wind tunnel measurements.

8.0 Findings and Recommendations

The Technical Assessment was limited in scope to the review of existing project technical reports and briefings. The findings below are for the most part based on a review of these documents and conversations with engineers involved with the SOFIA project. Some findings are based on the independent analysis performed by the team.

8.1 General Findings

The SOFIA project appropriately accounted for and designed an aperture treatment for flow control to mitigate or suppress telescope cavity resonances. The final design, a semi-circular aft-ramp, was found to be robust with respect to changes in airplane sideslip angle, TA elevation angle and airplane angle of attack in the 7 percent scale model wind tunnel tests. These test results also indicated that there were no strong resonant conditions over a Mach number range of 0.4 to 0.88. However, there were no analyses and only limited wind tunnel test results for the cavity door failed-open configuration. Therefore, there are uncertainties whether an uncontrolled cavity resonance will occur with the cavity door failed open during descent to landing from cruise altitude. These uncertainties are mitigated through a thorough, incremental building-block approach to opening the door during the flight test phase of the program.

The cavity fatigue analysis and DTA has started, but was not completed during the time period of this assessment. The validity of some aspects of the proposed approach could not be substantiated and require verification prior to flight. This technical area requires further evaluation before flight with the cavity open door.

Flight test planning for either the door closed or opened door flights has not been completed. Some initial planning for technical areas related to this assessment, such as opening the cavity door, has been completed and indicates a cautious approach to hazardous testing and to areas where uncertainties exist. Instrumentation in some areas require supplementation for appropriate real-time monitoring during flight and for adequate post-flight data reduction.

The assessment team provided 22 specific findings, 3 observations, and 7 recommendations to the SOFIA project which can be found in the detailed findings and recommendations section (Section 8.0) of this report. The recommendations, once implemented, will reduce the uncertainties and lead to a better understanding of the acoustical environment within the cavity.

Overall, the analysis, structural design and proposed approach to the cavity door open flight test taken by the project was found to be sound and conservative with the exception of the acoustic fatigue and damage tolerance assessment which the project had not completed at the time of this review.

8.1.1 Specific Findings and Observations

F-1 The SOFIA project appropriately accounted for and designed an aperture treatment for flow control to mitigate or suppress telescope cavity resonances. The final design, a semi-circular aft-ramp, was found to be robust with respect to changes in sideslip angle, TA elevation angle and angle of attack in the 7 percent scale model wind tunnel tests. There were no strong resonant conditions over the Mach number range of 0.4 to 0.88. (Section 6.2.1.1)

F-2 Wind tunnel tests of a 3 percent scale SOFIA model were conducted. The primary purpose of the model was to examine the effects of the cavity on the stability and control of the SOFIA airplane. The cavity opening was found to have a negligible effect on airplane stability and control and airplane handling qualities. (Section 6.2.1.1)

F-3 Acoustic environment data was also acquired during the 3 percent scale model tests. The 3 percent scale model consistently exhibited higher overall acoustic resonance amplitudes, including uncontrolled resonances, compared to the 7 percent scale model, which was the result of the boundary layer not being properly scaled (too thin relative to that expected in flight). (Section 6.2.1.1)

F-4 Limited wind tunnel testing was accomplished with the 7 percent scale model for the cavity door partial open configuration. The uncertainty of the acoustic resonance levels with a partial door opening can not be determined from the 7 percent scale model testing. (Section 6.2.1.1)

F-5 The full-scale SOFIA cavity structure sound pressure level will be less than the properly scaled sound pressure level measured in the wind tunnel. These lower acoustic pressure levels are a result of the damping provided by the interior cavity structure, and a reduction in the pressure load due to the reduction of the cavity spatial coherence. (Section 6.2.1.1)

F-6 The cavity acoustic resonant frequencies are neither the cavity structure's natural frequencies, nor the purely acoustic resonant frequencies but a set of frequencies of the coupled system. The worst case scenario places a Rossiter mode frequency at a coupled cavity-structural resonance which is not a "triple resonance" effect. (Section 7.1)

F-7 The cavity fatigue and damage tolerance analysis (DTA) has started but is not complete. (Section 6.2.2.4)

F-8 The numerical values of the acoustic fatigue life were not provided. Therefore, the adequacy of the various cavity structural components could not be evaluated. (Section 6.2.2.4)

F-9 The 3 percent scale model wind tunnel data was used as the input forcing spectra for acoustic fatigue analysis. This data exhibited higher overall acoustic resonance amplitudes than the 7 percent scale model data and therefore provide an element of conservatism to the analysis. (Section 6.2.2.4)

F-10 The project assumed that the structural components will have the shortest fatigue life when excited at their fundamental frequency with a relatively low assumed structural damping. Higher frequency modes which could have higher stress levels were not considered for the cavity structure. (Section 6.2.2.4.1)

F-11 The calculation on the dynamic response on the aft bulkhead is possibly unconservative. The Miles equation is sensitive to input load, and is only recommended for use when the input PSD is flat and broadband. The input PSD for the aft bulkhead was not flat and the standard form of the Miles equation was not used in the case reviewed. (Section 6.2.2.4.2)

F-12 The project used the classic "safe life" approach for the evaluating acoustic fatigue for the flight test phase of the program. This approach does not taken into account existing cracks in the structure. Damage tolerance assessment analyses, which includes crack growth and residual strength analyses, are planned once cavity flight test data is acquired. However, the classic "safe life" approach cannot assure that existing cracks that may be present will not reach critical lengths during the flight test phase. Inspections are being planned to detect structural cracks in the cavity. (Section 6.2.2.4.3)

F-13 Damage tolerance assessment analysis method will be validated by means of structural component and coupon tests. (Section 6.2.2.4.4)

F-14 The fundamental resonant frequency of several cavity structural components used in fatigue analyses is not planned to be measured during the SOFIA ground vibration test. (Section 6.2.2.6.1)

F-15 The overall SPL on the fuselage downstream of the cavity was shown to be 3-5 dB greater than the closed-door levels in the 7 percent scale model wind tunnel tests. It could not be determined if these increased levels were taken into account in the acoustic fatigue-life calculations. (Section 6.2.2.4.5)

F-16 The SOFIA project has recognized important lessons learned from the DC-10 WASP flight test experience with a large fuselage cavity. These lessons have been implemented into the project's flight test planning for opening the cavity door during flight. (Section 6.2.3.2.1)

F-17 Flight test plans for opening the cavity door, such as those in Vol. II, Appendix F, draw upon the experience of the DC-10 WASP airplane and provides a conservative build-up approach to opening the cavity door in flight. (Section 6.2.3.3.1)

F-18 Initial cavity flight instrumentation does not indicate the use of tufting inside and outside of the cavity with video camera monitoring. (Section 6.2.3.3.1)

F-19 The flutter analysis has been validated through parametric studies and comparison of results with published Boeing data, baseline flight test data and modal test data. Preliminary flutter analysis results indicate that there is no flutter within the flight envelope for the modified airplane (SOFIA) configuration. (Section 6.2.2.5.1)

F-20 Detailed flight flutter test planning has started with the cavity door closed configuration to determine the flutter characteristics of the airplane. Testing is being planned for multiple fuel configurations at several different altitudes. Preliminary planning for flight flutter testing with the cavity door open indicates testing at altitudes outside of the design altitude band where the possibility of unstable acoustic resonances exist. (Section 6.2.3.5.1)

F-21 The installation of the telescope in the cavity forced a significant rerouting of the control surface cables. All appropriate precautions are being taken by the project. These include control cable tension and strength tests, comparison of control surface rotation frequencies for the baseline and SOFIA configurations and control surface free-play tests. Indication of adverse effects from the rerouting of the control surface cables will be monitored closely during the flight flutter test phase. (Section 6.2.3.5)

F-22 Servoelastic testing of the telescope is not called out in the ground vibration test plan or flight test plan. An understanding of the potential coupling of the structure with the telescope assembly is essential. (Section 6.2.2.6.1)

O-1 The Strouhal number is the appropriate scaling parameter for comparing wind tunnel model and flight data. (Section 6.2.1.1)

O-2 The SOFIA project has contingency plans, such as leading edge boundary layer thickeners that can be implemented, to attempt to eliminate or mitigate uncontrolled cavity resonance should it occur during the normal cruise observing cavity door open flight conditions. (Section 6.2.1.1)

O-3 Ground vibration testing of the SOFIA airplane is planned and data acquired from the test will be used to update the dynamics model for more accurate flutter analysis results. (Section 6.2.2.6)

8.2 Recommendations

R-1 Implement a flight envelope expansion plan similar to the one in Vol. II, Appendix F for opening the cavity door in flight. This flight test plan has the proper fidelity and conservatism necessary to conduct this type of testing safely. (Findings F-4, F-16 and F-17)

R-2 Install tufting in the cavity interior and aft fuselage exterior, including the empennage and provide a means of video recording during flight. (Finding F-18)

R-3 Perform a comprehensive modal test of the cavity to include the telescope assembly, forward bulkhead, aft bulkhead, cavity fuselage structure and components used for fatigue calculations. (Findings F-12 and 14)

R-4 Conduct servo-elastic testing during the SOFIA ground vibration test and during flight to determine coupling effects of the Telescope Assembly with the SOFIA airplane structure. (Finding F-22)

R-5 Acquire flight data for use in fatigue and damage tolerance analyses to track cavity structural life used during the flight test program and to project the fatigue life of the fuselage with the telescope assembly modification. (Findings F-7, F-11 and F-12)

R-6 Develop and implement inspection techniques and intervals for critical cavity structural locations for use during the flight test program. (Finding F-12)

R-7 Complete the acoustic fatigue life calculations for open door cruise and door failed open descent environments before cavity open door flight. An independent review, either by the NESC or other independent team, is required in order to provide findings and recommendations to the SOFIA project and the ARC Airworthiness and Flight Safety Review Board. This review is to include an evaluation of the rationale that structural components will have the shortest fatigue life when excited at their fundamental frequency with a relatively low assumed structural damping and the aft bulkhead acoustic fatigue analysis methodology. (Findings F-7 and F-11)

9.0 Lessons Learned

There were no lessons learned during this assessment.

10.0 Definition of Terms

Definition of Terms

Corrective Actions	Changes to design processes, work instructions, workmanship practices, training, inspections, tests, procedures, specifications, drawings, tools, equipment, facilities, resources, or material that result in preventing, minimizing, or limiting the potential for recurrence of a problem.
Finding	A conclusion based on facts established during the assessment/inspection by the investigating authority.
Lessons Learned	Knowledge or understanding gained by experience. The experience may be positive, as in a successful test or mission, or negative, as in a mishap or failure. A lesson must be significant in that it has real or assumed impact on operations; valid in that it is factually and technically correct; and applicable in that it identifies a specific design, process, or decision that reduces or limits the potential for failures and mishaps, or reinforces a positive result.
Observation	A factor, event, or circumstance identified during the assessment/inspection that did not contribute to the problem, but if left uncorrected has the potential to cause a mishap, injury, or increase the severity should a mishap occur.
Problem	The subject of the independent technical assessment/inspection.
Requirement	An action developed by the assessment/inspection team to correct the cause or a deficiency identified during the investigation. The requirements will be used in the preparation of the corrective action plan.
Root Cause	Along a chain of events leading to a mishap or close call, the first causal action or failure to act that could have been controlled systemically either by policy/practice/procedure or individual adherence to policy/practice/procedure.

11.0 List of Acronyms

ARC	Ames Research Center
CDR	Critical Design Review
CFD	Computational Fluid Dynamics
dB	decibal
DLR	Deutches Zentrum für Luft und Raumfahrt
DTA	Damage Tolerance Analysis
FAA	Federal Aviation Administration
ft	feet
GVT	Ground Vibration Test
Hz	Hertz
in.	Inch(es)
ITA	Independent Technical Assessment
KAO	Kuiper Airborne Observatory
LaRC	Langley Research Center
LFD	Lower Flex Door
NASA	National Aeronautics and Space Administration
NESC	NASA Engineering and Safety Center
NRB	NESC Review Board
PSD	Power Spectral Density
psf	Pounds per square foot
psi	Pounds per square inch
SCA	Shuttle Carrier Airplane
SME	Subject Matter Expert
SOFIA	Stratospheric Observatory for Infrared Astronomy
SPL	Sound Pressure Levels
SSMOC	Science and Mission Operations Center
TA	Telescope Assembly
T/A	Telescope/aperture
TIM	Technical Interchange Meeting
URD	Upper Rigid Door
WASP	Widebody Airplane Sensor Platform

12.0 References

Eberhard, S. and Ulrich, W., "The Suspension Assembly of SOFIA, the Key Subsystem Connecting the Telescope with the Aircraft." Proceedings of the Society of Photo-Optical Instrumentation Engineers (SPIE) Conference, Munich, Germany, Vol. 4014, March 2000.

Frey, M. L., "Observatory Flight Test Plan for the Stratospheric Observatory for Infrared Astronomy (SOFIA) Program." L3 Communications Document 96160001-001, September 29, 2003.

Honaker, Michael, "Preliminary Assessment of Stress Levels in the TA Due to Aero-Acoustic Loads and 1 G Gravity Effects." SOFIA project Technical Note TN-MAH-013, August 10, 2000.

Kunz, N., "Trip Report for Visit to DC-10 Open Cavity Project." SOFIA Project Memo for the Record, December 17, 2003.

Lee et al. *Fatigue and Damage Tolerance Component Test Plan for the SOFIA 747SP*. Raytheon Aircraft Integration Systems, Doc. No. 96188003-002, 2001.

Martin, E. L., *Baseline Flutter Analysis for the Stratospheric Observatory for Infrared Astronomy (SOFIA) Program*. L3 Communications Document 96186001-001, February 18, 2005.

Matthews, L.S. *Vibroacoustic Assessment of SOFIA's Aft Bulkhead*. Rep No. LDG-00-004-SDS, Raytheon Systems Company, March, 2000.

McIntyre, M. J. *SOFIA V Wind Tunnel Test Report, Telescope Loads and Cavity Aero-acoustics*. NASA Ames Research Center, Moffett Field, CA, Document number 05-N-19980423-001, April 23, 1998.

_____. *Comparison of NASA and RSC Wind Tunnel Test Results*. NASA Ames Research Center, Moffett Field, CA, Document number 02-N-20000616-001, June 16, 2000.

Metallic Materials and Elements for Aerospace Vehicle Structures. MIL-HDBK-5J, 31 January, 2003.

Miles, John. "On Structural Fatigue Under Random Loading," *Journal of the Aeronautical Sciences* (November 1954).

Ospring, M. J. "SOFIA Dynamic Analysis Procedures, Revision B." SOFIA Project Memo for the Record, December 21, 2002.

_____. "SOFIA Cavity Door Analysis Procedures." SOFIA Project Memo for the Record, October 3, 2003.

_____. "Trip Report – ATS Engineering Modified DC-10." SOFIA Project Memo for the Record, October 30, 2003.

Ospring, M.J., and Harry Gobler. *Dynamic Analysis Using Power Spectral Density*. Project Memo for the Record, December, 1983.

Page, D. L. *Baseline Flight Test Report for the Stratospheric Observatory for Infrared Astronomy (SOFIA) Program*. L3 Communications Document 96156002-001, Revision A, September 10, 1998.

Preliminary Phase One Flight Test Plan for the Stratospheric Observatory for Infrared Astronomy (SOFIA) Program. L3 Communications Document 9616XXXX-000, December 2004.

Puglise, J. *Observatory Ground Vibration Test Plan for the Stratospheric Observatory for Infrared Astronomy (SOFIA) Program*. L3 Communications Document TP96157011-000, December 15, 2004.

Rose, J. A. "Wind Tunnel Test Report for the Stratospheric Observatory for Infrared Astronomy (SOFIA) Program." Raytheon Systems Company Technical Report, Sept., 21, 2000.

Rose, W. C. *SOFIA-Aft Cavities Wind Tunnel Test, SOFIA II Final Report*. Incline Village, NV: Rose Engineering & Research, Inc., 31 December 1994.

_____. *SOFIA-Telescope Torque Wind Tunnel Test, SOFIA III Final Report*. Incline Village, NV: Rose Engineering & Research, Inc., 31 March 1995.

_____. *SOFIA-Conceptual Door Design and Aero-Optics Wind Tunnel Test, SOFIA IV Final Report.* Incline Village, NV: Rose Engineering & Research, Inc., 31 March 1996.

_____. "*SOFIA V Design Validation Test Final Report*." NASA Ames Research Center, Moffett Field, CA, Document number 05-N-19980415 - 001, April 15, 1998.

_____. *Synopsis of Low-speed Wind Tunnel Test Report*. NASA Ames Research Center, Moffett Field, CA, Document number 05-N-19980930-001, September 30, 1998.

_____. *Synopsis of High-speed Wind Tunnel Test Report*. NASA Ames Research Center, Moffett Field, CA, Document number 05-N-19981118-001, November 18, 1998.

Steinberg, David. *Designing Electronic Equipment for Random Vibration*. Seminar Handout, 1983.

Stratospheric Observatory For Infrared Astronomy (SOFIA) Systems Interface Requirements Specification SOF-1030. Moffett Field, CA: National Aeronautics and Space Administration Ames Research Center, Original Issue August 1988, Revision 4 June. 2001.

Thompson, W.T. *Theory of Vibrations with Applications*. 5th Ed. Prentice-Hall, 1965.

13.0 Minority Report

There were no dissenting opinions in the Assessment Report.

Volume II: Appendices

Appendix A. NESC ITA/I Request Form (NESC-003-FM-01

NASA Engineering and Safety Center Request Form

Submit this ITA/I Request, with associated artifacts attached, to: nrbexecsec@nasa.gov, or to NRB Executive Secretary, M/S 105, NASA Langley Research Center, Hampton, VA 23681

Section 1: NESC Review Board (NRB) Executive Secretary Record of Receipt

Received (mm/dd/yyyy h:mm am/pm) 9/1/2004 2:27 PM	Status: New	Reference #: 04-073-E
Initiator Name: Estelle P. Condon	E-mail: Estelle.P.Condon@nasa.gov	Center: ARC
Phone: (650)-604-6071, Ext _____	Mail Stop: 200-2	

Short Title: SOFIA Acoustical Resonance

Description: The SOFIA modification includes a large open port cavity that is larger than any previous flown open port cavity. Despite numerous wind tunnel tests and extensive analysis there remains uncertainties regarding the acoustic environment within the cavity, especially in the off nominal failed door open descent flight regime where some degree of acoustic resonance is expected to occur. There is the potential for structural damage from acoustical resonance or tones in the SOFIA telescope cavity especially if they occur at or near a structural mode. In the worst case, the potential consequence is structural failure including loss of vehicle and crew. Independent expert opinion is requested to determine if the approach taken by the Contractor in the analysis, structural design and proposed approach to flight test are sound and conservative. First Flight of the SOFIA aircraft is planned for January 2005 and the associated Flight Readiness Review process will culminate in November and December of this year.

Source (e.g. email, phone call, posted on web): EMAIL

Type of Request: ITA

Proposed Need Date: 10/29/2004

Date forwarded to Systems Engineering Office (SEO): (mm/dd/yyyy h:mm am/pm):

Section 2: Systems Engineering Office Screening

Section 2.1 Potential ITA/I Identification

Received by SEO: (mm/dd/yyyy h:mm am/pm): 9/2/2004 12:35 PM

Potential ITA/I candidate? ☒ Yes ☐ No

- Assigned Initial Evaluator (IE): Michael Freeman
- Date assigned (mm/dd/yyyy): 9/3/2004
- Due date for ITA/I Screening (mm/dd/yyyy): 9/13/2004

Section 2.2 Non-ITA/I Action

Requires additional NESC action (non-ITA/I)? ☐ Yes ☐ No

- If yes:
  - Description of action:
  - Actionee:
  - Is follow-up required? ☐ Yes ☐ No If yes: Due Date:
  - Follow-up status/date:
- If no:
  - NESC Director Concurrence (signature):

Request closure date:

Section 3: Initial Evaluation		
Received by IE: (mm/dd/yyyy h:mm am/pm):		
Screening complete date:		
Valid ITA/I candidate? ☐Yes ☐ No		
Initial Evaluation Report #: NESC-PN-		
Target NRB Review Date:		
Section 4: NRB Review and Disposition of NCE Response Report		
ITA/I Approved: ☐Yes ☐ No	Date Approved:	Priority: - Select -
ITA/I Lead: , Phone ( ) - , x		
Section 5: ITA/I Lead Planning, Conduct, and Reporting		
Plan Development Start Date:		
ITA/I Plan # NESC-PL-		
Plan Approval Date:		
ITA/I Start Date	Planned:	Actual:
ITA/I Completed Date:		
ITA/I Final Report #: NESC-PN-		
ITA/I Briefing Package #: NESC-PN-		
Follow-up Required? ☐Yes ☐ No		
Section 6: Follow-up		
Date Findings Briefed to Customer:		
Follow-up Accepted: ☐Yes ☐ No		
Follow-up Completed Date:		
Follow-up Report #: NESC-RP-		
Section 7: Disposition and Notification		
Notification type: - Select -	Details:	
Date of Notification:		
Final Disposition: - Select -		
Rationale for Disposition:		
Close Out Review Date:		

Form Approval and Document Revision History

Approved: _____ _____
NESC Director Date

Version	Description of Revision	Office of Primary Responsibility	Effective Date
1.0	Initial Release	Principal Engineers Office	29 Jan 04

Appendix B. Tutorials

B1.0 Aero-acoustic Physics Description

In this section an overview of the aero-acoustic physics associated with the SOFIA cavity is presented. The SOFIA aircraft has a large cylindrical cavity with an opening (aperture) in the fuselage measuring approximately 10.6 feet long by 9.25 feet wide. The configuration sets the stage for an aero-acoustic feedback process that produces large amplitude acoustic tones in the cavity near field and large amplitude oscillations in the flow around the aperture.

The aero-acoustic process can be described as follows. The incoming turbulent boundary layer separates from the leading edge of the aperture and forms a free shear layer spanning the cavity. The free shear layer is highly unstable and disturbances within the shear layer grow and convect downstream. Eventually, the shear layer rolls up into a spanwise coherent vortex structure that propagates downstream and impacts the trailing edge of the aperture. The ensuing unsteady vortex-corner interaction gives rise to a sound source. Noise from this source drives an acoustic response of the cavity. Acoustic energy is then fed into the shear layer at the aperture leading edge via a complex receptivity process. This feedback process leads to a discrete number of high-amplitude oscillations/tones in the cavity flow commonly referred to as “Rossiter modes” after the researcher who first studied them. In Figure B1.0-1, a Schlieren image of a resonating cavity flow with annotations describing the physical elements of the aero-acoustic feedback process is shown. The cavity in this image has a length-to-depth ratio of 2 but, due to limitations in the optical setup, the full depth of the cavity is not visible.

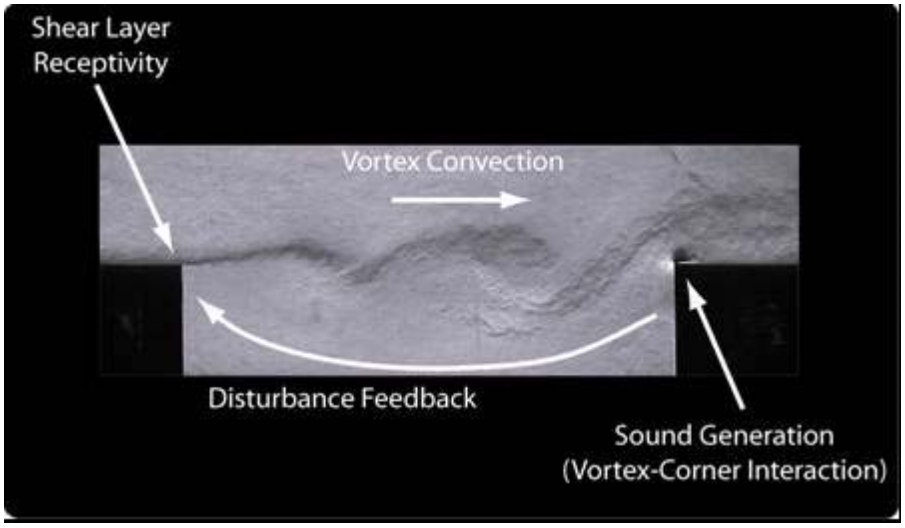

Figure B1.0-1: Schlieren image of a resonating cavity flow (Kegerise, 1999).

A semi-empirical model for possible Rossiter-mode frequencies is given as:

$$St_m = \frac{f_m \lambda}{U_\infty} = \frac{m - \alpha}{M_\infty \left(1 + \frac{\gamma - 1}{2} M_\infty^2\right)^{-1/2} + 1/\kappa}, \quad m = 1,2,3,\mathrm{K}\ ,$$

where *St* is a Strouhal number, α is an empirical constant (typically equal to 0.25), and κ is the ratio of vortex-convection velocity to freestream velocity (typically equal to 0.55). Note that the Rossiter modes are not integer multiples of one another. Furthermore, they vary with freestream Mach number. It is also important to note that this model does not tell us which Rossiter modes will occur at any given Mach number nor does it give an indication of their amplitudes. But it does give us a scaling relation to convert measured model frequencies to full scale conditions.

The acoustic response of the cavity can be a controlling factor in the selection of Rossiter modes and their amplitudes. If at some Mach number a Rossiter mode coincides with (or lies near) an acoustic resonance of the cavity, a very large-amplitude acoustic tone can be generated.

There are several governing parameters in the cavity-tone problem: the geometry (length, depth, etc.), the freestream Mach number, the freestream dynamic pressure, and the state/character of the incoming boundary layer. Wind tunnel testing on a scale model at the appropriate Mach numbers is usually not a problem. The Reynolds number in wind tunnel testing will be lower than at flight, but this does not present a problem because cavity oscillations are the result of an inviscid mechanism. Previous measurements of cavity oscillations over a Reynolds number range greater than a factor of ten showed that unsteady pressure amplitudes can be scaled with the dynamic pressure. Comparisons of unsteady pressures in weapons-bay cavities at flight and wind tunnel scales also show that the dynamic pressure is the proper scaling parameter. There is one caveat in that statement: the incoming boundary layer characteristics must be matched between the wind tunnel model scale and the full-scale aircraft. The cavity-tone amplitudes are known to be highly dependent on the state of the incoming boundary layer and so it is crucial that it be properly scaled.

B1.1 Structural Acoustical Resonance Phenomenon

Resonance of a mechanical system occurs when there is harmonic excitation at one of the system's natural frequencies. A free oscillation can occur at such frequencies because the restorative forces associated with the system's elasticity are cancelled by the inertial loads stemming from acceleration of the system mass. Because of such cancellation, the sole resistance to a forced excitation at a natural frequency is associated with dissipation effects,

which are much weaker. Consequently, large velocities, and therefore large displacement amplitudes, are generated to balance the applied excitation.

The similarity of the nature of structural and acoustic cavity resonances causes concern that both phenomena occur at the same frequency. The concern is that large pressures will be generated with in the cavity, and that these pressures will be applied to a structure that has little ability to resist these structures. Thus, the magnification factors associated with each resonant response would be multiplied, leading to a potentially dangerous level of vibration. This level might be sufficiently large to cause an immediate failure. If not, is still could be large enough to significantly reduce fatigue life due to excessive vibration amplitudes over any number of cycles. Further concern then arises from the fact that the acoustic response in this scenario is generated by a source associated with the turbulence generated at the cavity opening. Resonances associated with Rossiter modes significantly enhance the source levels at certain frequencies. If the Rossiter mode frequencies align with the structure and acoustic natural frequencies, one is confronted with the possibility of a triple resonance, which would seem to imply the potential for a catastrophic condition.

In fact, it is not obvious whether any of the preceding reasoning is correct. It is based on the assumption that the pressure causing the structure to vibrate is known, whereas any vibration of the structure will modify the acoustic field because it pushes the fluid particles that are in contact with the structure. Another assumption that is contained in the "triple resonance scenario" discussed previously is an assumption that the occurrence of the Rossiter modes is unaffected by the interior acoustic pressure. Whether this is the case is extremely difficult to answer because it requires a full computational fluid dynamics (CFD) simulation. A conservative approach is to assume that the Rossiter modes do occur, and that they can occur at any frequency. Then given that assumption one can explore how the interaction of the structure and the acoustic medium in the cavity affect the structure's vibration amplitude.

An acoustic cavity is a region of fluid surrounded by any type of boundary. If the boundaries are rigid solid surfaces, or if they correspond to surfaces where the cavity is exposed to a larger outer acoustic region that is not excited, the elasticity effects for a resonance stem from the fluid's compressibility, and the mass is that of the fluid. The natural frequencies and mode functions, which describe the pressure distribution for a free oscillation at the corresponding natural frequency, are governed by the Helmholtz equation,

$$\nabla^2 P + k^2 P = 0$$

where P is the complex amplitude of the pressure and $k = \omega/c$, with ω being the frequency of the oscillation and c being the speed of sound. Despite the simple nature of this equation, computer solutions are necessary unless the cavity's shape is relatively simple, such as a box.

Excitation of the cavity can originate in either of two ways. The conventional one, which has received considerable attention, is of interest in applications such as noise reduction in an aircraft cabin. In this case the vibration of one or more boundaries is taken as the input, and the task is to identify the interior pressure amplitude at all locations at a specified frequency, from one can extract sound pressure levels. It is irrelevant to this problem whether the boundary is itself an elastic system capable of resonance, because the boundary motion is considered to be specified. In other words, the acoustical analysis seeks to determine a transfer function describing the interior acoustic field produced by a specified boundary motion. The free vibration version of this problem, which describes the natural frequencies of the cavity, is obtained by taking the vibrating boundary to not move. This is equivalent to considering these boundaries to not move, so one finds that the cavity resonances are those of a cavity having the same shape, but with rigid walls. This is particularly relevant to SOFIA, because all wind tunnel measurements, as well as the supporting CFD evaluations, were based on a structural model that had negligible compliance in the frequency range where turbulence was found to generate the largest pressures.

The interior acoustic problem that has received little attention is that where the interior pressure fluctuations are generated by an acoustic source, rather than by vibration of the walls. This is the case for SOFIA when one considers the effect of the Rossiter modes. Like all aircraft, SOFIA has walls that are flexible. In this case the determination of acoustical natural frequencies must consider the compliance of the walls. Such compliance has spring-like features, owing to the elastic effects, and inertial features associated with the structure's mass. Determining the natural frequencies in this case is further complicated, beyond the issue of complexity of the cavity's shape. This is so because the boundary conditions for the acoustic medium depend on the structure's ability to resist the pressure that is applied to it. For example, if one were to consider the cavity's natural frequencies based on considering the walls to be rigid, that analysis would be invalidated if the structure were to resonate, because the structure has little ability to sustain a pressure loading when it resonates. Thus, the determination of the resonant frequencies, as well as any analysis of the vibration levels generated by the acoustical source of a Rossiter mode, requires that one formulate a fully coupled problem. A fundamental feature of the fully-coupled nature of such problems is that there is one set of natural frequencies, at which the pressure and structural response are magnified in unison. This is not to imply that the vibration amplitudes are magnified less than they would be if the resonances of the cavity and structure were uncoupled. Rather it points to the complexity of the question, and the need for some analysis to understand the phenomenon.

B1.2 Structural Integrity

Acoustic resonance and related structural acoustic interactions results in issues of structural integrity in terms of high dynamic stresses, vibrations, fatigue and fracture. The determination

of the effect of the dynamic stresses requires acoustic fatigue strength and fracture analyses (Damage tolerance analysis (damage tolerance assessment) and residual strength analysis).

Acoustic fatigue failures typically occur in structures lying close to, or in the path of, jet engine exhaust**.** Similar failures have occurred in other regions of pressure fluctuation, such as within the intake duct of fan engines, close to propeller tips, and in regions of separated flow near control surfaces, such as elevators, flaps, rudders, or near items such as spoilers, which are used on some aircraft during maneuvers.

Structural acoustic fatigue issues are addressed to satisfy requirements such as:

1. Qualify the structural components/structures according to the requirements of the airworthiness requirements.
2. Reduce maintenance problems which are known from experience to be very costly (repairs, modifications, down-times etc.) when they are due to acoustic sources of excitation.
3. Understand and define rational solutions when acoustic problems appear.

To predict the acoustic fatigue life of structures, three main issues have to be addressed:

1. Loads applied to the structure (dynamic characteristics of the acoustic excitation).
2. Structural dynamic response evaluation which provide stresses (S_{rms}) and frequencies.
3. Acoustic fatigue strength data for the materials and the selected design (rivets, etc.)

B1.2.1 Mechanics of Fatigue

MIL-HDBL-5J, Metallic Materials and Elements for Aerospace Vehicle Structures Handbook, provides typical fatigue and crack growth properties information for metallic materials used in civil and military aircraft structures. For the classic metallic materials, the handbook provides data in the form of charts and tables. Figure B1.2-1 shows a S-N curve for notched coupons. The Srms, which is the root mean square value of stress at a reference position on the failure line, is given as a function of the number of cycles to failure. Such curves are used for calculating the fatigue life at a given stress level. Methods are available to take into account the mean stress effects and variable amplitude loadings. Typically, Miners cumulative damage theory is used to track the fatigue life expended.

Crack growth analyses are performed to determine the time that observed crack sizes grow to critical crack sizes for structural components. Inspection intervals are normally arrived at by crack growth calculations taking into consideration the detectable crack sizes during inspections. Allowable crack sizes are determined such that the structure meets residual strength requirements. Figure B1.2-2 show these relationships.

Damage tolerance assessments are best carried out by representative tests on full- scale structure. When full- scale testing is not accomplished, a large amount of reliance must be based on analysis. If analysis is used, sufficient testing must be performed to validate all aspects of the analytical methods. Appropriate margins of safety must be shown if flight safety is to be assured.

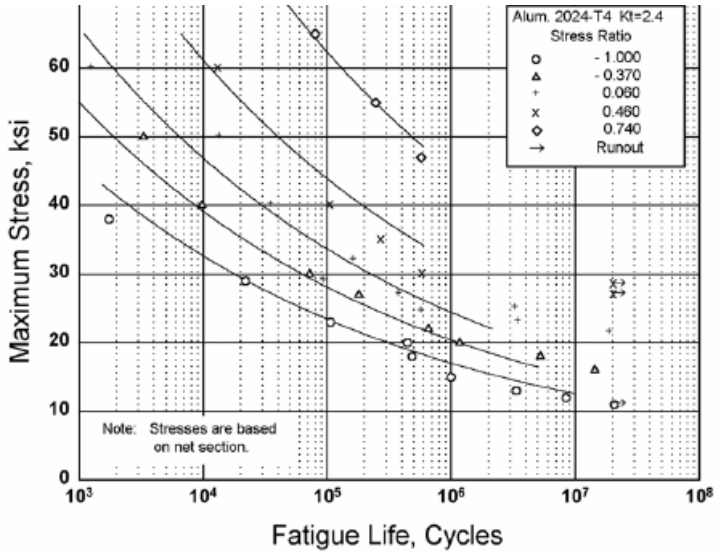

Figure 3.2.3.1.8(c). Best-fit S/N curves for notched, K_t = 2.4, 2024-T4 aluminum alloy bar, longitudinal direction.

Figure B1.2-1. Typical best-fit S/N curves for notched 2024-T4 aluminum alloy bar.

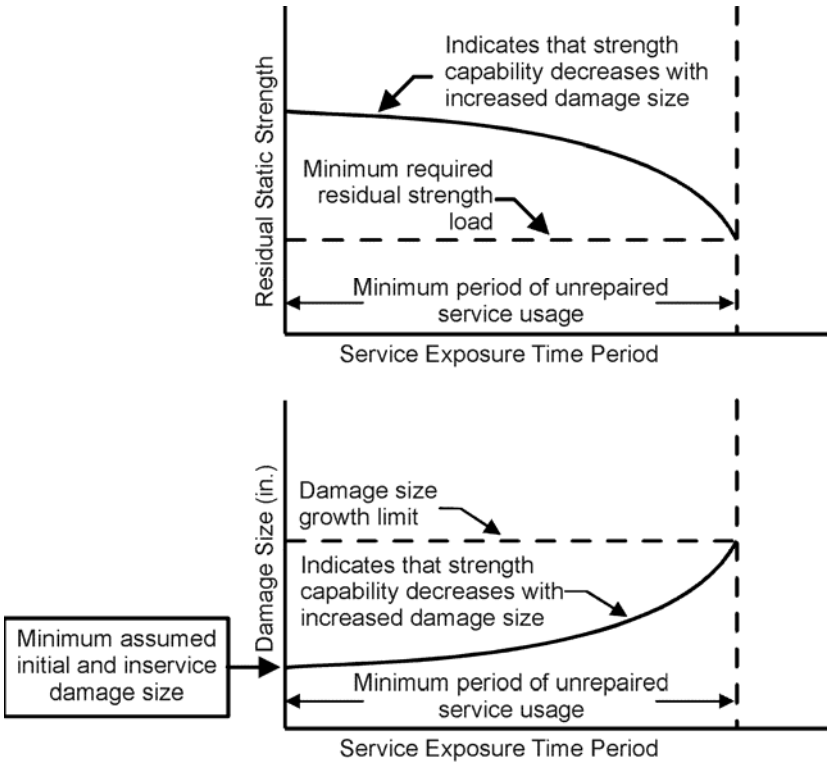

Figure B1.2-2 shows charts relating residual strength, crack length and service life.

Such curves need to be generated to develop inspection intervals and NDI methodologies.

B1.3 Flutter

Aeroelastic flutter involves the adverse interaction of aerodynamic, elastic and inertia forces on structures to produce an unstable oscillation that often results in structural failure. Energy is extracted from the air stream to excite the structural modes over which air flows and the resulting vibrations grow in magnitude until structural failure occurs. Flutter is dependent upon the mass and stiffness distribution of a structure, and any structural modifications involving changes to these distributions can significantly change the flutter characteristics.

The cavity cut-out on the aft fuselage of the SOFIA airplane is a significant structural modification. In addition to the structural changes, a nearly 40,000 pound telescope assembly has been installed in a fairly small area of the aft fuselage. Adding to the complexity of the modification is the acoustical environment that will be present with the cavity door open during flight.

The flutter characteristics are defined early in an aircraft's development cycle. Preliminary analytical flutter analyses are performed to define the vehicle's flutter characteristics, such as predicted flutter speed, mode participation (flutter mechanism) and frequency of flutter. The structural mode frequencies that participate in flutter mechanism of large transport type aircraft, such as the B-747SP, are typically below 5 Hz. The flutter frequency of the basic B-747SP is between 2 and 3 Hz and the flutter mechanism involves the antisymmetric first wing bending mode coupling with an engine nacelle lateral mode. There is some aft fuselage torsion motion that is part of the flutter mechanism mode shape. However, it is important to note that the fuselage torsion mode is at a higher frequency and is not coupled with the other two modes.

In the case of the SOFIA airplane, there are cavity acoustical resonances that occur with the cavity door open during flight. The two lowest major peaks found in the wind tunnel tests are at a frequency of 35 Hz and 47 Hz. These frequencies are considerably higher than the basic structural modes of the airplane. Even if acoustical resonance frequencies coincided with airframe structural frequencies, the result would be a forced vibration and not flutter. However, the energy contained in the acoustic resonances and in particular when an instability occurs within the cavity, can cause sonic fatigue damage to the structure on which this energy impinges. An example is the B-58 weapons bay that initially had high amplitude acoustical resonances and the cavity structure developed cracks within 30 flight hours.

Flutter wind tunnel model testing and full- scale ground vibration testing are often performed to verify the aerodynamic and structural models used in the preliminary flutter analysis. Flutter analyses are usually performed after the models have been updated followed by dedicated flight flutter testing. Flight flutter testing is conducted to verify the absence of flutter within an airplane's operational flight envelope. The scope of flutter testing can easily become quite large particularly with aircraft that require testing of multiple fuel configurations.

The typical approach to flight flutter testing is to fly the aircraft at several stabilized test points arranged in increasing order of dynamic pressure and Mach number. The aircraft structure is excited by some means of excitation and the response is recorded by instrumentation usually consisting of strain gages and/or accelerometers sampled at high rates. The structural responses are nearly always monitored in real time and often acquired by a digital computer for extraction of response frequencies and damping ratios. These data establish trends as a function of airspeed. Information is then extrapolated to predict the stability of the next planned test point.

Flutter testing, however, is still a hazardous test for several reasons. First, one still must fly close to actual flutter speeds before imminent instabilities can be detected. Second, subcritical damping trends cannot be accurately extrapolated to predict stability at higher airspeeds. Third, the aeroelastic stability may change abruptly from a stable condition to one that is unstable with only a few knots' change in airspeed.

B1.4 Flight Testing

Flight testing of a newly designed or a modified aircraft is undertaken to verify that the aircraft conforms to its basic design requirements, such as performance, stability and control, structural loads, aeroelasticity, etc. Flight testing is accomplished to confirm the satisfactory operation of those characteristics that which cannot be fully verified by ground testing, to verify the airworthiness of the vehicle, to identify significant discrepancies between actual flight behavior and that predicted from analyses and ground tests, and to acquire flight test data to improve the accuracy of models and simulations.

Flight testing of a new or modified airplane is carried out with the initial purpose of defining a flight envelope which is safe. Once the airworthiness of the airplane has been demonstrated and found to be acceptable, the vehicle may then be flown to demonstrate its capability of meeting the requirements of its intended purpose.

Expanding an airplane's flight envelope is a task that must be cautiously and systematically approached cautiously and systematically and requires the cooperation and coordination of the many technical disciplines. In general, the flight test program and the associated test procedures are put together by a flight test team. The test procedures take into account the importance of accomplishing the test objectives and the risk involved in achieving them.

The project usually conducts a risk assessment by means of a formal hazard analysis designed to identify and evaluate all potential problems associated with the flight test. An independent review of the flight test plan and risk assessment is accomplished to confirm that:

1. all relevant data has been considered
2. the safety criteria of the organization has been applied
3. no potential hazards have been missed
4. the importance of the acquired data justifies the risks incurred

Responsibility for this safety review and the approval of the proposed flight test program may rest with the supervisory chain for each technical discipline or assigned to a review board that which consists of experts in each technical discipline.

Appendix C. A Simple Method of Structural Response Due to an Interior Cavity Resonance

A Simple Model of Structural Response Due to an Interior Cavity Resonance

Jerry H. Ginsberg

Contents:

Pages 1-12: Analysis
Pages 13-28: Evaluation of formulas
Pages 28-37: Parameter studies

Background

- Possible cavity resonances:
  - Vortical behavior - internal reflection of vortices generated by shear flow over the opening.
  - Acoustical behavior - ideal fluid, analogous to resonance of a mechanical system or electrical circuit.
- Present focus is *acoustical resonance*
- Initial reasoning:
  - Any cavity has natural frequencies at which a pressure oscillation occurs without an disturbance other than an initial nonuniform pressure distribution.
  - If an excitation is applied to a cavity at a frequency that is close to a natural frequency, very large pressures within the cavity will result.
  - Large pressure oscillations will lead to large structural motions.
  - The situation will be much worse if the frequency for the acoustic resonance aligns with a structural natural frequency because both cavity pressure and structure response are greatly magnified.

Further Considerations

- The frequencies at which acoustical resonances occur depend on the size and shape of the cavity, and the boundary conditions.
- Sturdy surfaces, such as building walls, act as though they are rigid if the excitation frequency is below the coincidence frequency, which corresponds to flexural waves in the wall propagating at the acoustical speed.
- Well below the first resonance, all structures behave in a quasi-static manner, i.e. their impedance is mainly elastic.
- If one were to calculate the acoustic resonances assuming the structure was essentially elastic, the analysis would not be valid if the acoustical resonant frequency matched a structure natural frequency, because the structural impedance would be mainly resistive due to damping, rather then reactive (elasticity).
- This seems to lead to a dilemma of conflcting tendencies.

A Simple Model

- Consider a one-dimensional cavity, that is, a tube.
- One end of the tube is open to the air, at which there is an acoustic excitation.
- The other end of the tube is terminated by an arbitrary elastic structure.

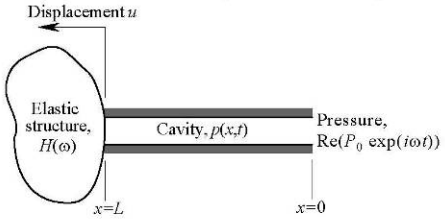

Governing Equations

- Frequency domain analysis:
  - Cavity pressure: $p(x,t) = \mathrm{Re}\left(P(x)\exp(i\omega t)\right)$
  - Structure displacement: $u = \mathrm{Re}\left(U\exp(i\omega t)\right)$
- Helmholtz equation:

$$\frac{d^2P}{dx^2} + k^2P = 0$$

$k = \omega/c$, speed of sound c

- Boundary conditions:
  - Open end: $P = P_0$ at x
  - Structural termination: Cavity cross section area A

$$U = H(\omega)\,P_0A$$

Frequency response function $H(\omega)$

- Euler's equation: $dP/dx = -\rho\omega^2U$

Solution

- Cavity pressure:

$$P(x) = P_0 \left[\frac{\sin(kL) + \rho c \omega A H(\omega) \cos(kL)}{\cos(kL) - \rho c \omega A H(\omega) \sin(kL)} \sin(kx) + \cos(kx) \right]$$

- Structure response:

$$U = A P_0 \frac{H(\omega)}{\cos(kL) - \rho c \omega A H(\omega) \sin(kL)}$$

- Nondimensionalize:

$$P_0 = \rho c^2 \hat{P}_0, \quad U = L\hat{U}$$
$$U = H(\omega) P_0 A \implies \hat{U} = \hat{H}(kL) \hat{P}_0$$
$$\hat{H}(kL) = \rho c^2 \frac{A}{L} H(kc)$$

Structural response:

$$U = P_0 \left(\frac{H(kL)}{\cos(kL) - kLH(kL)\sin(kL)} \right)$$

$$P(x) = P_0 \left(\frac{\cos(kL - kx) - H(\omega)\sin(kL - kx)}{\cos(kL) - kLH(kL)\sin(kL)} \right)$$

- One-degree-of-freedom model:
  - Static flexibility coefficient H_{static}
  - Natural frequency (nondimensional) κ
  - Structural damping loss factor γ

$$H(kL) = \frac{H_{\text{static}}}{1 + i\gamma - \left(\frac{kL}{\kappa}\right)^2}$$

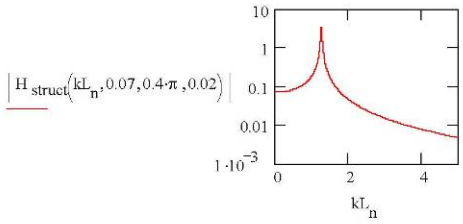

Resonances

- Structural resonance $\kappa L = \kappa$:
  - Peak of $H(kL) \Longrightarrow$ Maximizes numerator of U
- Acoustic resonance:
  - Frequency $kL = \Omega$ at which U is maximized:

$$\frac{d}{d(kL)} \left| \cos(kL) - kLH(\omega) \sin(kL) \right| = 0 \text{ at } \kappa L = \Omega$$

- Observations:
  - The denominators of $P(x)$ and U are the same.
  - If kL differs significantly from κ, then the numerator for U varies relatively slowly.
  - If Ω differs sufficiently from κ, then U will show a local maximum at $kL = \Omega$.

Evaluation of Acoustic Resonant Frequencies

- Seek to minimize $|\cos(kL) - \rho c \omega A H(\omega) \sin(kL)|$
- Imaginary part of $H(\kappa L)$ is very small compared to the real part, except at $kL \approx \kappa$

$$\mathrm{Re}(H(kL)) = H_{\text{static}} \frac{1 - \left(\frac{kL}{\kappa}\right)^2}{\left[1 - \left(\frac{kL}{\kappa}\right)^2\right]^2 + \gamma^2}$$

$$\mathrm{Im}(H(kL)) = -H_{\text{static}} \frac{\gamma}{\left[1 - \left(\frac{kL}{\kappa}\right)^2\right]^2 + \gamma^2}$$

- Consequently, the root for acoustic resonance should be well approximated by

$$\cos(kL) - kL\,\mathrm{Re}(H(kL))\sin(kL) = 0 \iff H_{\text{static}} \tan(\Omega) = \frac{1 - \Omega^2/\kappa^2}{\Omega}$$

►

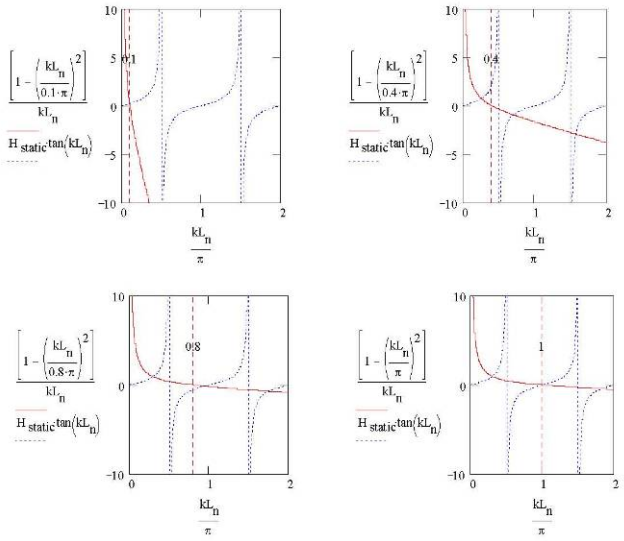
0.1
0.4
0.8
1
kL_n / π

Structure Response at a Pure Cavity Resonance

- The only case where the structure's natural frequency aligns with a cavity resonance is

$$\kappa = n\pi \implies \Omega = n\pi$$

- Even if $\kappa = n\pi$, there are multiple resonances at other frequencies
- Let Ω_j denote a root. Estimate the denominator when $\kappa \neq n\pi$.

$$\mathrm{Re}\left(\mathcal{D}\right) \approx \cos\left(\Omega_j\right) - H_{\text{static}} \frac{\Omega_j}{1-\left(\Omega_j/\kappa\right)^2} \sin\left(\Omega_j\right) = 0$$

$$\mathrm{Im}\left(\mathcal{D}\right) \approx -H_{\text{static}} \frac{\gamma\Omega_j}{\left[1-\left(\Omega_j/\kappa\right)^2\right]^2} \sin\left(\Omega_j\right)$$

When $\Omega_j \neq \kappa$, damping is unimportant for $H\left(\Omega_j\right)$:

$$H\left(\Omega_j\right) \approx \frac{H_{\text{static}}}{1-\left(\Omega_j/\kappa\right)^2}$$

- Structural displacement at pure cavity resonances:

$$\frac{|U|}{P_0} = \frac{|H\left(\Omega_j\right)|}{|\mathcal{D}|} = \frac{1-\left(\Omega_j/\kappa\right)^2}{\gamma\Omega_j \sin\left(\Omega_j\right)}$$

Pure Structural Resonance

- Set $kL = \kappa$ but $kL \neq \Omega_j$:

$$H(\kappa) = \frac{H_{\text{static}}}{i\gamma}, \quad \mathcal{D} = \cos(\Omega_j) + i\frac{H_{\text{static}}}{\gamma}\sin(\Omega_j) \approx i\frac{H_{\text{static}}}{\gamma}\sin(\Omega_j)$$

$$\frac{|U|}{P_0} = \frac{|H(\Omega_j)|}{|\mathcal{D}|} = \frac{1}{\sin(\Omega_j)} \tag{1}$$

One-Dimensional Structure-Acoustic Resonance-Loss Factor

$$H_{struct}(kL, H_{static}, \kappa, \gamma) := \frac{H_{static}}{1 - \left(\frac{kL}{\kappa}\right)^2 + i \cdot \gamma}$$

$$Denominator(kL, H_{static}, \kappa, \gamma) := \cos(kL) - H_{struct}(kL, H_{static}, \kappa, \gamma) \cdot kL \cdot \sin(kL)$$

$$U_{magnification}(kL, H_{static}, \kappa, \gamma) := \frac{H_{struct}(kL, H_{static}, \kappa, \gamma)}{Denominator(kL, H_{static}, \kappa, \gamma)}$$

Assume 1% of critical damping: $\gamma := 0.02$ $H_{static} := 0.7$

$N := 40000$ $n := 1 .. N + 1$ $kL_n := \frac{n - 1}{N} \cdot 2 \cdot \pi$ $\Delta := \frac{2 \cdot \pi}{N}$

Pure acoustic resonances:

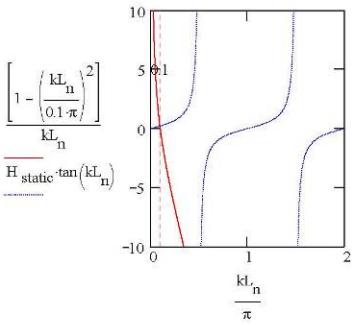

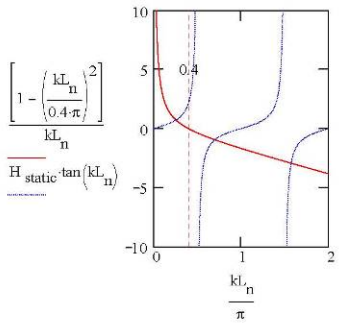

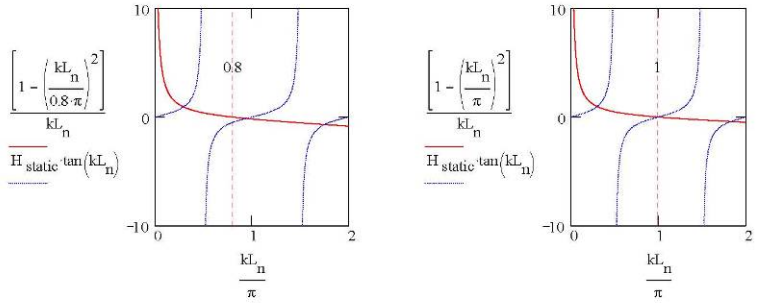

Set natural frequency different from a multiple of π: $\kappa := 0.4 \cdot \pi$

Search for kL value giving minimum denominator magnitude:

$H_n := H_{struct}(kL_n, H_{static}, \kappa, \gamma)$ $D_n := Denominator(kL_n, H_{static}, \kappa, \gamma)$ $U_n := \frac{H_n}{D_n}$

First resonance: $z := 0.25 \cdot \pi$ $\Omega_1 := root\left[\cot(z) - H_{static} \cdot \frac{z}{1 - \left(\frac{z}{\kappa}\right)^2}, z\right]$

Second resonance: $z := 0.7 \cdot \pi$ $\Omega_2 := root\left[\cot(z) - H_{static} \cdot \frac{z}{1 - \left(\frac{z}{\kappa}\right)^2}, z\right]$

$$\frac{\Omega}{\pi} = \begin{bmatrix} 0.2566 \\ 0.7029 \end{bmatrix}$$

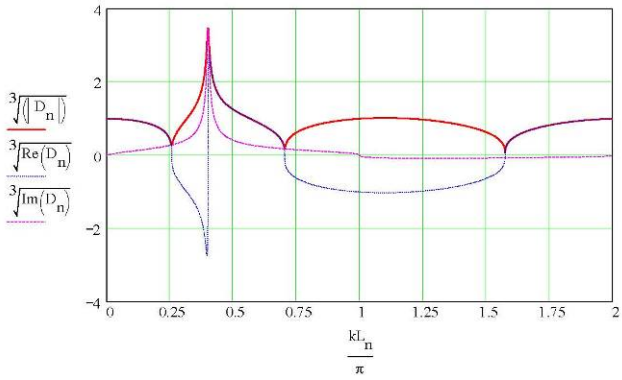
4
2
0
−2
−4
0
0.25
0.5
0.75
1
1.25
1.5
1.75
2
$\sqrt[3]{|D_n|}$
$\sqrt[3]{Re(D_n)}$
$\sqrt[3]{Im(D_n)}$
$\frac{kL_n}{\pi}$

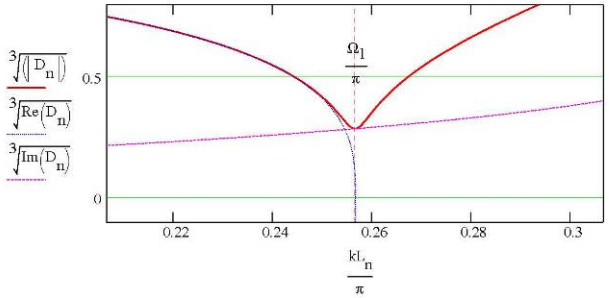
0.5
0
0.22
0.24
0.26
0.28
0.3
$\frac{\Omega_1}{\pi}$
$\sqrt[3]{|D_n|}$
$\sqrt[3]{Re(D_n)}$
$\sqrt[3]{Im(D_n)}$
$\frac{kL_n}{\pi}$

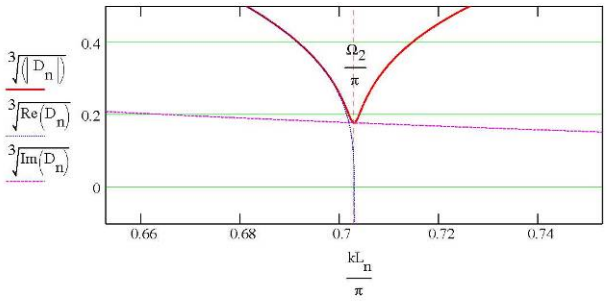
0.4
0.2
0
0.66
0.68
0.7
0.72
0.74
Ω2/π
kLn/π

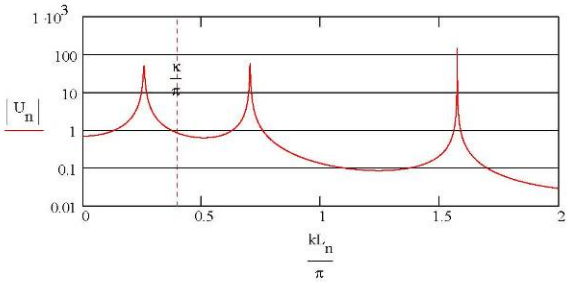
1·10^3
100
10
1
0.1
0.01
0
0.5
1
1.5
2
|Un|
k/π
kLn/π

Test formula for U at acoustic resonances:

$$\max\left(\text{submatrix}\left(\overrightarrow{|U|}, 1, \frac{N}{4}, 1, 1\right)\right) = 50.5629 \qquad \max\left(\text{submatrix}\left(\overrightarrow{|U|}, \frac{N}{4}, \frac{N}{2}, 1, 1\right)\right) = 58.8143$$

$$\frac{\left|1 - \left(\frac{\Omega_1}{\kappa}\right)^2\right|}{\gamma \cdot \Omega_1 \cdot \sin(\Omega_1)} = 50.5617 \qquad \frac{\left|1 - \left(\frac{\Omega_2}{\kappa}\right)^2\right|}{\gamma \cdot \Omega_2 \cdot \sin(\Omega_2)} = 58.8186$$

Test formula for U at structural resonances:

$$U_{\text{magnification}}(\kappa, H_{\text{static}}, \kappa, \gamma) = -0.8367 - 6.181i \cdot 10^{-3}$$

$$\frac{1}{\kappa \cdot \sin(\kappa)} = 0.8367$$

Case where natural frequency is very low: $\kappa := 0.1 \cdot \pi$

$H_n := H_{\text{struct}}(kI_n, H_{\text{static}}, \kappa, \gamma)$ $\quad D_n := \text{Denominator}(kI_n, H_{\text{static}}, \kappa, \gamma)$ $\quad U_n := \frac{H_n}{D_n}$

First resonance: $z := 0.05 \cdot \pi$ $\quad \Omega_1 := \text{root}\left[\cot(z) - H_{\text{static}} \cdot \frac{z}{1 - \left(\frac{z}{\kappa}\right)^2}, z\right]$

Second resonance: $z := 0.7 \cdot \pi$ $\quad \Omega_2 := \text{root}\left[\cot(z) - H_{\text{static}} \cdot \frac{z}{1 - \left(\frac{z}{\kappa}\right)^2}, z\right]$

$$\frac{\Omega}{\pi} = \begin{bmatrix} 0.0966 \\ 0.5141 \end{bmatrix}$$

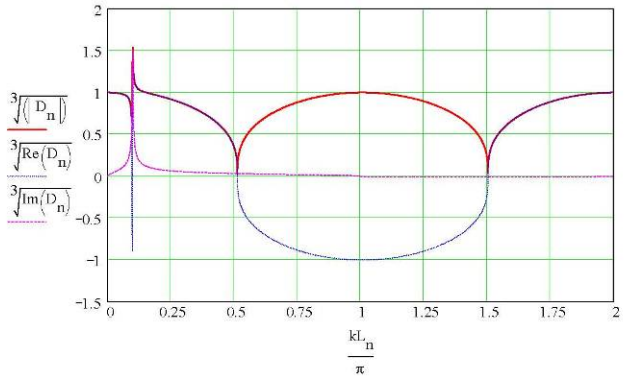
2
1.5
1
0.5
0
−0.5
−1
−1.5
0
0.25
0.5
0.75
1
1.25
1.5
1.75
2
$\sqrt[3]{\langle D_n \rangle}$
$\sqrt[3]{\mathrm{Re}(D_n)}$
$\sqrt[3]{\mathrm{Im}(D_n)}$
$\frac{kL_n}{\pi}$

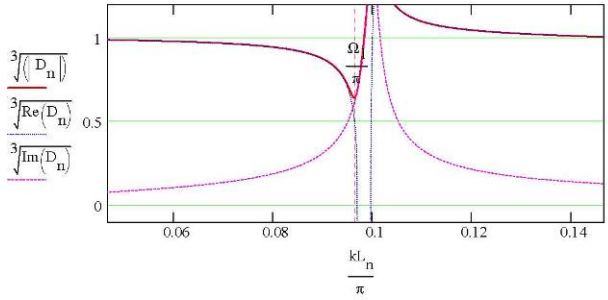
1
0.5
0
0.06
0.08
0.1
0.12
0.14
$\frac{\Omega}{\pi}$
$\sqrt[3]{\langle D_n \rangle}$
$\sqrt[3]{\mathrm{Re}(D_n)}$
$\sqrt[3]{\mathrm{Im}(D_n)}$
$\frac{kL_n}{\pi}$

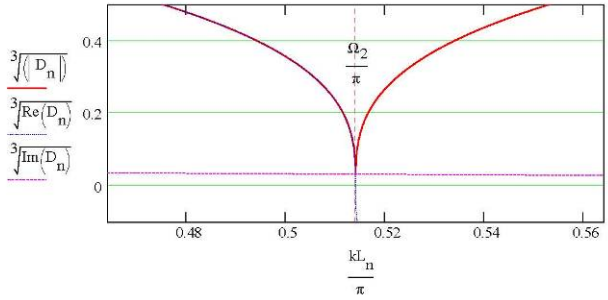
0.4
0.2
0
0.48
0.5
0.52
0.54
0.56

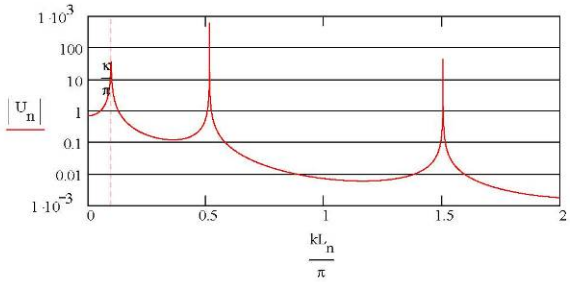
1·10^3
100
10
1
0.1
0.01
1·10^-3
0
0.5
1
1.5
2

Test formula for U at acoustic resonances:

$$\max\left(\text{submatrix}\left(\left|\overrightarrow{U}\right|, 1, \frac{N}{5}, 1, 1\right)\right) = 36.6713 \qquad \max\left(\text{submatrix}\left(\left|\overrightarrow{U}\right|, \frac{N}{5}, \frac{N}{2}, 1, 1\right)\right) = 603.1229$$

$$\frac{\left|1 - \left(\frac{\Omega_1}{\kappa}\right)^2\right|}{\gamma \cdot \Omega_1 \cdot \sin\left(\Omega_1\right)} = 36.6765 \qquad \frac{\left|1 - \left(\frac{\Omega_2}{\kappa}\right)^2\right|}{\gamma \cdot \Omega_2 \cdot \sin\left(\Omega_2\right)} = 788.1028$$

This value actually is better than the computed peak because a finer scan is required.

c

Test formula for U at structural resonances:

$$\left|U_{\text{magnification}}\left(\kappa, H_{\text{static}}, \kappa, \gamma\right)\right| = 9.9195$$

$$\frac{1}{\kappa \cdot \sin(\kappa)} = 10.3007$$

Somewhat larger approximation error because k is close to Ω_2, so $H(\kappa)$ has a larger imaginary part

Case of a high natural frequency: $\kappa := 1.2 \cdot \pi$

Search for kL value giving minimum denominator magnitude:

$H_n := H_{struct}(kL_n, H_{static}, \kappa, \gamma)$ $D_n := Denominator(kL_n, H_{static}, \kappa, \gamma)$ $U_n := \frac{H_n}{D_n}$

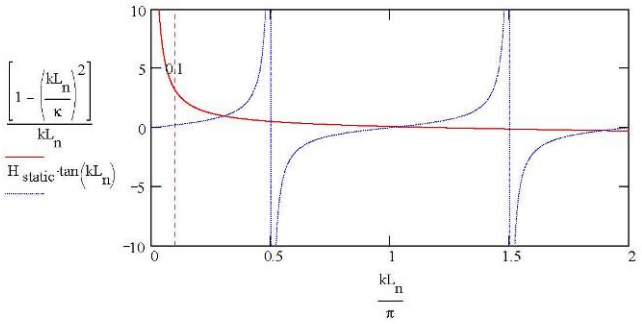

First resonance: $z := 0.3 \cdot \pi$ $\Omega_1 := root\left[\cot(z) - H_{static} \cdot \frac{z}{1 - \left(\frac{z}{\kappa}\right)^2}, z\right]$

Second resonance: $z := 1.1 \cdot \pi$ $\Omega_2 := root\left[\cot(z) - H_{static} \cdot \frac{z}{1 - \left(\frac{z}{\kappa}\right)^2}, z\right]$

$$\frac{\Omega}{\pi} = \begin{bmatrix} 0.3031 \\ 1.0355 \end{bmatrix}$$

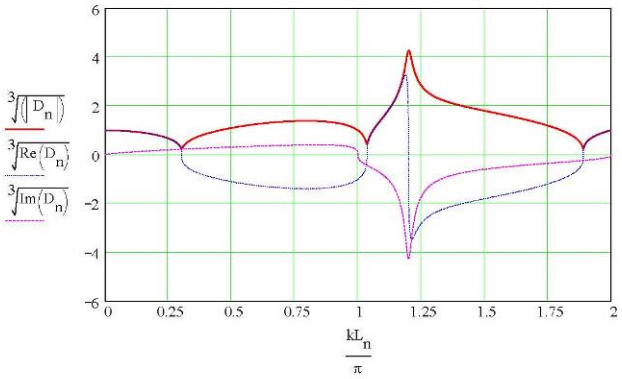
6
4
2
0
−2
−4
−6
0
0.25
0.5
0.75
1
1.25
1.5
1.75
2
$\frac{kL_n}{\pi}$
$\sqrt[3]{|D_n|}$
$\sqrt[3]{Re(D_n)}$
$\sqrt[3]{Im(D_n)}$

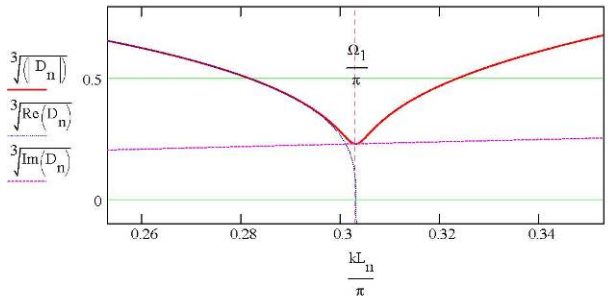
0.5
0
0.26
0.28
0.3
0.32
0.34
$\frac{\Omega_1}{\pi}$
$\frac{kL_n}{\pi}$
$\sqrt[3]{|D_n|}$
$\sqrt[3]{Re(D_n)}$
$\sqrt[3]{Im(D_n)}$

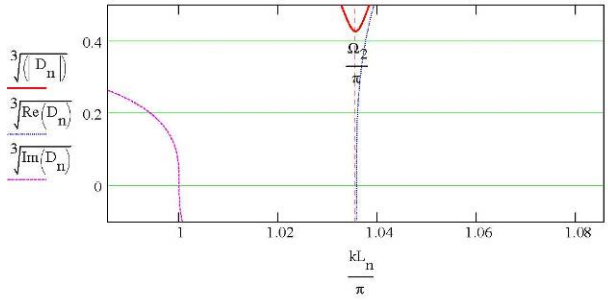
0.4
0.2
0
1
1.02
1.04
1.06
1.08
kL_n / π
Ω2 / π

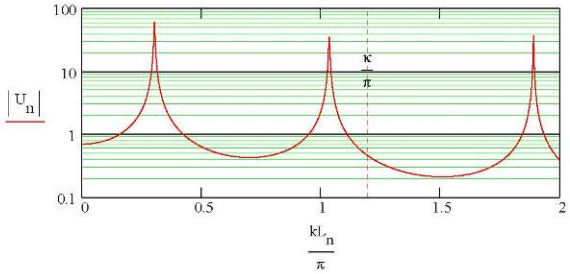
100
10
1
0.1
0
0.5
1
1.5
2
|U_n|
kL_n / π
κ / π

Test formula for U at acoustic resonances:

$$\max\left(\text{submatrix}\left(\overrightarrow{|U|},1,\frac{N}{4},1,1\right)\right)=60.3518 \qquad \max\left(\text{submatrix}\left(\overrightarrow{|U|},\frac{N}{4},\frac{3\cdot N}{4},1,1\right)\right)=35.219$$

$$\frac{\left|1-\left(\frac{\Omega_1}{\kappa}\right)^2\right|}{\gamma\cdot\Omega_1\cdot\sin\left(\Omega_1\right)}=60.35 \qquad \frac{\left|1-\left(\frac{\Omega_2}{\kappa}\right)^2\right|}{\gamma\cdot\Omega_2\cdot\sin\left(\Omega_2\right)}=-35.2193$$

Test formula for U at structural resonances:

$$\left|U_{\text{magnification}}\left(\kappa,H_{\text{static}},\kappa,\gamma\right)\right|=0.4513$$

$$\frac{1}{\kappa\cdot\sin(\kappa)}=-0.4513$$

Combined Acoustic-Structure Resonance

$\kappa := 1.0 \cdot \pi$

Search for kL value giving minimum denominator magnitude:

$H_n := H_{struct}(kL_n, H_{static}, \kappa, \gamma)$ $D_n := Denominator(kL_n, H_{static}, \kappa, \gamma)$ $U_n := \frac{H_n}{D_n}$

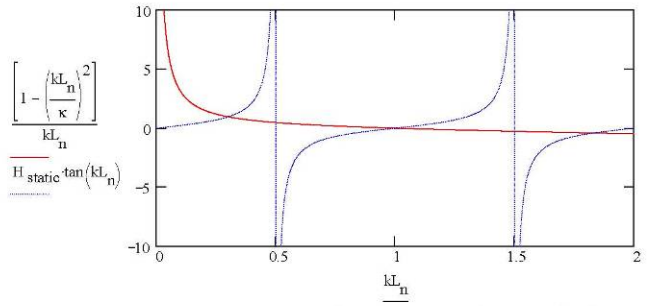

First resonance: $z := 0.3 \cdot \pi$ $\Omega_1 := root\left[H_{static} \cdot \tan(z) - \frac{\left[1 - \left(\frac{z}{\kappa}\right)^2\right]}{z}, z\right]$

Second resonance: $z := 1.0 \cdot \pi$ $\Omega_2 := root\left[H_{static} \cdot \tan(z) - \frac{\left[1 - \left(\frac{z}{\kappa}\right)^2\right]}{z}, z\right]$

$\frac{\Omega}{\pi} = \begin{bmatrix} 0.3002 \\ 1 \end{bmatrix}$

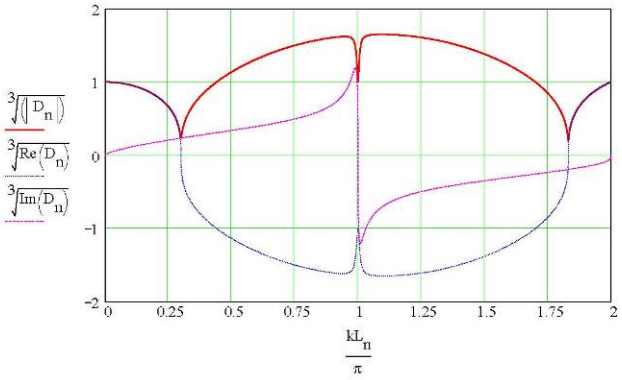
2
1
0
−1
−2
0
0.25
0.5
0.75
1
1.25
1.5
1.75
2
$\frac{kL_n}{\pi}$
$\sqrt[3]{|D_n|}$
$\sqrt[3]{Re(D_n)}$
$\sqrt[3]{Im(D_n)}$

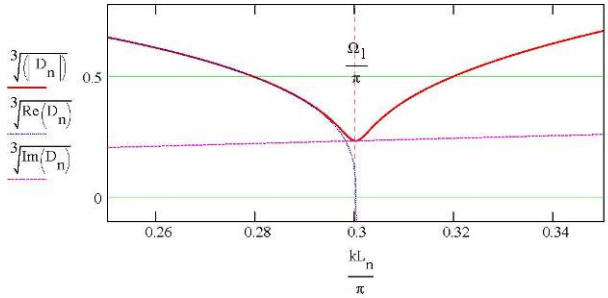
0.5
0
0.26
0.28
0.3
0.32
0.34
$\frac{\Omega_1}{\pi}$
$\frac{kL_n}{\pi}$
$\sqrt[3]{|D_n|}$
$\sqrt[3]{Re(D_n)}$
$\sqrt[3]{Im(D_n)}$

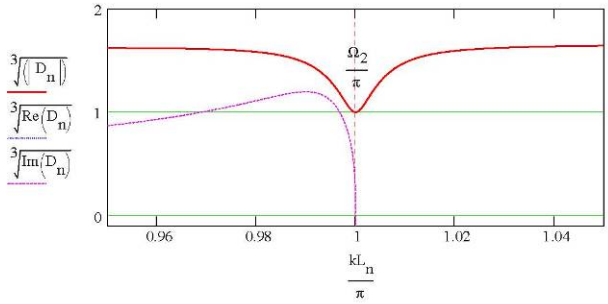
2
1
0
0.96
0.98
1
1.02
1.04
Ω2/π
kLn/π

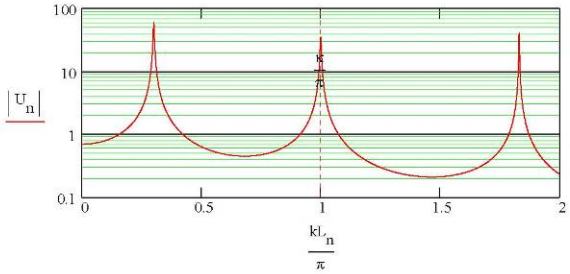
100
10
1
0.1
0
0.5
1
1.5
2
|Un|
kLn/π

Test formula for U at acoustic resonances:

$$\max\left(\text{submatrix}\left(\left|\overrightarrow{U}\right|, 1, \frac{N}{4}, 1, 1\right)\right) = 59.5971 \qquad \max\left(\text{submatrix}\left(\left|\overrightarrow{U}\right|, \frac{N}{4}, \frac{3\cdot N}{4}, 1, 1\right)\right) = 35$$

$$\frac{\left|1 - \left(\frac{\Omega_1}{\kappa}\right)^2\right|}{\gamma\cdot\Omega_1\cdot\sin\left(\Omega_1\right)} = 59.5978 \qquad \frac{H_{static}}{\gamma} = 35$$

One-Dimensional Structure-Acoustic Resonance
Parameter Studies-Structural Damping

$$H_{struct}(kL, H_{static}, \kappa, \gamma) := \frac{H_{static}}{1 - \left(\frac{kL}{\kappa}\right)^2 + i \cdot \gamma}$$

$$Denominator(kL, H_{static}, \kappa, \gamma) := \cos(kL) - H_{struct}(kL, H_{static}, \kappa, \gamma) \cdot kL \cdot \sin(kL)$$

$$U_{magnification}(kL, H_{static}, \kappa, \gamma) := \frac{H_{struct}(kL, H_{static}, \kappa, \gamma)}{Denominator(kL, H_{static}, \kappa, \gamma)}$$

$N := 10 \cdot 10^4$ $\quad n := 1 .. N + 1$ $\quad kL_n := \frac{n - 1}{N} \cdot 2 \cdot \pi$ $\quad \Delta := \frac{2 \cdot \pi}{N}$

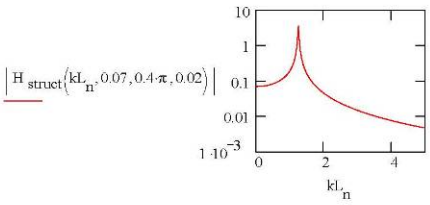

Effect of changing H_{static} with constant natural frequency

Since κ is held constant here, this is the effect of changing stiffness and mass in constant proportion.
Note that increasing H_{static} corresponds to decreasing stiffness.

Moderately stiff system, $\kappa = 0.4\pi$

$|U_{magnification}(kL_n, 0.007, 0.4\cdot\pi, 0.02)|$

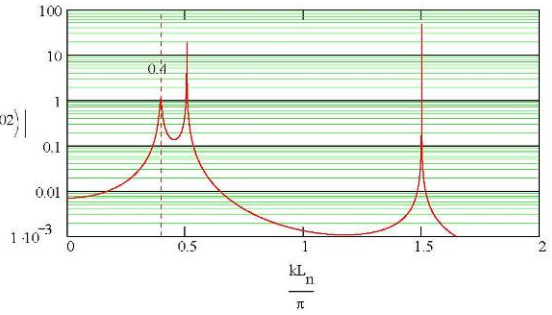

$|U_{magnification}(kL_n, 0.07, 0.4\,\pi, 0.01)|$

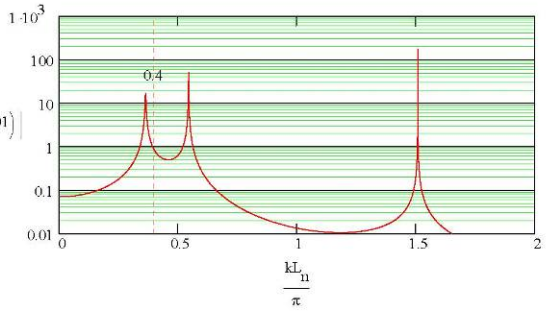

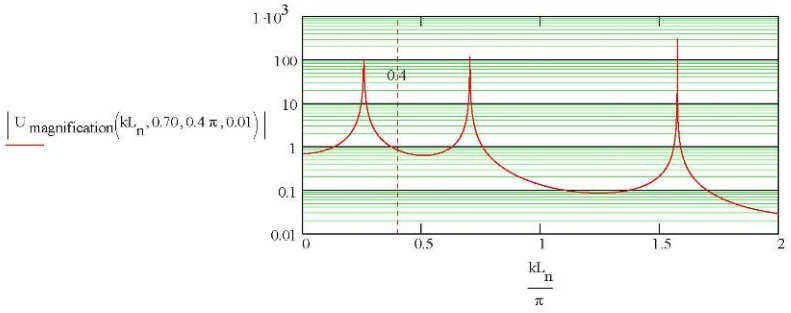

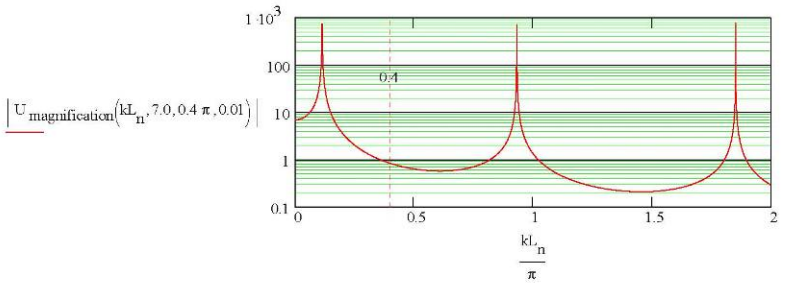

Observation: Raising H_{static}, i.e. lower stiffness with proportional decrease of mass (κ is constant), significantly increases the largest resonance peaks.

Very stiff system, $\kappa = 40\pi$

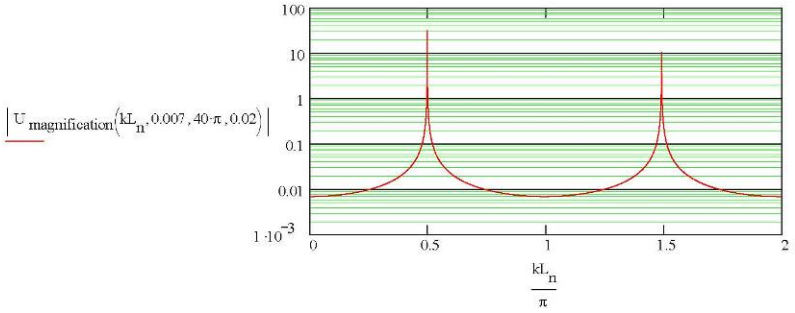

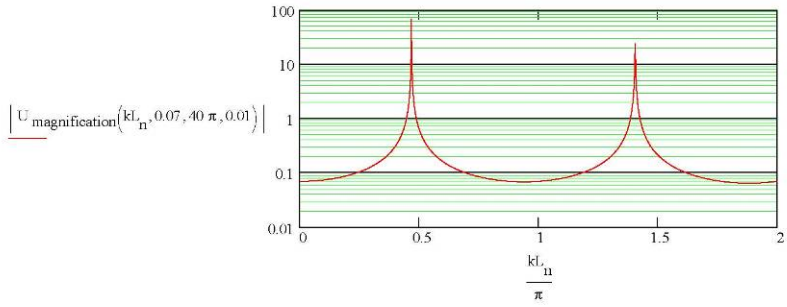

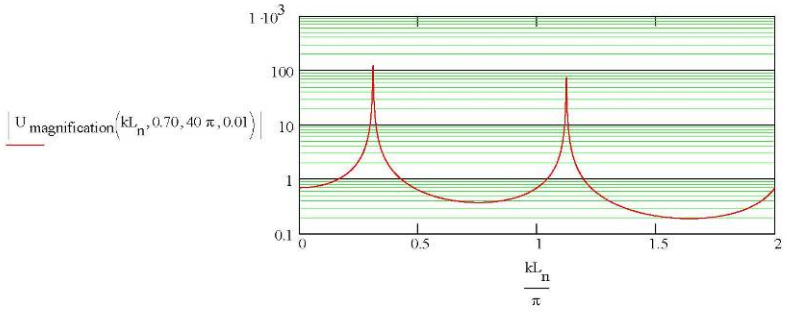

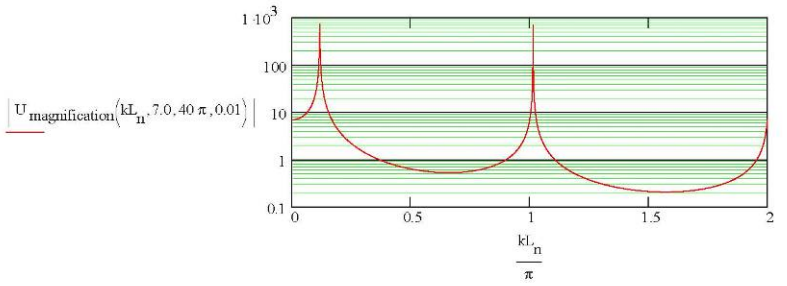

Observation: For a stiff system, raising H_{static} significantly increases the largest resonance peaks only for very high values of H_{static}.

Effect of Changing Stiffness with Constant Mass

Increase H_{static}, with $\kappa^2 H_{static}$ held constant:

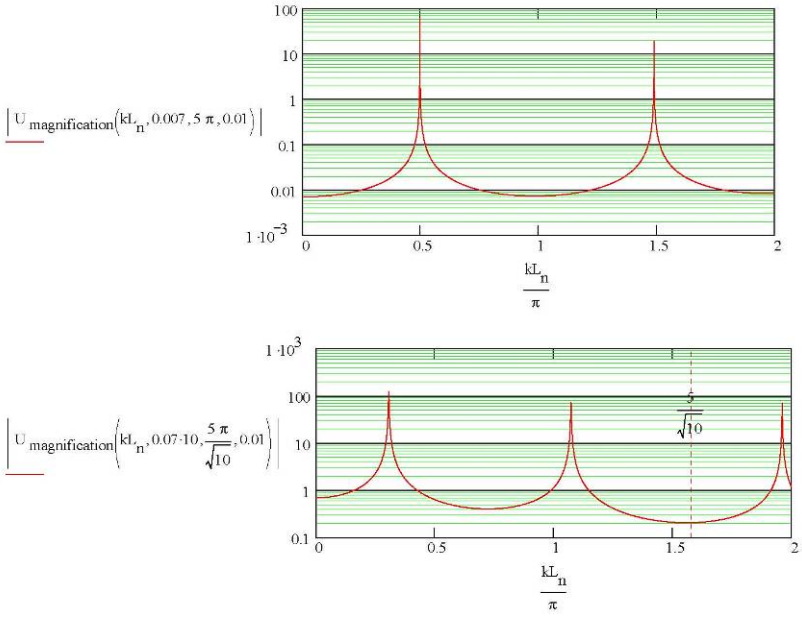

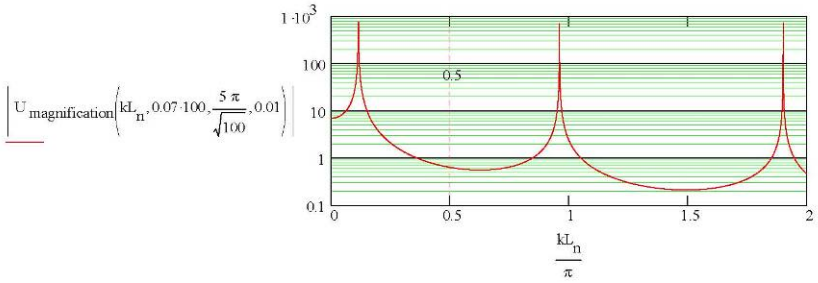

Observation: Raising H_{static}, i.e. lower stiffness, with mass held constant, has little effect on the resonance peaks for stiff cases, but raises peaks for flexible structures.

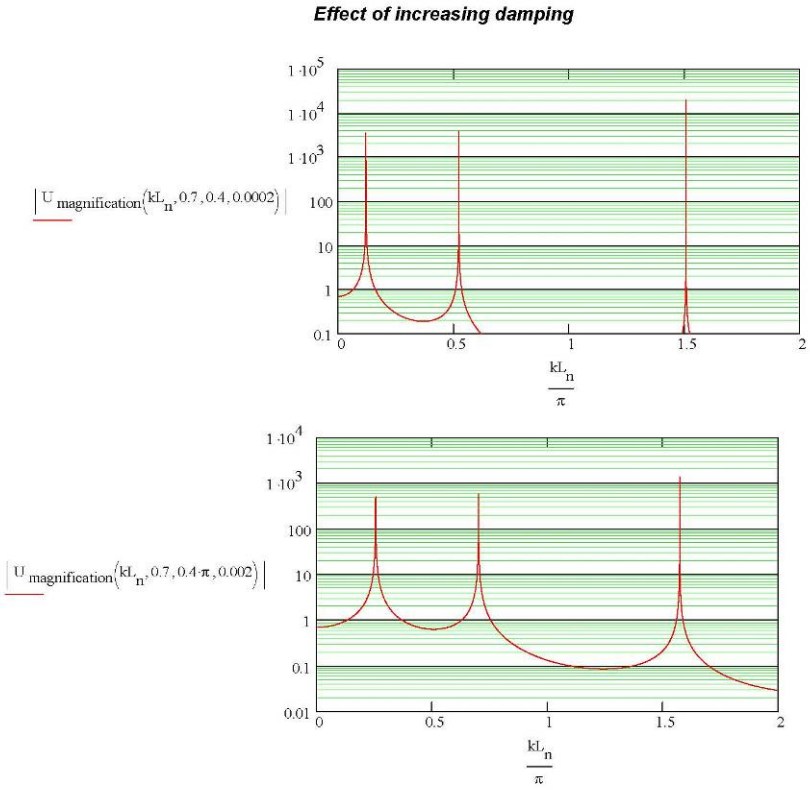
Effect of increasing damping
|U magnification(kL_n, 0.7, 0.4, 0.0002)|
1·10^5
1·10^4
1·10^3
100
10
1
0.1
0
0.5
1
1.5
2
kL_n / π
|U magnification(kL_n, 0.7, 0.4·π, 0.002)|
1·10^4
1·10^3
100
10
1
0.1
0.01
0
0.5
1
1.5
2
kL_n / π

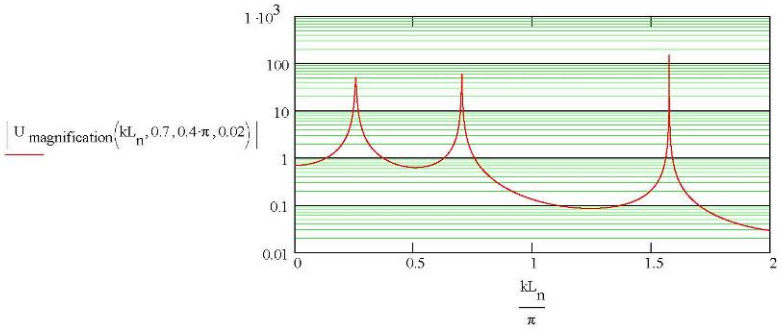

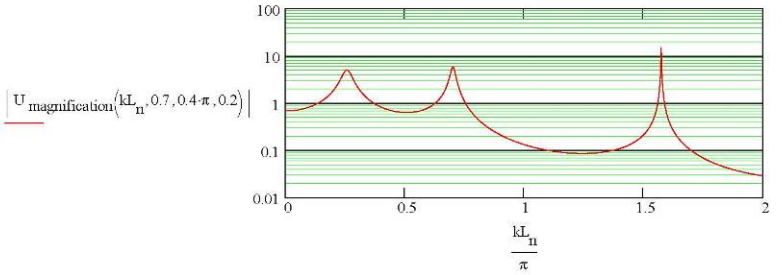

The peak values are inversely proportional to the amount of damping.

Appendix D. Two-Dimensional Model of Coupled Acoustic Cavities – Structure Resonance

Two-Dimensional Model of Coupled Acoustic Cavity - Structure Resonance

Jerry H. Ginsberg
G. W. Woodruff School of Mechanical Engineering
Georgia Institute of Technology

Prepared: 7 January 2005
Analysis section rewritten: 20 June 2005

Contents

(1) Description of model

(2) Analysis

(3) Matlab (Release 12) program

(4) Results for RMS displacement as a function of excitation frequency

(5) Discussion

(6) Analysis of Pressure

(7) Pressure as a function of excitation frequency at selected locations

Description of model

- Rectangular acoustic cavity:
  - Length $= L$, width $= b$
  - Rigid parallel walls at $y = 0$ and $y = b$
  - Open end at $x = L$
  - Acoustic source at $x = L$, $y = 0$ (This is a line source in a three-dimensional perspective)
- Elastic plate at $x = 0$:
  - Thickness $= h$
  - Edges at $y = 0$ and $y = b$ are clamped (no displacement or cross-section rotation)
  - Structural damping loss factor σ, which corresponds to modal critical damping ratios being constant at $\sigma/2$
- Rationale for the model:
  - Determine if it is significant that structural modes and acoustic modes have different spatial patterns
  - Provide a model that is recognizable as being relevant to SOFIA
  - Create a structural model where changing parameters

is apparent in its meaning. (In the one-dimensional model changing stiffness affected the natural frequency and scaled the complex frequency response.)

- Analysis leads to a transfer funtction of the RMS plate displacement for a unit source strength as a function of frequency
- Fluid mechanics would give the source strength as a function of frequency. The full RMS plate response would be the product of the this frequency dependence and the transfer function between the source strength and the RMS displacement

A Two-Dimensional Model of Coupled

Acoustic Cavity-Structure Resonance

Consider a rectangular cavity in which there is no variation of response in the z direction. Two parallel walls are rigid. These form the boundaries $y = 0$ and $y = b$. The wall at $x = 0$ is an elastic plate, and $x = L$ is open. A line source, extending infinitely in the z direction is present very close to the corner at $x = L$, $y = 0$. The system is depicted in the below figure. Significant parameters for the fluid within the cavity are the density ρ and sound speed c. The properties of the elastic plate are the Young's modulus E, density ρ_e, and thickness h. The source has frequency ω, and the analysis is performed in the frequency domain, so the dependence of the pressure field and plate displacement are taken to be

$$\begin{aligned} &\text{Interior pressure:} \quad p = \mathrm{Re}\left(P\left(x,y\right)e^{i\omega t}\right) \\ &\text{Plate displacement:} \quad w = \mathrm{Re}\left(W\left(x\right)e^{i\omega t}\right) \end{aligned} \tag{1}$$

The basic equations for the acoustic domain are the Helmholtz equation which must satisfy boundary conditions derived from the Euler equation at the solid boundaries,

$$\nabla^2 P + k^2 P = 0, \quad k = \frac{\omega}{c} \tag{2}$$

$$\frac{\partial P}{\partial y} = 0 \text{ at } y = 0 \text{ and } y = b \tag{3}$$

$$\frac{\partial P}{\partial y} = -\rho\omega^2 W \text{ at } x = 0 \tag{4}$$

$$P = bP_0\delta\left(y\right) \text{ at } x = L \tag{5}$$

In the last boundary condition bP_0 is the source strength, with b introduced because the Dirac delta function, $\delta\left(y\right)$, along a line of constant x has units of length.

The plate is governed by classical plate theory wih a transverse pressure load that is the acoustic field in its surface,

$$D\frac{d^4W}{dy^4} - \rho_e h\omega^2 W = -\left. P\right|_{x=0}, \quad D = \frac{Eh^3}{12\left(1-\nu^2\right)} \tag{6}$$

Both edges of the plate are taken to be clamped, so

$$W = \frac{dW}{dy} = 0 \text{ at } y = 0 \text{ and } y = b \tag{7}$$

The basic analysis procedure entails describing the response of each medium based on considering the other field to be known. Then the equations of each medium are coupled.

1. Modal Analysis of the Plate

The normalized vibration modes of the plate are denoted as $\Psi_j(y)$. They are known to be

$$\Psi_j(y) = C_{1j}\sin\left(\alpha_j\frac{y}{b}\right) + C_{2j}\cos\left(\alpha_j\frac{y}{b}\right) + C_{3j}\sinh\left(\alpha_j\frac{y}{b}\right) + C_{4j}\cosh\left(\alpha_j\frac{y}{b}\right) \tag{8}$$

The coefficients C_{nj} and eigenvalues α_n are obtained by seeking nontrivial solutions of the equation of motion subject to the boundary conditions and the normalizing condition,

$$\frac{d^4\Psi_j}{dy^4} - \alpha_j^4\Psi_j = 0, \quad \alpha_j = \left(\frac{\rho_e h\omega^2}{D}\right)^{1/4} \tag{9}$$

$$\Psi_j = \frac{d\Psi_j}{dy} = 0 \text{ at } y = 0 \text{ and } y = b \tag{10}$$

$$\int_0^b \rho_e h\left(\Psi_j\right)^2 dy = \rho_e hb \tag{11}$$

Modes that have been normalized in this manner have a modal mass of $\rho_e hb$ and a modal stiffness of equal to $\rho_e hb\omega_j^2$.

Although a frequency domain representation is the ultimate analysis, the initial analysis is done in the time domain. The plate modes form the basis function for a modal series representation of displacememt in which the coefficients η_j are time functions to be determined,

$$w = \sum_{j=1} \Psi_j(y)\,\eta_j(t) \tag{12}$$

Unless indicated otherwise, all sums extend to infinity. The virtual work associated with the pressure loading is

$$\begin{aligned} \delta W &= \int_0^b (-p|_{x=0})\,\delta w(y,t)\,dy \\ &= -\int_0^b p|_{x=0} \left(\sum_j \Psi_j \delta\eta_j\right) dy \end{aligned} \tag{13}$$

Thus the generalized forces are

$$Q_j = -\int_0^b p|_{x=0}\,\Psi_j dy \tag{14}$$

When the pressure is represented in the frequency domain as in Eq. 1, the generalized forces become

$$Q_j = \mathrm{Re}\left(bG_j \exp^{i\omega t}\right) \tag{15}$$

where the coefficients G_j, which have units of pressure, are given by

$$G_j = -\frac{1}{b}\int_0^b P(x=0,y)\,\Psi_j dy \tag{16}$$

The equations governing the modal coordinates are

$$\rho_e hb\left(\ddot{\eta}_j + \omega_j^2 \eta_j\right) = Q_j \tag{17}$$

For a response at frequency ω, the modal coordinates are

$$\eta_j = \mathrm{Re}\left(X_j e^{i\omega t}\right) \tag{18}$$

which corresponds to a modal series for the frequency domain plate displacement given by

$$W = \sum_{j=1} \Psi_j X_j \tag{19}$$

Substitution of the harmonic forms of the modal coordinates, Eq. 18, and generalized forces, Eq. 15, into the modal differential equations leads to

$$X_j = \frac{1}{\rho_e h}\left[\frac{G_j}{\omega_j^2\left(1+i\sigma\right)-\omega^2}\right] \tag{20}$$

2. Acoustical Response

The boundary conditions $\partial P/\partial y = 0$ at $y = 0$ and $y = b$ are identically satisfied by representing the pressure field in terms of a Fourier cosine series in the y direction,

$$P\left(x,y\right) = \sum_{j=1} F_j\left(x\right)\cos\left[\frac{\left(j-1\right)\pi y}{b}\right] \tag{21}$$

Substitution of this expression into the Helmholtz equation, in combinations with the orthogonality of the cosine functions, leads to

$$\frac{d^2F_j}{dx^2} + \left[k^2 - \frac{\left(j-1\right)^2\pi^2}{b^2}\right]F_j = 0 \tag{22}$$

This leads to alternative forms for the general solution, depending on whether the coefficient of F_j in the above is positive or negative,

$$F_j = d_{1j}\sin\left(\beta_j\frac{x}{L}\right) + d_{2j}\cos\left(\beta_j\frac{x}{L}\right) \text{ if } j-1 < \frac{kb}{\pi} \tag{23a}$$

$$F_j = d_{1j}\sinh\left(\beta_j\frac{x}{L}\right) + d_{2j}\cosh\left(\beta_j\frac{x}{L}\right) \text{ if } j-1 > \frac{kb}{\pi} \tag{23b}$$

where

$$\beta_j = \begin{cases} \left[k^2L^2 - \frac{L^2}{b^2}\pi^2\left(j-1\right)^2\right]^{1/2} & \text{if } j-1 < \frac{kb}{\pi} \\ \left[\frac{L^2}{b^2}\pi^2\left(j-1\right)^2 - k^2L^2\right]^{1/2} & \text{if } j-1 > \frac{kb}{\pi} \end{cases} \tag{24}$$

The coefficients d_{1j} and d_{2j} are determined by satisfying the boundary conditions at $x = 0$ and $x = b$. Requiring that the series expansion satisfy Eq. 4 leads to

$$\sum_{j=1} \left. \frac{dF_j}{dx} \right|_{x=0} \cos\left[\frac{(j-1)\,\pi y}{b}\right] = -\rho\omega^2 \sum_{j=1} \Psi_j X_j \tag{25}$$

To exploite the orthogonality property multiply the preceding by a specific cosine function in the series and integrate over $0 < x < b$, which yields

$$\frac{b}{2} \left. \frac{dF_n}{dx} \right|_{x=0} = -\rho\omega^2 \sum_{j=1} X_j \int_0^b \Psi_j \cos\left[\frac{(n-1)\,\pi y}{b}\right] dy \tag{26}$$

This leads to coupling coefficients defined by

$$\Lambda_{nj} = \frac{1}{b} \int_0^b \Psi_j \cos\left[\frac{(n-1)\,\pi y}{b}\right] dy \tag{27}$$

Correspondigly, the boundary condition reduces to

$$\left. \frac{dF_n}{dx} \right|_{x=0} = -2\rho\omega^2 \sum_{j=1} \Lambda_{nj} X_j \tag{28}$$

Regardless of the case for the index j, substitution of either of Eqs. 23 into the preceding leads to

$$\frac{\beta_n}{L} d_{1n} = -2\rho\omega^2 \sum_{j=1} \Lambda_{nj} X_j \text{ for all } n \tag{29}$$

The only condition remaining to be satisfied is the pressure at the open end where the source is located. Substitution of the pressure series, Eq. 21, into Eq. 5 gives

$$\sum_{j=1} F_j\,(x = L) \cos\left[\frac{(j-1)\,\pi y}{b}\right] = bP_0\delta\,(y) \tag{30}$$

Orthogonality of Fourier series basis functions leads to the boundary value of each F_j. Thus, multiply this equation by a specific cosine term and integrate over $0 < y < b$. The Dirac delta integral property then leads to

$$F_n\,(x = L) = 2P_0 \tag{31}$$

This in turn leads to a relation for the coefficients in the general solution for F_j. When Eq. 23 is substituted into this condition, the result is

$$d_{1n}\sin(\beta_n) + d_{2n}\cos(\beta_n) \text{ if } n-1 < \frac{kb}{\pi} \tag{32a}$$

$$d_{1n}\sinh(\beta_n) + d_{2j}\cosh(\beta_n) \text{ if } n-1 > \frac{kb}{\pi} \tag{32b}$$

The last step is to describe the G_j coefficients describing the generalized forces. Substitution of the Fourier pressure series into Eq. 21 gives

$$\begin{aligned} G_j &= -\frac{1}{b}\int_0^b P(x=0,y)\,\Psi_j dy \\ &= \int_0^b \sum_{n=1} F_n(x=0)\cos\left[\frac{(n-1)\pi y}{b}\right]\Psi_j dy \\ &= -\frac{1}{b}\sum_{n=1} F_n(x=0)\int_0^b \cos\left[\frac{(n-1)\pi y}{b}\right]\Psi_j dy \\ &= -\sum_{n=1}\Lambda_{nj}F_n(x=0) = -\sum_{n=1}\Lambda_{nj}d_{2n} \end{aligned} \tag{33}$$

3. Assembly of Equations

It clearly is not possible to extend the series to infinite length, so each is truncated at N terms. The adequacy of the choice of N must be validated by verifying that evaluation of the series gives convergent pressure and displacement fields. The previous sections derived a complete and solvable set of equations governing the coefficients of the pressure and displacement series. Recognition of this fact, as well as identification of a solution strategy, is best done by writing the relevant relations in matrix form. Equation 32 describing the pressure condition at $x = L$ may be written as

$$\boxed{[S]_{N\times N}\{d_1\}_{N\times 1} + [C]_{N\times N}\{d_2\}_{N\times 1} = \{2\}_{N\times 1}P_0} \tag{34}$$

where $\{2\}$ merely denotes an N length matrix whose elements equal 2. Both the $[S]$ and $[C]$ matrices are diagonal, with elements defined as

$$S_{n,n} = \begin{cases} \sin\beta_n \text{ if } n-1 < bk/\pi \\ \sinh\beta_n \text{ if } n-1 > bk/\pi \end{cases}$$
$$C_{n,n} = \begin{cases} \cos\beta_n \text{ if } n-1 < bk/\pi \\ \cosh\beta_n \text{ if } n-1 > bk/\pi \end{cases} \tag{35}$$

The acceleration continuity conditions at $x = 0$, Eq. 29, written in matrix form is

$$\boxed{\{d_1\}_{N\times 1} = -2\rho\omega^2 L\,[E]_{N\times N}\,[\Lambda]_{N\times N}\,\{X\}_{N\times 1}} \tag{36}$$

where $[E]$ is a diagonal array, defined to be

$$E_{n,n} = \frac{1}{\beta_n} \tag{37}$$

Writing Eq. 33 for the generalized force coefficients gives

$$\{G\}_{N\times 1} = -\,[\Lambda]^{\mathrm{T}}\,\{d_2\} \tag{38}$$

This leads to Eq. 20 becoming

$$\boxed{\{X\}_{N\times 1} = \frac{1}{\rho_e h}\,[H]_{N\times N}\,\{G\}_{N\times 1} = -\frac{1}{\rho_e h}\,[H]_{N\times N}\,[\Lambda]^{\mathrm{T}}_{N\times N}\,\{d_2\}_{N\times 1}} \tag{39}$$

where $[H]$ is diagonal, with elements defined to be

$$H_{n,n} = \frac{1}{\omega_j^2(1+i\sigma) - \omega^2} \tag{40}$$

Rather than solving for all of the coefficients simultaneously, a better stategy is to eliminate $\{d_1\}$ and $\{d_2\}$ algebraically. Subsitution of Eq. 36 into Eq. 34 yields

$$\begin{aligned} \{d_2\} &= [C]^{-1}\left\{\{2\}\,P_0 - [S]\,\{d_1\}\right\} \\ &= [C]^{-1}\,\{2\}\,P_0 + 2\rho\omega^2 L\,[C]^{-1}\,[S]\,[E]\,[\Lambda]\,\{X\} \end{aligned} \tag{41}$$

A set of equations for $\{X\}$ then results from substitution of this expression into Eq. 39,

$$\begin{aligned}\{X\} &= -\frac{1}{\rho_e h}[H][\Lambda]^{\mathrm{T}}\{d_2\} \\ &= -\frac{P_0}{\rho_e h}[H][\Lambda]^{\mathrm{T}}[C]^{-1}\{2\} \\ &\quad -\frac{2\rho\omega^2 L}{\rho_e h}[H][\Lambda]^{\mathrm{T}}[C]^{-1}[S][E][\Lambda]\{X\}\end{aligned} \tag{42}$$

Collecting coefficients of $\{X\}$ yields the equations to be solved,

$$\boxed{\begin{aligned}&\left[[I] + 2\frac{\rho L}{\rho_e h}\omega^2[H][\Lambda]^{\mathrm{T}}[C]^{-1}[S][E][\Lambda]\right]\{X\} \\ &\qquad = -\frac{P_0}{\rho_e h}[H][\Lambda]^{\mathrm{T}}[C]^{-1}\{2\}\end{aligned}} \tag{43}$$

4. Nondimensional Equations

Computations are most meaningful if done nondimensionally. Therefore introduce the following nondimensional quantities:

$$\begin{aligned}&\text{Excitation frequency: } \Omega = kL = \frac{\omega L}{c} \\ &\text{Plate natural frequencies: } \hat{\omega}_j = \left(\frac{DL^2}{\rho_e c^2 h b^4}\right)^{1/2}\alpha_j^2 = \left(\frac{Eh^2L^2}{12(1-\nu^2)\rho_e c^2 b^4}\right)^{1/2}\alpha_j^2 \\ &\qquad\qquad = \left(\frac{1}{12(1-\nu^2)}\right)^{1/2}\left(\frac{c_e}{c}\right)\left(\frac{hL}{b^2}\right)\alpha_j^2 \\ &\text{Source pressure level: } \hat{P}_0 = \frac{P_0}{\rho_0 c^2}\end{aligned} \tag{44}$$

where $c_e = (E/\rho_e)^{1/2}$ is the propagation speed of extensional waves in a bar composed of the plate's material. The only coefficient matrix that is dimensional is $[H]$, which is also nondimensionalized such that

$$\left[\hat{H}\right] = \frac{c^2}{L^2}[H] \tag{45}$$

The displacement has units of length, so it is nondimensionalized by L. Also, it is useful to consider the displacement generated by a unit amplitude source. Thus, let

$$\left\{\hat{X}\right\} = \frac{1}{\hat{P}_0 L}\{X\} \tag{46}$$

Thus, the nondimensional equations to solve are

$$\boxed{\left[[I] + 2\frac{\rho L}{\rho_e h}\Omega^2 \left[\hat{H}\right] [\Lambda]^{\mathrm{T}} [C]^{-1} [S] [E] [\Lambda]\right] \left\{\hat{X}\right\} = -\left(\frac{\rho L}{\rho_e h}\right) \left[\hat{H}\right] [\Lambda]^{\mathrm{T}} [C]^{-1} \{2\}} \tag{47}$$

The elements of $[\Lambda]$ are given by Eq. 27 and the other coeffient matrices are diagonal, being given by

$$\hat{H}_{j,j} = \frac{1}{\hat{\omega}_j^2 (1 + i\sigma) - \Omega^2}$$

$$\beta_j = \begin{cases} \left[\Omega^2 - \frac{L^2}{b^2}\pi^2 (j-1)^2\right]^{1/2} & \text{if } j - 1 < \frac{\Omega}{\pi}\frac{b}{L} \\ \left[\frac{L^2}{b^2}\pi^2 (j-1)^2 - \Omega^2\right]^{1/2} & \text{if } j - 1 > \frac{\Omega}{\pi}\frac{b}{L} \end{cases}$$

$$S_{j,j} = \begin{cases} \sin\beta_j \text{ if } j - 1 < \frac{\Omega}{\pi}\frac{b}{L} \\ \sinh\beta_j \text{ if } j - 1 > \frac{\Omega}{\pi}\frac{b}{L} \end{cases} \tag{48}$$

$$C_{j,j} = \begin{cases} \cos\beta_j \text{ if } j - 1 < \frac{\Omega}{\pi}\frac{b}{L} \\ \cosh\beta_j \text{ if } j - 1 > \frac{\Omega}{\pi}\frac{b}{L} \end{cases}$$

$$E_{j,j} = \frac{1}{\beta_j}$$

Solution of these equations gives $\left\{\hat{X}\right\}$ at a specified Ω. In addition to Ω such a solution will depend on the value of a few nondimensional parameters:

$$\begin{gathered} \text{Wave speed ratio: } \frac{c_e}{c} \\ \text{Density ratio: } \frac{\rho_e}{\rho} \\ \text{Poisson's ratio: } \nu \\ \text{Cavity aspect ratio: } \frac{L}{b} \\ \text{Plate thickness: } \frac{h}{b} \\ \text{Structural loss factor: } \sigma \end{gathered} \tag{49}$$

After the value of $\left\{\hat{X}\right\}$ has been evaluated at a specific Ω, the complex displacement amplitude at any location y is evaluated from the modal series,

$$W(y) = P_0 L \sum_{j=1}^{N} \Psi_j(y) \hat{X}_j \tag{50}$$

The mean-squared amplitude, averaged over the span length b, is found to be

$$(W_{\mathrm{RMS}})^2 = \frac{1}{b}\int_0^b W(y) W(y)^* \, dy = P_0 P_0^* \frac{L^2}{b} \int_0^b \left(\sum_{j=1}^{N} \Psi_j(y) \hat{X}_j\right)\left(\sum_{n=1}^{N} \Psi_n(y) \hat{X}_n^*\right) dy \tag{51}$$

The orthogonality condition of the mode functions, Eq. 11, reduces this to

$$\boxed{(W_{\mathrm{RMS}})^2 = |P_0|^2 L^2 \sum_{j=1}^{N} \hat{X}_j \hat{X}_j^* = L^2 \left\{\hat{X}\right\}^{\mathrm{T}} \left\{\hat{X}\right\}} \tag{52}$$

5. Conventional Acoustic Resonance

Consider the situation where the cavity walls are rigid and there is an opening at $x = L$. The acoustic modes in this case are the eigensolutions satisfying the Helmholtz equation

$$\nabla^2 P + k^2 P = 0, \quad k = \frac{\omega}{c} \tag{53}$$

subject to the boundary conditions that

$$\frac{\partial P}{\partial y} = 0 \text{ at } y = 0 \text{ and } y = b, \quad \frac{\partial P}{\partial x} = 0 \text{ at } x = 0, \quad P = 0 \text{ at } x = L \tag{54}$$

A cosine dependence satisfies the boundary conditions at $y = 0$ and $y = L$, so let

$$P = F(x) \cos\left[\frac{(j-1)\pi y}{b}\right] \tag{55}$$

Substitution of this into the Helmholtz equation leads to

$$\frac{d^2 F}{dx^2} + \frac{\beta_j^2}{L^2} F = 0 \tag{56}$$

This is like the case of the plate boundary, except that the only nontrivial solutions will be obtained for $(j-1) < (\Omega/\pi)(b/L)$. Thus, F is trigonometric,

$$F = d_1 \sin\left(\beta_j \frac{x}{L}\right) + d_2 \cos\left(\beta_j \frac{x}{L}\right) \tag{57}$$

Satisfying the rigid boundary conditions at $x = 0$ leads to

$$\frac{\partial P}{\partial x} = 0 \implies d_1 = 0 \tag{58}$$

Then the pressure free condition at $x = L$ requires that

$$\cos\left(\beta_j\right) = 0 \tag{59}$$

so that the eigenvalues are

$$\beta_j = \frac{(2n-1)\pi}{2}, \quad n = 1, 2, \ldots \tag{60}$$

Thus, for each j representing a specific wavelength in the y direction, there are an infinite number of wave numbers n describing the variation in the x direction,

$$\beta_{j,n} = \left[\Omega_{j,n}^2 - \frac{L^2}{b^2}(j-1)^2\pi^2\right]^{1/2} = \frac{(2n-1)\pi}{2}, \quad j, n = 1, 2, \ldots \tag{61}$$

where $\Omega_{j,n}$ denotes the nondimensional natural frequency of a cavity mode. Solving the preceding for this frequency yields

$$\Omega_{j,n} = \left[\frac{(2n-1)^2\pi^2}{4} + \frac{L^2}{b^2}(j-1)^2\pi^2\right]^{1/2} \tag{62}$$

When L/b is close to unity, the fundamental frequency corresponds to $j = 1$ (plane wave relative to the y dependence) and $n = 1$, which gives $\Omega_{\text{fundament}} = \pi/2$. This is much higher than the combined cavity-structure resonant frequency.

```
%%%%%%%%%%%%%%%%%%%%%%   MATLAB PROGRAM   %%%%%%%%%%%%%%%%%%%%%%%%

% Two dimensional model of acoustical resonance
% Parameters are set here
% clear all
syms y real;
c_ratio = 5000/1480; %c(plate)/c(air)
rho_ratio = 7800/1.2; % density(plate)/density(air at sea level)
L_b = 1; % cavity aspect ratio
h = 0.1; % plate thickness (inches)
b = 8; % cavity length (meter)
h_b = h * 0.0254/8; % thickness ratio: h/b
sigma = 0.05; % loss factor
nu = 0.3; % Poisson's ratio

% Series length
N=12;

% Solve eigenvalue problem for plate modes, standard formulas for a clamped
-clamped beam
for j=1:N
    u0 = (j + 0.5)*pi; % Generate an initial guess for the root
    alpha(j) = fzero(inline('cos(x)-1/cosh(x)'),u0); % Solve characteristic
 equation
    % Evaluate ratio of terms for a mode function:
    R(j) = (sin(alpha(j)) - sinh(alpha(j)))/(cos(alpha(j)) - cosh(alpha(j))
);
end
nat_freq = (1/sqrt(12 * (1 - nu^2))) * c_ratio * L_b *h_b * alpha.^2;

% Mode functions using the Symbolic Toolbox
for j = 1:N
    % Acoustic mode functions in y direction:
    theta(j) = cos((j - 1)*pi*y);
    % Use the asmptotic approximation of beam mode functions above the four
th mode because
    % the hyperbolic functions cause numerical difficulty when their argume
nt is large
    if j < 5
        psi(j) = (sin(alpha(j)*y) - sinh(alpha(j)*y)) - R(j) * (cos(alpha(j
)*y) - cosh(alpha(j)*y));
    else
        psi(j) = sin(alpha(j)*y) - cos(alpha(j)*y) + exp(-alpha(j)*y)-((-1)
^j)*exp(-alpha(j)*(1-y));
    end
```

```
end

% Normalize the mode functions
for j=1:N;
    MU = int(psi(j)^2,y,0,1); %Modal mass for unnormalized functions
    mu(j) = double(MU);
    PSI(j) = psi(j)/sqrt(mu(j));
end
for j=1:N;  for n=1:N;
            lambda(j,n)=int(psi(j)*theta(n),y,0,1);
end; end

LAMBDA = real(double(lambda)); % Convert symbolic to numerical value

im = i;
% Evaluate response at M frequencies up to the natural frequency of mode N/↙
2
M = 1000; d_OMEGA = 1.1 * nat_freq(N/2)/M;

% Begin computation of complex amplitudes
for m = 1:M
    OMEGA(m) = d_OMEGA * m;
    if 20*floor(m/20)==m
        [m OMEGA(m)]
    end
    for j = 1:N
        H(j,j) = 1/(nat_freq(j)^2 * (1 + im*sigma) - OMEGA(m)^2);
        if (j-1)<OMEGA(m)/(L_b * pi)
            beta(j) = sqrt(OMEGA(m)^2 - (j-1)^2 * L_b^2 * pi^2);
            S(j,j) = sin(beta(j));
            C(j,j) = cos(beta(j));
        else
            beta(j) = sqrt((j-1)^2 * L_b^2 * pi^2 - OMEGA(m)^2);
            S(j,j) = sinh(beta(j));
            C(j,j) = cosh(beta(j));
        end
        E(j,j) = 1/beta(j);
    end
    % System of equations is [A] {X} = {B}
    A = eye(N) + 2 * (1/rho_ratio) * (L_b/h_b) * OMEGA(m)^2 * H * LAMBDA.' ↙
* C^(-1) * S * E * LAMBDA;
    B = - (1/rho_ratio) * (L_b/h_b) * H * LAMBDA.' * C^(-1) * diag(2 * eye(↙
N));
    X(:,m) = A\B;
    RMS(m) = norm(X(:,m));
```

```
    % Evaluate norm of [H], which will be large at natural frequencies of st
ructure
    H_mag(m) = norm(H,'fro');
    % Evaluate determinant of [A] which will be small at the resonances of t
the coupled system
    Det_A(m) = abs(det(A));
end

% This plot monitors the dependence of each coefficient. It is not needed.
figure(1)
semilogy(OMEGA,abs(X(1,:)),'-', OMEGA,abs(X(2,:)), ':',...
    OMEGA,abs(X(3,:)),'-.', OMEGA,abs(X(4,:)),'--',...
    OMEGA,abs(X(5,:)),'-', OMEGA,abs(X(6,:)),'-', 'LineWidth',2)
title(['h = ', num2str(h), ' inches,  \sigma = ', num2str(sigma)])
xlabel('Excitation frequency \Omega'); ylabel('Modal coefficients');
legend('X(1)', 'X(2)', 'X(3)', 'X(4)', 'X(5)', 'X(6)');

% This plot shows the frequency dependences of the RMS displacement, as wel
l as det_A and H_mag.
% Natural frequencies are shown as diamond symbols
figure(2)
x_nat_freq = nat_freq(1:N/2);
y_dum(1:N/2) = 2 * min([H_mag,Det_A,RMS]);
semilogy(OMEGA,RMS,'r-', OMEGA,H_mag,'b:', OMEGA,Det_A,'m-.',...
    x_nat_freq, y_dum,'kd', 'LineWidth',2)
title(['h = ', num2str(h), ' inches,  \sigma = ', num2str(sigma)])
xlabel('Excitation frequency \Omega');
legend('RMS displacement', 'mag(H)', 'det(A)', 'Plate natural freqs.');
```

Results: Steel plate, air at sea level

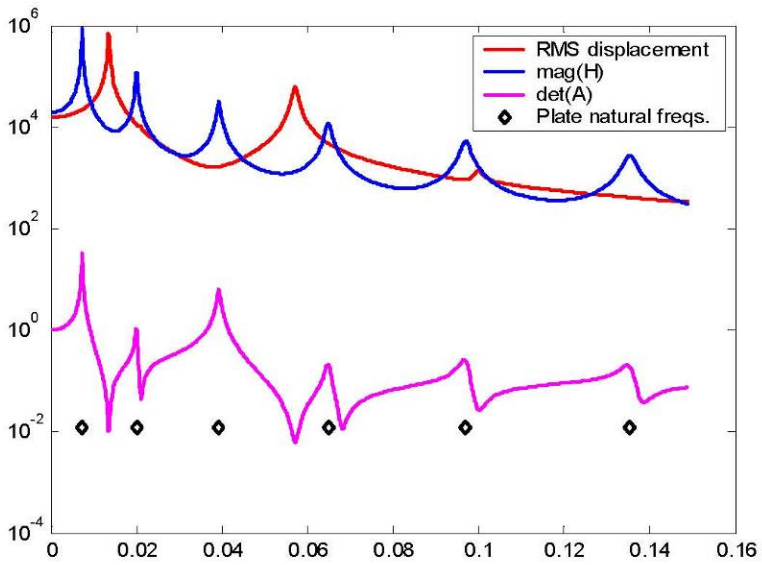

$h = 0.1$ in., $\sigma = 0.02$

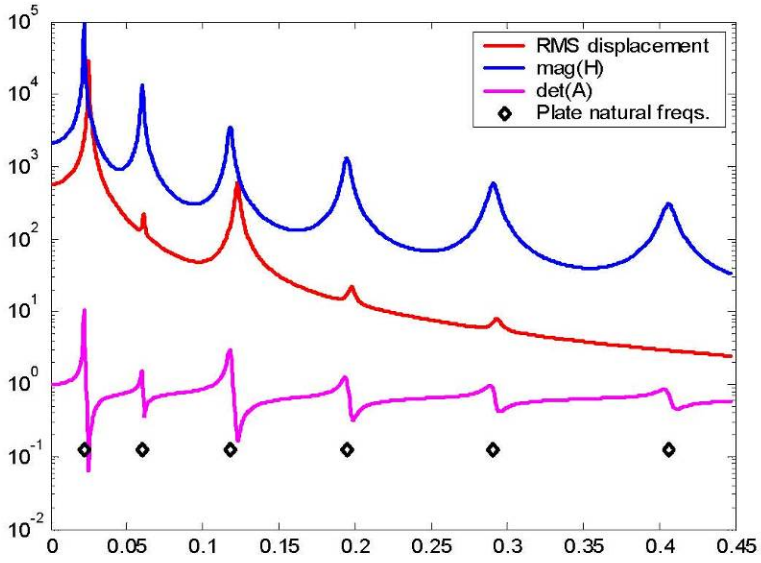

$h = 0.3$ in., $\sigma = 0.02$

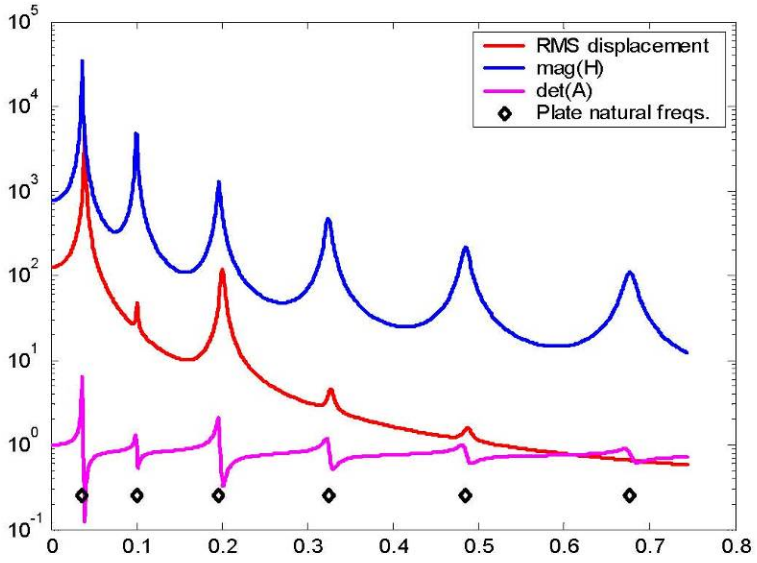

$h = 0.5$ in., $\sigma = 0.02$

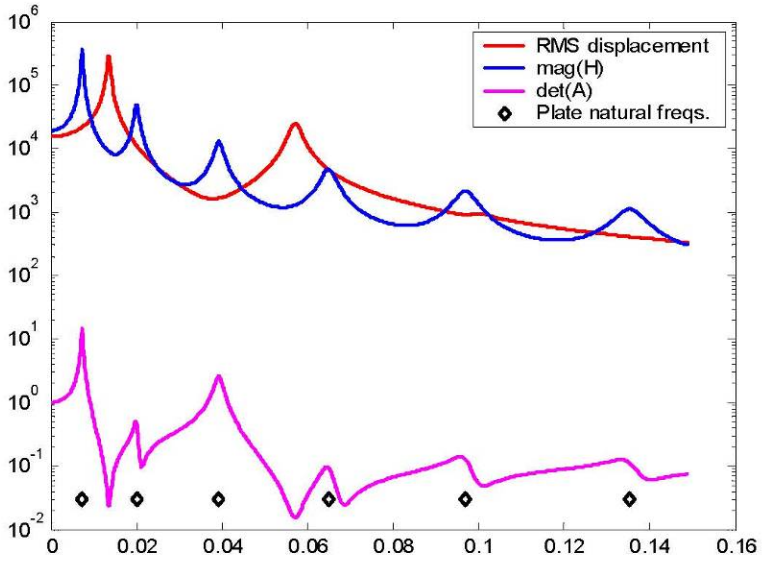

$h = 0.1$ in., $\sigma = 0.05$

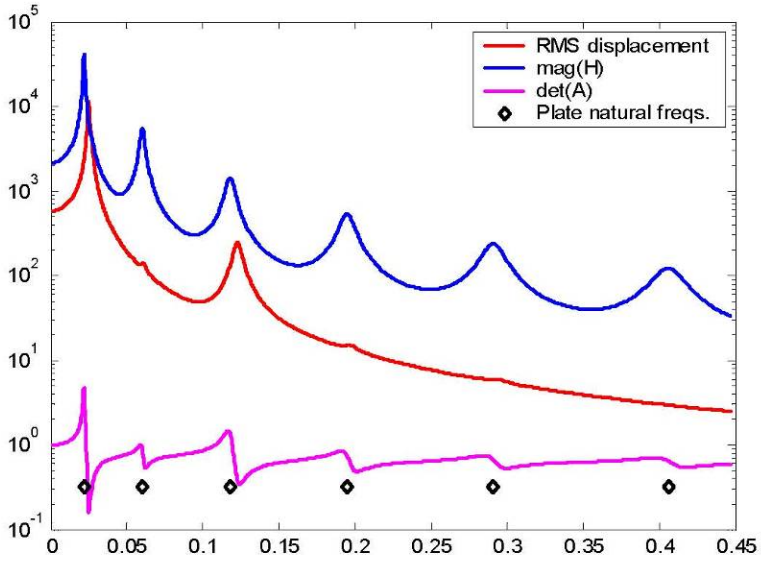

$h = 0.3$ in., $\sigma = 0.05$

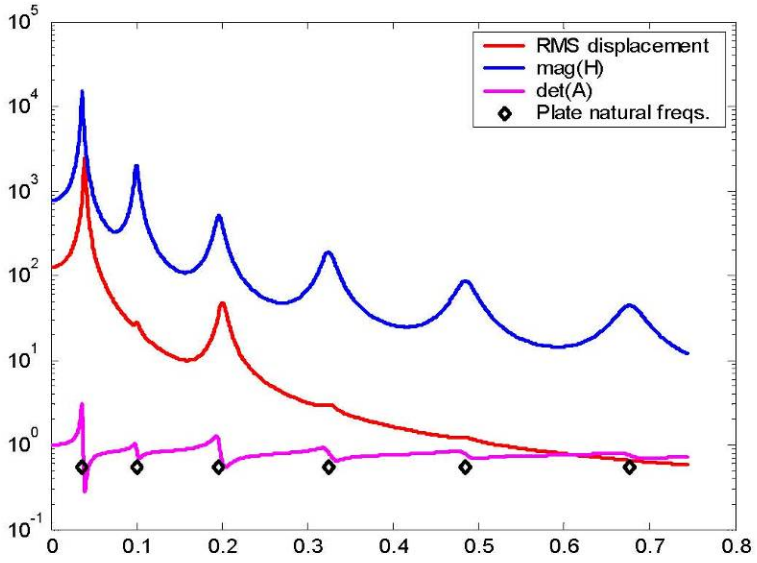

$h = 0.5$ in., $\sigma = 0.05$

Discussion of Plate Displacement

- The general form of the matrix equation for $\{X\}$ is like that in the one-dimensional model. To see this, multiply eq. (22) in the analysis by $[H]^{-1} = [D]$, which is the dynamic stiffness. This leads to

$$\left[[D] + 2\frac{\rho L}{\rho_e h}\Omega^2 [\Lambda]^{\mathrm{T}} [C]^{-1} [S] [1/\beta] [\Lambda]\right] \{X\} = -\frac{\rho L}{\rho_e h} [\Lambda]^{\mathrm{T}} [C]^{-1} \left(\hat{P}_0 L\right)$$

  The left coefficient matrix is the structural stiffness plus the acoustic impedance.
  - At structural resonances, $[D]$ becomes small so the response is decided by the acoustic impedance
  - At coupled resonances, the determinant of the coefficient of $\{X\}$ would be zero if there were no damping, $\sigma = 0$, which makes $[H]$ real.
- The density of air occurs solely as $\rho L/\rho_e L$, which multiplies $[H]$ in eq. (22). The nondimensional plate natural frequencies, eq. (23), are inversely proportional to the sound speed in air, which is the only occurrence of c. In both occurrences, the fluid property occurs reciprocally with the plate thickness h. Raising the

altitude decreases ρ significantly and c slightly. Thus, increasing altitude is like increasing h.

- Consider the plots for various h at fixed σ :
  - The frequency scale increases as h increases because the natural frequencies of the plate are proportional to h.
  - Increasing h shifts the resonance frequencies upward.
  - For the largest $h = 0.5$ inch the acoustic resonances occur at frequencies that are slightly above the natural frequencies. This is analogous to the stiff structure case in the one-dimensional model. Decreasing h leads to acoustic resonances that occur at frequencies that are above the corresponding plate natural frequency.
  - The RMS displacement is largest at the first acousic resonance for each h.
    The peak RMS displacement (first resonance) is almost inversely proportionately to h. This suggests that making the structure stiffer is beneficial.
  - For the thinnest case, $h = 0.1$ inch, there is no resonance in the plate response at three frequencies where $\det([A])$ becomes small. This suggest that

a modal analysis of the SOFIA acoustic cavity that accounts for the structural compliance will provide a conservative estimate of potentially dangerous frequencies.

- Consider the plots for two σ values at fixed h :
  - The peak RMS displacement (first resonance) is almost inversely proportionately to σ.
  - Some resonances dissappear with increasing σ
- General conclusions:
  - If resonances should be found to be a problem, the only recourse from a structural viewpoint is strengthening the structure, which is not feasible, or increasing the damping, which can be done.
  - The plots of RMS displacement vs frequency are for a constant source strength. The Rossiter mode (?) model for a turbulent source gives a strength that also shows resonances. If these resonances occur at the acoustic-structure coupled resonances, the result could be disastrous.
  - Since coupling between the cavity acoustic domain and the structure has apparently not been quantitatively examined for SOFIA, either analytically or

experimentally, insufficient information is available to determine whether a serious resonance might occur.

6. Pressure Evaluation

After Eq. 47 has been solved for $\left\{\hat{X}\right\}$ at a specified Ω, the pressure field can be evaluated by returning to the intermediate equations to determine the coefficients d_{1n} and d_{2n}. Replacing the dimensional parameters in Eq. 36 with the nondimensional definitions gives

$$\boxed{\{d_1\} = -2\rho\left(\frac{c\Omega}{L}\right)^2 L\,[E]\,[\Lambda]\,\hat{P}_0 L\left\{\hat{X}\right\} = -\left(\rho c^2 \hat{P}_0\right) 2\Omega^2\,[E]\,[\Lambda]\left\{\hat{X}\right\}} \tag{63}$$

The corresponding operations applied to Eq. 41 leads to

$$\boxed{\begin{aligned}\{d_2\} &= [C]^{-1}\{2\}\left(\rho c^2 \hat{P}_0\right) + 2\rho\left(\frac{c\Omega}{L}\right)^2 L\,[C]^{-1}\,[S]\,[E]\,[\Lambda]\,\hat{P}_0 L\left\{\hat{X}\right\} \\ &= \left(\rho c^2 \hat{P}_0\right)\left\{[C]^{-1}\{2\} + 2\Omega^2\,[C]^{-1}\,[S]\,[E]\,[\Lambda]\left\{\hat{X}\right\}\right\}\end{aligned}} \tag{64}$$

Note that $\rho c^2 P_0$ is the dimensional source level, so the accompanying factors in the expressions for $\{d_1\}$ and $\{d_2\}$ are transfer functions.

The pressure at any location is given by the Fourier series, Eq. 21, and the general solution in Eq. 23. To use them in conjunction with the solutions for $\{d_1\}$ and $\{d_2\}$, define

$$\Phi_{S,j}(x,y) = \begin{cases} \sin\left(\beta_j \frac{x}{L}\right)\cos\left(\frac{(j-1)\pi y}{b}\right) & \text{if } j-1 < \frac{kb}{\pi} \\ \sinh\left(\beta_j \frac{x}{L}\right)\cos\left(\frac{(j-1)\pi y}{b}\right) & \text{if } j-1 > \frac{kb}{\pi} \end{cases}$$

$$\Phi_{C,j}(x,y) = \begin{cases} \cos\left(\beta_j \frac{x}{L}\right)\cos\left(\frac{(j-1)\pi y}{b}\right) & \text{if } j-1 < \frac{kb}{\pi} \\ \cosh\left(\beta_j \frac{x}{L}\right)\cos\left(\frac{(j-1)\pi y}{b}\right) & \text{if } j-1 > \frac{kb}{\pi} \end{cases} \tag{65}$$

This allows Eq. 21 to be written as

$$\boxed{\begin{aligned}P(x,y) &= \sum_{j=1}^{N}\left[\Phi_{S,j}(x,y)\,d_{1j} + \Phi_{C,j}(x,y)\,d_{2j}\right] \\ &= [\Phi_S]\{d_1\} + [\Phi_C]\{d_2\}\end{aligned}} \tag{66}$$

Pressures @ $y/b = 0,\ 0.5$,and 1 for fixed x

$h = 0.1, \sigma = 0.2$

Max scale $= 10^3$

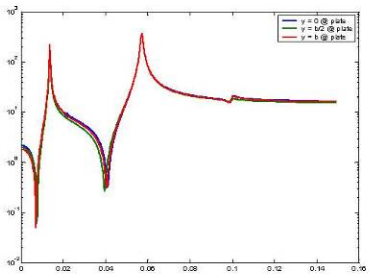

$x/L = 0$

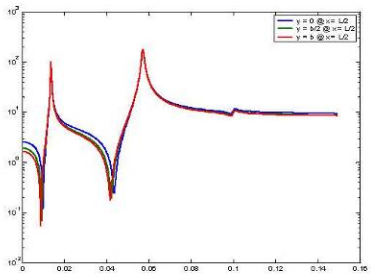

$x/L = 0.5$

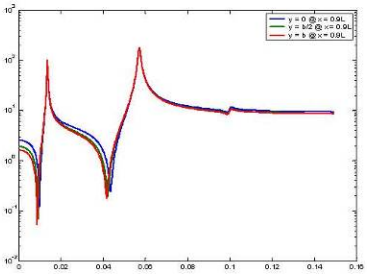

$x/L = 0.9$

Pressure @ $y/b = 0,\ 0.5$,and 1 for fixed x

$h = 0.3, \sigma = 0.2$

Max scale $= 10^2$

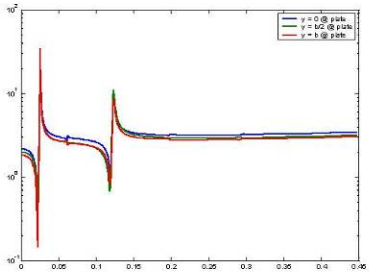

$x/L = 0$

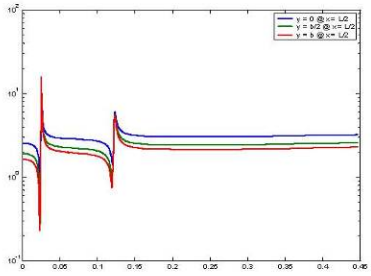

$x/L = 0.5$

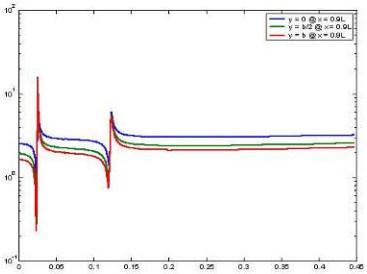

$x/L = 0.9$

Pressure @ $y/b = 0,\ 0.5$,and 1 for fixed x

$h = 0.5, \sigma = 0.2$

Max scale $= 10^2$

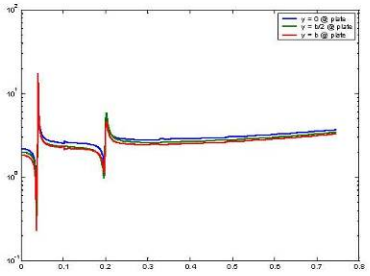

$x/L = 0$

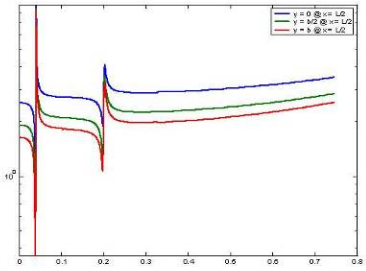

$x/L = 0.5$

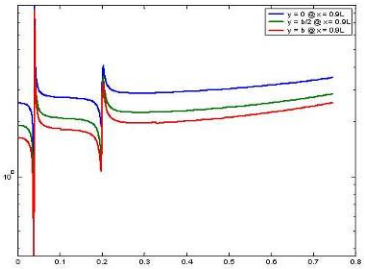

$x/L = 0.9$

Pressure @ $y/b = 0,\ 0.5$,and 1 for fixed x

$h = 0.1, \sigma = 0.5$

Max scale $= 10^3$

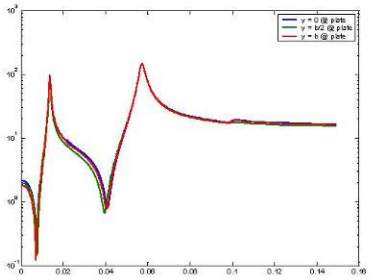

$x/L = 0$

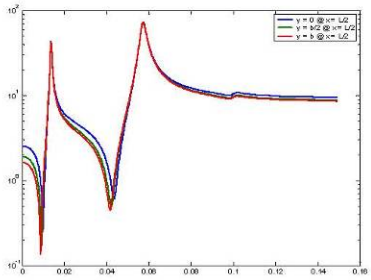

$x/L = 0.5$

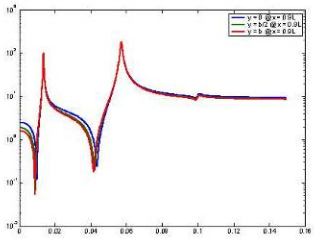

$x/L = 0.9$

Pressure @ $y/b = 0,\ 0.5$,and 1 for fixed x

$h = 0.3, \sigma = 0.5$

Max scale $= 10^2$

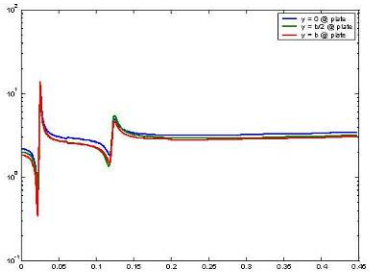

$x/L = 0$

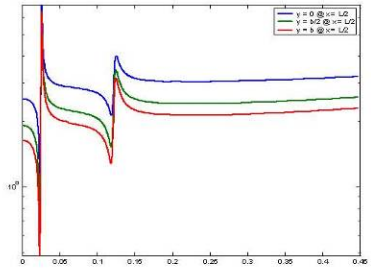

$x/L = 0.5$

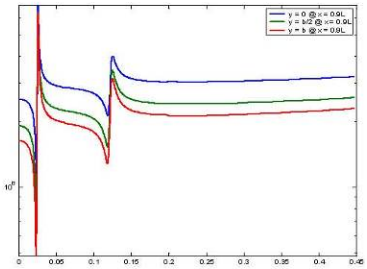

$x/L = 0.9$

Pressure @ $y/b = 0,\ 0.5$,and 1 for fixed x

$h = 0.5, \sigma = 0.5$

Max scale $= 10$

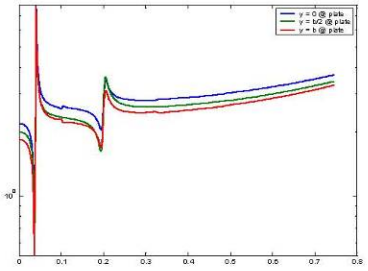

$x/L = 0$

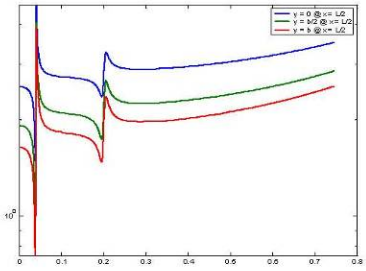

$x/L = 0.5$

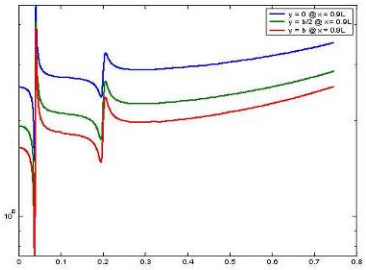

$x/L = 0.9$

Appendix E. A General Analysis of the Responseof an Acoustic Cavity Bounded by an Elastic Structure

A General Analysis of the Response of an Acoustic Cavity Bounded by an Elastic Structure to Acoustic Excitation

Jerry H. Ginsberg

19 March 2005

Problem Description

(1) An arbitrarily shaped acoustic cavity.

(2) An arbitrary elastic structure with structural damping bounding some or all of the cavity.

(3) Two types of boundary conditions:
- Local impedance: pressure at a point on the surface is taken to be proportional to local velocity in the normal direction.
- Elastic structure: local pressure globally excites surface displacement.

(4) Combine governing equations:
- Structural response to a known surface pressure.
- Acoustic response to known motion of structure and acoustic source.

(5) Eliminate excess variables to determine:
- Transfer function for structural response generated by a known acoustic source.
- Transfer function for acoustic field generated by a known acoustic source.

(6) Derive global conclusions from general equations.

Basic Governing Equations

- Acoustic domain:
  - Acoustic source excitation at frequency ω distributed over some region.
  - Helmholtz equation governs complex pressure amplitude at all locations in cavity.
  - Boundary conditions: Relate pressure and normal particle velocity in fluid at boundary location $\bar{x}_B$.
  - Local impedance regions:
    - Compliant material $P(\bar{x}_B) = -Z(\bar{x}_B)\,\bar{v}(\bar{x}_B) \cdot \bar{n}(\bar{x}_B)$.
    - Specific impedance Z is a known material property that may depend on location.
      - Model often used for acoustical liners.
      - Limiting cases: Rigid walls, $Z \to \infty$, and pressure-release regions, $Z = 0$.

* Cavity opening:
  - To a first approximation $Z = 0$, but this breaksdown for SOFIA, where the opening is large compared to an acoustic wavelength.
  - A reasonable approximation is that Z has a small real part, corresponding to acoustic radiation to the atmosphere.
  - Euler's equation: $\nabla P = i\omega\rho_0\bar{v}$, so the impedance boundary converts to Robin-type boundary condition on pressure. Hence, the particle velocity on this portion of the boundary is removed from the problem.

– Elastic boundary:
  * · Complex amplitude of structural displacement on boundary is $\bar{U}(\bar{x}_B)$, velocity is $i\omega\bar{U}$.
  - Structural displacement at all locations are mutually coupled.
  - Consequently, enforcing Euler's equation does eliminate velocity variables.

- Acoustic field modeled by a discretizing procedure (boundary elements, finite elements, surface variational principle, Ritz series) .
  - Source excitation $\mathrm{Re}\{P_S\}\exp(i\omega t)$.
  - Pressure variables: Complex amplitudes consitute an array of J unknowns $\{P\}$.
  - Structural displacements at all locations described by N complex amplitudes $\{U\}$.

– Governing equation:

$$[A(\omega)]_{J\times J}\{P\}_{J\times 1} = \omega^2 [B]_{J\times N}\{U\}_{N\times 1} + [D]\{P_S\} \quad (1)$$

* Notes:
  - $[A]$, $[B]$, and $[D]$ are the result of the discretization modeling procedure.
  - Although $\{U\}$ consists of all displacement variable, in cases where they represent mesh point displacements, $[B]$ will have nonzero elements only for the wet surface displacements in the normal direction. (This is irrelevant to the following analysis.)
  - $[A]$ may be complex, $[B]$ and $[D]$ are real. (This too is not essential to the analysis.)

- Structural Dynamics
  - Generalized coordinates for displacement $\{U\}$
  - Standard modeling techniques yield stiffness $[K]$ and inertia $[M]$
  - Structural damping: loss factor σ
  - Map pressure field into generalized forces: $[B]$
  - Governing equation:

$$\left[[K](1+i\sigma)-\omega^2[M]\right]_{N\times N}\{U\}_{N\times 1}=[\Lambda]_{N\times J}\{P\}_{J\times 1} \tag{2}$$

  - Define complex frequency response (transfer function):

$$[H_S(\omega)]=\left[[K](1+i\sigma)-\omega^2[M]\right]^{-1} \tag{3}$$

  - Displacement for a known pressure field:

$$\{U\}=[H_S(\omega)][\Lambda]\{P\} \tag{4}$$

- Coupled Equations
  - Use eq. (4) to eliminate $\{U\}$ from pressure equations:

$$[A(\omega)]\{P\} = \omega^2 [B][H_S(\omega)][\Lambda]\{P\} + [D]\{P_S\} \quad (5)$$

  - Solve for pressure $\Longrightarrow$ Source to pressure transfer function:

$$[H_P(\omega)] \equiv \left[[A(\omega)] - \omega^2 [B][H_S(\omega)][\Lambda]\right]^{-1} \quad (6)$$

  - Pressure field generated by the source:

$$\{P\} = [H_P(\omega)][D]\{P_S\} \quad (7)$$

  - Displacement generated by the source:

$$\{U\} = [H_S(\omega)][\Lambda][H_P(\omega)][D]\{P_S\} \quad (8)$$

Direct Observation

- Resonant frequencies:
  - Structural: Natural frequencies are values of ω that give

$$\min\left(\left|[K](1+i\sigma)-\omega^2[M]\right|\right) \Longrightarrow \max\left[H_S(\omega)\right] \quad (9)$$

  - Acoustic: Values of ω that give

$$\min\left(\left|[A(\omega)]-\omega^2[B][H_S(\omega)][\Lambda]\right|\right) \Longrightarrow \max\left[H_P(\omega)\right] \quad (10)$$

  - Acoustic cavity with rigid walls:
    - $[K] \rightarrow \infty \Longrightarrow [H_S(\omega)] \rightarrow 0$
    - If there is no place to dissipate energy, which means that $\mathrm{Re}(Z) = 0$ at boundaries, then

$$\text{Rigid cavity resonance} \implies |[A(\omega)]| = 0 \quad (11)$$

- General trends
  - At a structural resonance frequency, norm($[H_S(\omega)]$) is large.
  - Because $[A(\omega)]$ has no singularities, $|[A(\omega)] - \omega^2[B][H_S(\omega)][\Lambda]$ will not be small, so

    Structural natural frequencies will not match resonance frequencies of coupled system

  - The dominant term in $[H_P(\omega)]$ is the contribution of $[H_S(\omega)]$, so eq. (8) is approximated as

$$\{U\} = -\omega^{-2}[H_S(\omega)][\Lambda][[B][H_S(\omega)][\Lambda]]^{-1}[D]\{P_S\} \quad (12)$$

  - Thus, the singularity of $[H_S(\omega)]$ is annihilated. In other words, the poles of the $[H_S(\omega)]$ transfer function are near-zeros of the $[H_P(\omega)]$ transfer function. Consequently,

    The displacement will not be large at the structure's natural frequencies

– Away from structural resonances, $[H_S(\omega)]$ decreases as the structure's stiffness increases, so

Acoustic resonance frequencies approach the structure's natural frequencies as the stiffness increases

Further Analysis

- Need to derive analytical expressions that enable comparisons:
  - Peak transfer function values at various types of resonances
  - Relation of peak transfer functions in wind-tunnel experiments vs. what can be expected at full scale
- Pole-residue representations of the transfer functions
  - Structural dynamics:
    - Classical modal analysis: General eigenvalue problem:

$$[\Phi]^{\mathrm{T}}[M][\Phi] = [I], \quad [\Phi]^{\mathrm{T}}[K][\Phi] = \mathrm{diag}\left(\omega_S^2\right) \qquad (13)$$

where $\mathrm{diag}\left(\omega_S^2\right)$ denotes a diagonal array of squares of the natural frequencies and $[\Phi]$ is the normal mode matrix.

* Complex amplitudes of the response to an arbitrary set of forces $\{F\}$ at excitation frequency ω :

$$\{U\} = [H_S(\omega)]\{F\} \tag{14}$$

where

$$[H_S(\omega)] = \sum_{n=1}^{N} \frac{\{\Phi_n\}\{\Phi_n\}^{\mathrm{T}}}{(\omega_S)_n^2(1+i\sigma) - \omega^2} \tag{15}$$

* Resonance occurs when ω equals any of the natural frequencies and σ is small. The $(\omega_s)_j$ values consititute a double pole, and the corresponding numerator is the residue.

– Coupled acoustic cavity and structure:
  * The transfer function $[H_P(\omega)]$ can be represented in pole-residue form. In some formulations this can be developed directly from the equation for $[H_p(\omega)]$, and experimental modal analysis algorithms always can be used for this purpose.
  * The poles are complex eigenvalues,

$$\left|[A(\omega)] - \omega^2[B][H_S(\omega)][\Lambda]\right| = 0 \iff \lambda = (\lambda_P)_j \tag{16}$$

* These eigenvalues occur as conjugate pairs:
  - $\mathrm{Im}(\lambda_P)_j = \pm(\omega_P)_j$: the natural frequency of a cavity mode
  - $\mathrm{Re}(\lambda_p)_j = -(\zeta_P)_j(\omega_P)_j$: the damping ratio of the cavity mode
* The residues $[R_P]_j$ are complex coefficients that are independent of frequency:

$$[H_P(\omega)] = \sum_{j=1}^{J}\left[\frac{[R_P]_j}{i\omega - (\lambda_P)_j} + \frac{[R_P]_j^*}{i\omega - (\lambda_P)_j^*}\right] \qquad (17)$$

* Suppose the dissipation is moderate,
  - $\mathrm{Re}(Z) \ll \rho_0 c$ (the characteristic impedance of the air)
  - Loss factor $\sigma < 0.1$
  - Then to a first order approximation

$$\mathrm{Im}(\lambda_P)_j \equiv (\omega_P)_j \text{ is independent of } \mathrm{Re}(Z) \text{ and } \sigma$$
$$\mathrm{Re}(\lambda_P)_j \approx \beta_1 \times \text{average}(\mathrm{Re}(Z)) + \beta_1 \times \sigma \tag{18}$$

– Rigid-walled cavity:
  * This is the special case of the acoustic cavity when the structure is rigid.
  * Let $(\lambda_R)_j$ denote the eigenvalues in this case,

$$|[A(\omega)]| = 0 \implies \omega = (\lambda_P)_j \tag{19}$$

  * Correspondingly, the residue factors in eq. (17) are denoted $[R_R]_j$.

Resonances

- At any resonance, the response is dominated by the near singular pole:
  - Structural resonance

$$\omega \approx (\omega_S)_n \implies \text{peak}\left[H_S(\omega)\right] = \frac{\{\Phi_n\}\{\Phi_n\}^{\mathrm{T}}}{(\omega_S)_n^2(1+i\sigma)-\omega^2} \tag{20}$$

  - Coupled cavity-structural resonance:

$$\omega \approx (\omega_P)_j \implies \text{peak}\left[H_P(\omega)\right] = \frac{[R_P]_j}{i\omega-(\lambda_P)_j} \tag{21}$$

  - Rigid-walled cavity resonance:

$$\omega \approx (\omega_R)_j \implies \text{peak}\left[H_R(\omega)\right] = \frac{[R_P]_j}{i\omega-(\lambda_R)_j} \tag{22}$$

- If dissipation is moderate, which means that all eigenvalues are such that $|\mathrm{Re}(\lambda_j)| \ll \left|\mathrm{Im}(\lambda)_j\right|$, then the largest corresponding response occurs when the excitation frequency equals $\mathrm{Im}(\lambda_j)$. This is referred to as the resonance peak.
  - Resonance may occur for any eigenvalue. The one leading to the largest response is the mode for which $\mathrm{norm}\left([R]_j\right) / \mathrm{Re}(\lambda)_j$ is a maximum.
  - Thus, the maximum values of the transfer functions are well approximated as
    - Structural resonance

$$\omega = (\omega_S)_n \implies \max\left[H_S(\omega)\right] = \frac{\{\Phi_n\}\{\Phi_n\}^{\mathrm{T}}}{i(\omega_S)_n^2 \sigma} \tag{23}$$

    - Coupled cavity-structural resonance:

$$\omega = (\omega_P)_j \implies \max\left[H_P(\omega)\right] = \frac{[R_P]_j}{-\mathrm{Re}(\lambda_P)_j} \tag{24}$$

    - Rigid-walled cavity resonance:

$$\omega = (\omega_R)_j \implies \max\left[H_R(\omega)\right] = \frac{[R_R]_j}{-\mathrm{Re}(\lambda_R)_j} \tag{25}$$

Comparison of Wind Tunnnel and Full-Scale Behavior

- Characteristics of the wind tunnel model:
  - Solid boundaries are nearly rigid and dissipate little.
  - Pressure-release condition at opening is approximate:
    - $Z = 0$ is descriptive of cavity openings that are small relative to an acoustic wavelength
    - Actually $\mathrm{Re}(Z) \ll \rho_0 c$, but nonzero. (Energy dissipated from the cavity actually is energy that is radiated to the atmosphere.
- Characteristics of the full-scale SOFIA:
  - Solid boundaries are compliant and dissipate more than wind tunnel model, but still small.
  - Pressure-release condition at opening is the same, so acoustic dissipation is the same between model and full-scale.
  - Corrolaries:
    - Acoustic resonances occur at different frequencies

$$(\omega_P)_j \neq (\omega_R)_j \tag{26}$$

* Dissipation is stronger in full-scale

$$\left|\mathrm{Re}\left(\lambda_P\right)_j\right| > \left|\mathrm{Re}\left(\lambda_R\right)_j\right| \tag{27}$$

- The one-dimensional and two dimensional cavity models, as well as the probabily that the structure is relatively stiff, suggest that the acoustic residue factors are comparable between the wind tunnel and SOFIA,

$$\left[R_P\right]_j \approx \left[R_R\right]_j \tag{28}$$

- Conclusions from eqs. (24) and (25):

Resonance frequencies identified in wind tunnel, after scaling, will not match frequencies at which displacement is maximized in SOFIA

Pressure field measured in the wind tunnel will be higher than in SOFIA

Maximum Structural Displacement Amplitude

- Consider excitation at the structural natural frequency, $\omega = (\omega_S)_n$.
  - Maximum structure transfer function given by eq. (23).
  - Substitute into eq. (6) for pressure transfer function,

$$[H_P((\omega_S)_n)] \equiv \left[[A(\omega)] - (\omega_S)_n^2 [B] \left(\frac{\{\Phi_n\}\{\Phi_n\}^{\mathrm{T}}}{i(\omega_S)_n^2 \sigma} \right) [\Lambda] \right]^{-1} \quad (29)$$

  - Because of the smallness of σ, the second term is dominant,

$$[H_P((\omega_S)_n)] \equiv -\left[\frac{[B]\{\Phi_n\}\{\Phi_n\}^{\mathrm{T}}[\Lambda]}{i\sigma} \right]^{-1} \quad (30)$$

- Use $\max\left[H_S\left(\omega\right)\right]$ and corresponding $\left[H_P\left(\left(\omega_S\right)_n\right)\right]$ to evaluate displacemement $\left\{U\right\}$,

$$\left\{U\right\} = -\frac{\left\{\Phi_n\right\}\left\{\Phi_n\right\}^{\mathrm{T}}}{\left(\omega_S\right)_n^2}\left[\Lambda\right]\left[\left[B\right]\left\{\Phi_n\right\}\left\{\Phi_n\right\}^{\mathrm{T}}\left[\Lambda\right]\right]^{-1}\left[D\right]\left\{P_S\right\} \tag{31}$$

- This is an order one effect $\Longrightarrow$ an analytical confirmation that the displacement at the natural frequency is not large.

Summary

- Structural natural frequencies will not match resonance frequencies of coupled system.
- The displacement will not be large at the structure's natural frequencies.
- Acoustic resonance frequencies approach structure natural frequencies as the stiffness increases.
- Resonance frequencies identified in wind tunnel, after scaling, will not match frequencies for SOFIA.
- Pressure field measured in the wind tunnel will be higher than in SOFIA.

Implications

- The worst case design procedure used by NASA for the door considered the RMS pressure from the envelope source PSD to act at the structural's natural frequency.
- This is a more conservative approach than the Raytheon procedure, which applied the measured PSD to the structure's transfer function, and then impose a safety factor.
- Both procedures will over predict the response, because the pressure PSD that acts on the full-scale SOFIA structure will be less than the properly scaled PSD measured in the wind tunnel.
- Thus, the Raytheon and NASA procedures yield conservative designs.

Appendix F. Tables- Door Position and Test Objectives

Test point	Flt. #	Alt.	Speed	Door position	Comments	Test objectives
1	1	0	180 KCAS	2 door positions, 40% crack, full open-40° position	Monitor data continuously during acceleration to 180KCAS. Need one taxi run per door position (q=.7, M=.28)	Get initial data on cavity performance for low M# and q. learn cavity primary acoustic modes. See what effects door position has on cavity acoustics.
2	2	5,000	200 KCAS	5 door positions, 10% crack, 40% crack,20-40-60	Need 10 seconds of data for each door position. Check data before proceeding to next condition. (q=.91, M=.34)	Check cavity aero acoustics for multiple door positions at low q and M#. See if other primary acoustic modes are present. Learn what the interaction between acoustic modes and structural modes are.
3-3'	3	10,000	200 KCAS-1.2Vso - 200KCAS	5 door positions (may be able to reduce # of positions after gaining experience from previous data points), 10% crack, 40% crack,20-40-60	Lower flaps and extend gear as speed decreases per normal procedures, see TIS 411.3. At 1.2V_{SO}, Increase power to simulate go-around. Check controllability in roll and yaw. (Side slip can be checked now or later in flight test program.) Check data before proceeding to next door position. (q=.91, M=.36)	Check controllability and aero acoustics of cavity in landing and go-around configuration. Insure aircraft can attempt a safe landing.
4-4'	3	5,000 - GL	200 KCAS- 0	5 door positions (may be able to reduce # of positions after gaining experience from previous data points), 10% crack, 40% crack,20-40-60	Fly test profile for each door position, continuously record data for all door positions through entire profile. Full stop landings may not be required if flight crew allows movement of door during run-out. (q=.91 - 0, M=.34 - 0)	Demonstrate that aircraft can be landed with door opened to any position
5 - 5'	4	10,000' - 45,000'	200- 215 KCAS	5 door positions (may be able to reduce # of positions or continuosly slew to full open position, after gaining experience from previous data points), 10% crack, 40% crack,20-40-60	Climb from 10,000' to45,000' in 5,000' increments, subsitute 41,000' for 40,000'. Take data after each climb increment for each door position. Slew TA to cause misalignment at 10,000', 25,000, and 41,000 to check effects of misalignment. Close door during climb. (q=.91, M=.36-.8)	Check the effects of M# on cavity aero acoustics at constant q for multiple door positions. See if acoustic modes change frequency or magnitude with Mach #. Check for new acoustic modes and forcing functions as a function of Mach #. Check interaction of acoustics with structure
6 - 6'	4	45,000'-10,000'	215- 200 KCAS	Door full open at 40° position.	Decent from 45,000' to 10,000'. Set door to 40° position and take continuous data during the decent. (q=.91, M=.8-.36)	Get continuous data for a fixed q at Mach numbers between .8 - .36
7 - 7'	5	10,000' - 39,000'	270 KCAS	5 door positions (may be able to reduce # of positions or continuosly slew to full open position, after gaining experience from previous data points), 10% crack, 40% crack,20-40-60	Similar to pt. 5 except at higher q and M# Climb from 10,000' to39,000' in 5,000' increments. Take data at each climb increment for each door position.Close door during climb. (q=1.7, M=.49-.87)	Help clear the mach envelope at higher q than test point 5

Test point	Flt. #	Alt.	Speed	Door position	Comments	Test objectives
8 - 8'	5	39,000'- 10,000'	270 KCAS	Door full open at 40° position.	Decent from 39,000' to 10,000'. Set door to 40° position and take continuous data during the decent. (q=1.49- 1.69, M=.87-.49)	Get continuous data for Mach numbers between .87 - .49
9 - 9'	5	45,000'- 10,000'	215- 320 KCAS	Use previous data to choose critical door positons.	Decent from 45,000' to 10,000' along Mmo curve and then along Vmo to 10,000' (q=.91- 2.4, M=.87-.59)	Clear the operational flight envelope for a cruise configuration.
10- 10'	5	10,000'	320- 200 KCAS	Use previous data to choose critical door positons.	Decelerate from 320 KCAS to 200 KCAS at critical door positions. Take continuous data.	Complete envelope expansion for emergency decent condition.

General Notes:
1) All initial door open test should be done with A/C wt. as light as possible to increase stall margin, reduce stress on brakes, and minimize alpha.

2) Additional testing will be required to understand effects of Beta and non-cruise and emergency configurations.

3) If cavity starts to experience high aero-acoustics recovery will be to start door close procedure and accelerate or decelerate to previous flight condition

4) Initial test points will be with Tuned Mass Dampers (TMD) active. After external reasonance loads are measured, TMD can be de-ativated or removed.

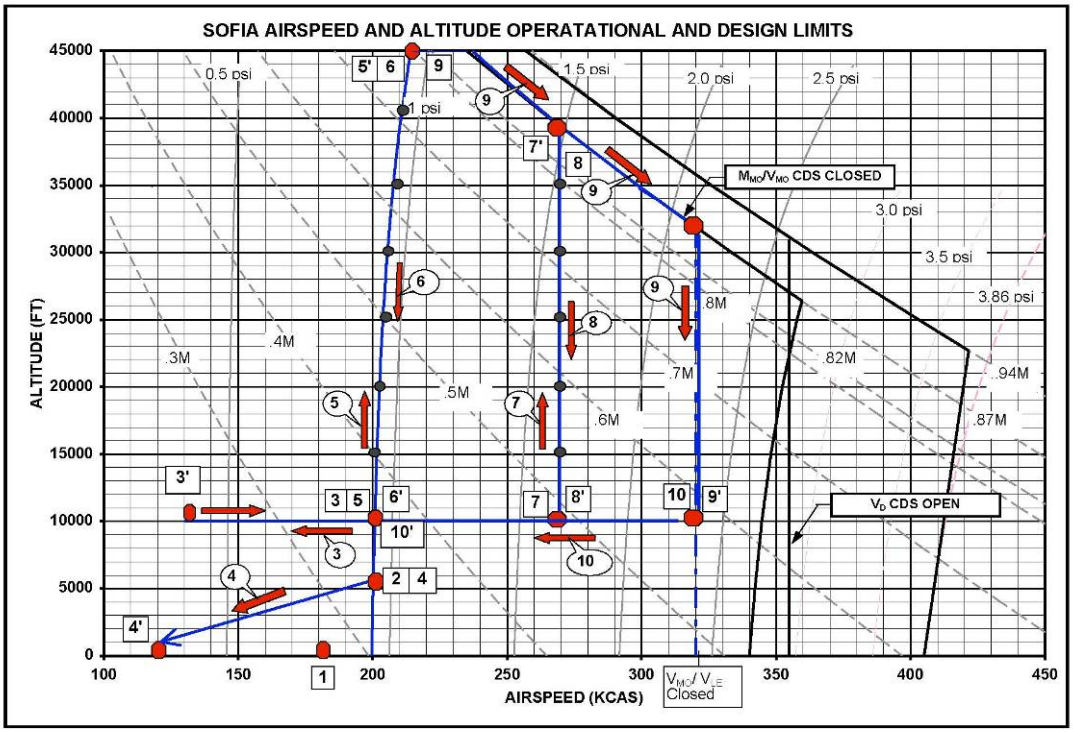
SOFIA AIRSPEED AND ALTITUDE OPERATATIONAL AND DESIGN LIMITS
ALTITUDE (FT)
AIRSPEED (KCAS)
45000
40000
35000
30000
25000
20000
15000
10000
5000
0
100
150
200
250
300
350
400
450
0.5 psi
1 psi
1.5 psi
2.0 psi
2.5 psi
3.0 psi
3.5 psi
3.86 psi
.3M
.4M
.5M
.6M
.7M
.8M
.82M
.87M
.94M
MMO/VMO CDS CLOSED
VD CDS OPEN
VMO/ VLE Closed

Document Approval and Revision History

Approved:	Original signed on file	10/6/05
	NESC Director	Date

Version	Description of Revision	Author	Effective Date
1.0	Initial Release	Principal Engineer's Office	9/22/05
2.0	Various changes as listed in email dated 10/2/05 from M. Kehoe (attached)	Principal Engineer's Office	10/6/05

Version 2.0 Changes – 10-6-05

Page 9 of 184 – Changed text "Section 8.2 to Section 8.0"
Page 25 of 184 – Changed text "figure 6.2.2.1-1 to figure 6.2.2-3"
Page 26 of 184 - Changed text "figure 6.2.2.1-2 to figure 6.2.2-4"
Page 51 of 184 – Enlarged figure 6.2.4-1 so Q did not appear as an O in CONSEQUENCE
Page 57 of 184 – Changed text "Section 8.2 to Section 8.0"
Page 73 of 184 – Changed text "Figure A1.0-1 to Figure B1.0-1"
Page 77 of 184 – Changed text "Figure A1.2-1 to Figure B1.2-1"
Page 77 of 184 - Added sentence at the end of the last paragraph "Figure B1.2-2 show these relationships."

Things that need to be changed in the report
Footnotes:

Footnote 6 should be
Rose, W. C. *SOFIA-Telescope Torque Wind Tunnel Test, SOFIA III Final Report*. Incline Village, NV: Rose Engineering & Research, Inc., 31 March 1995

Footnote 7 should be
Rose, W. C. *SOFIA-Conceptual Door Design And Aero-Optics Wind Tunnel Test, SOFIA IV Final Report*. Incline Village, NV: Rose Engineering & Research, Inc., 31 March 1996

Footnote 11 has two typos
Metallica should be *Metallic* and *Materal* should be *Materials.* Listing in the Reference Section is correct.

Footnote 12 should be
Matthews, L.S. *Vibroacoustic Assessment of SOFIA's Aft Bulkhead*. Rep No. LDG-00-004-SDS, Raytheon Systems Company, March, 2000. Currently Footnote 13

Footnote 13 should be
Honaker, Michael, "Preliminary Assessment of Stress Levels in the TA Due to Aero-Acoustic Loads and 1 G Gravity Effects", SOFIA project Technical Note TN-MAH-013, August 10, 2000. Currently Footnote 12

Footnote 17 has a typo
Ospring, J.J., and Harry Gobler should be Ospring, M.J., and Harry Gobler. This typo is also in the Reference Listing.

Other Comments

Text is document appears to be “blocked” except for the following pages where it is “left justified”

Pages 14, 25, 47, 49, 52, 58-62.

Figure on Page 19 (wind tunnel model) looks like it could fit on the previous page

REPORT DOCUMENTATION PAGE

Form Approved
OMB No. 0704-0188

The public reporting burden for this collection of information is estimated to average 1 hour per response, including the time for reviewing instructions, searching existing data sources, gathering and maintaining the data needed, and completing and reviewing the collection of information. Send comments regarding this burden estimate or any other aspect of this collection of information, including suggestions for reducing this burden, to Department of Defense, Washington Headquarters Services, Directorate for Information Operations and Reports (0704-0188), 1215 Jefferson Davis Highway, Suite 1204, Arlington, VA 22202-4302. Respondents should be aware that notwithstanding any other provision of law, no person shall be subject to any penalty for failing to comply with a collection of information if it does not display a currently valid OMB control number.
PLEASE DO NOT RETURN YOUR FORM TO THE ABOVE ADDRESS.

1. REPORT DATE *(DD-MM-YYYY)*	2. REPORT TYPE	3. DATES COVERED *(From - To)*
01- 05 - 2009	Technical Memorandum	Sept. 2004-Sept. 2005

4. TITLE AND SUBTITLE
Stratospheric Observatory for Infrared Astronomy (SOFIA) Acoustical Resonance Technical Assessment Report

5a. CONTRACT NUMBER

5b. GRANT NUMBER

5c. PROGRAM ELEMENT NUMBER

6. AUTHOR(S)
Kehoe, Michael W.; Gilbert, Michael G.; Gupta, Kajal K.; Ginsberg, Jerry H.; Kegerise, Michael A.; Kolar, Ramesh

5d. PROJECT NUMBER

5e. TASK NUMBER

5f. WORK UNIT NUMBER
869021.05.07.02.99

7. PERFORMING ORGANIZATION NAME(S) AND ADDRESS(ES)
NASA Langley Research Center
Hampton, VA 23681-2199

8. PERFORMING ORGANIZATION REPORT NUMBER
L-19668 NESC-RP-05-98/04-073-E

9. SPONSORING/MONITORING AGENCY NAME(S) AND ADDRESS(ES)
National Aeronautics and Space Administration
Washington, DC 20546-0001

10. SPONSOR/MONITOR'S ACRONYM(S)
NASA

11. SPONSOR/MONITOR'S REPORT NUMBER(S)
NASA/TM-2009-215730

12. DISTRIBUTION/AVAILABILITY STATEMENT
Unclassified - Unlimited
Subject Category 05-Aircraft Design, Testing and Performance
Availability: NASA CASI (443) 757-5802

13. SUPPLEMENTARY NOTES

14. ABSTRACT

A request was submitted on September 2, 2004 concerning the uncertainties regarding the acoustic environment within the Stratospheric Observatory for Infrared Astronomy (SOFIA) cavity, and the potential for structural damage from acoustical resonance or tones, especially if they occur at or near a structural mode. The requestor asked for an independent expert opinion on the approach taken by the SOFIA project to determine if the project's analysis, structural design and proposed approach to flight test were sound and conservative. The findings from this assessment are recorded in this document.

15. SUBJECT TERMS
LFD; NESC; SOFIA; SSMOC; TA; URD

16. SECURITY CLASSIFICATION OF:			17. LIMITATION OF ABSTRACT	18. NUMBER OF PAGES	19a. NAME OF RESPONSIBLE PERSON
a. REPORT	b. ABSTRACT	c. THIS PAGE			STI Help Desk (email: help@sti.nasa.gov)
					19b. TELEPHONE NUMBER *(Include area code)*
U	U	U	UU	192	(443) 757-5802